REGULATION OF MACROPHAGE PHENOTYPE BY S-NITROSYLATION DURING PULMONARY INFLAMMATORY RESPONSES

BY

SHERYSE TAYLOR

A dissertation submitted to the

School of Graduate Studies

Rutgers, The State University of New Jersey

In partial fulfillment of the requirements

For the degree of

Doctor of Philosophy

Graduate Program in Toxicology

Written under the direction of

Dr. Andrew Gow

And approved by

_____

_____

_____

_____

_____

_____

New Brunswick, New Jersey

MAY, 2019

ABSTRACT OF THE DISSERTATION

REGULATION OF MACROPHAGE PHENOTYPE BY S-NITROSYLATION DURING PULMONARY INFLAMMATORY RESPONSES

By: Sheryse Taylor

Dissertation Director: Andrew Gow, PhD

The pulmonary microenvironment is truly unique as it is continuously exposed to insult through inhalation of pollution and microbes, tasking the pulmonary immune system with active maintenance of homeostasis. In the lung the resident immune cell is the alveolar macrophage. These cells, along with bone marrow derived infiltrating macrophages are capable of developing responses that can be characterized along a pro-inflammatory or pro-repair spectrum, which is dictated in part by the microenvironment. For example, resident alveolar macrophages are largely anti-inflammatory as the lung contains a number of immunosuppressive mechanisms to prevent activation. These macrophages surveil the lung and when necessary, mount an immune response to preserve lung function. Key to this inflammatory response in macrophages is inducible Nitric Oxide Synthase (iNOS) and iNOS derived nitric oxide (NO). NO can react with a large number of biological targets, the majority of which fall under three major categories: reactive oxygen and nitrogen species (RONS), metals and thiols. NO's thiol based reactions serve as a signaling mechanism, forming S-nitrosothiols (SNOs) on proteins and small peptides. Formation of SNOs modifies the activity and function of a variety of proteins including enzymes and transcription factors, many of which have been implicated in macrophage activation and inflammatory signaling. Loss of NO has been found to alter the immune response in a model, and time dependent manner. Whether through genetic ablation or inhibition, loss of iNOS derived NO has been found to both reduce acute lung injury (ALI) in models of ozone, bleomycin, and LPS and worsen hyperoxia induced ALI,

and bleomycin induced fibrosis. It is unclear which of NO's bioactivity contributes to the previously observed effects, as well as the extent of NO's thiol based signaling on regulation of macrophage activation. Using models of acute lung injury, fibrosis and adenocarcinoma the present studies confirm previous findings of model induced changes in macrophage activation, and then determine how increased SNO formation affected macrophage phenotype in these models. Using multiple methods of immunophenotyping, we observed that SNO formation limited pro-inflammatory macrophage activation in models of pulmonary inflammation. Additionally, consistent with microenvironment/macrophage crosstalk, these changes altered immune signaling in the lung microenvironment. In general, these changes in macrophage phenotype and immune signaling led to alterations in biomarkers of disease progression. Also observed were the effects of SNO signaling in multiple macrophage subsets, primarily observing differences in resident lung populations as opposed to those recruited to the lung, and alveolar space during inflammatory signaling. Our findings suggest that NO's thiol based signaling present an opportunity to regulate inflammatory signaling and macrophage activation, as well as demonstrate the contribution of macrophage phenotype to the lung microenvironment.

DEDICATION

This dissertation is dedicated to my mother, Carlota “Aunty Halcyon” Jacobs-Taylor.

ACKNOWLEDGEMENTS

I would first like to thank Dr. Andrew Gow for his mentorship and guidance throughout the years. I am so grateful for his willingness to take me on as a student. He allowed to me explore my research interests even when they did not necessarily fit into what was previously studied in his laboratory. I am thankful for his understanding, empathy, and willingness to share his vast knowledge with me, and for preparing me for a career in science. Next, I would like to thank the entire Gow Lab, members past and present. Drs. Guo, Abramova, and Golden assisted me with so much throughout the years. I am eternally grateful and would not be here without them. From being extra hands when needed to giving life and science advice, thank you all so very much.

Next, I would like to thank Dr. Debra Laskin, whom, without I would not have been able to undertake my thesis project. During my rotation in her laboratory, I began learning many of the techniques I used to complete my work. I would like to thank her for her time, scientific advice, mentorship, and general support throughout the years. I am also grateful to Dr. Laskin for the great team she leads. The Laskin Lab's members both past and present have been instrumental in my completion of my dissertation. Dr. Gardner, Dr. Venosa, Dr. Mandal, Dr. Joseph, Dr. Smith, Kinal Vayas, Richard Sun, and Alexa Murray have been my friends, collaborators and support. Thank you all so much.

I would like to thank my thesis committee for their time, and attention as well as their advice and support. Thank you all for keeping me on track and focused in accomplishing my goals.

A special thank you goes to Dr. Lauren Aleksunes who helped me first as a professor and then as program director. Thank you for your guidance, advice, understanding and

simply your willingness to listen, to help in any way you can. I am so thankful for all your support during incredibly difficult times.

Thank you to my cohorts Stephanie Marco and Richard Sun. The lunches, study sessions, and comedic relief throughout the years were invaluable. Stephanie, you were with me every step of the way, and we grew especially close because of our mutual hardships. I'm proud of you. Thank you. I'd also like to thank Dr. Blessy George, PharmD. Thank you for all your company during classes as well as being will to carpool to downtown New Brunswick weekly. John, Jamie, Laura, Sara, Justin, and Allison thank you for your company as well as advice and resources when needed.

I also must thank all EOHSI staff and administration. The flow cytometry core as well as histopathology core played a huge role in completion of this work. Thank you Elizabeth Rossi, Linda Everett, Eva Link, and Sandi Selby for being patient with me, ensuring I took care of all administrative things I would ordinarily overlook.

I'd also like to thank the Sant'Angelo and Denzin labs for all their help, and advice on immune assays, techniques, and writing.

Lastly, but certainly not the least, I must thank my non-Rutgers support system. To my mother, I miss you daily. Without you I wouldn't have gotten here. Thank you so much for instilling a love of learning and curiosity in me. Thank you for giving me the strength and confidence to believe in myself, and always pushing me to be better. I wish you were here for this moment, but I know you are watching and I hope you know I love you and that I am thankful for all that you did. Even in your last days, you made me show you my work. I know you are proud. To my sister, thank you for being the support that I needed through all times. We survived, and though at times it hurts, we are made stronger, and our sisterly bond is strengthened as well. Thank you for always being my

biggest cheerleader, and hype man. Thank you for using your expertise as a teacher to help me improve my presentation skills. Thank you for always being there whenever I needed. I love you.

I'd like to thank my dad, your pride in me and support has always meant so much. I miss you always. Thank you for all you have given me, for listening and always having practical advice for me. Whenever I needed encouragement, I was able to find it in you. Love you and thank you. To my closest cousin and confidante Pashan, I love you. Thank you for always looking out for me and being there.

ACKNOWLEDGEMENT OF PUBLICATIONS

In preparation for submission

CHAPTER 2

Taylor, S., Francis, M., Murray, A., Abramova, E., Gow, A., Laskin, J., and Laskin, D. Increased S-nitrosylation Reduces Ozone Induced Lung Inflammation Through Reduced Macrophage Pro-inflammatory Activation.

In preparation for submission to American Journal of Respiratory Cell and Molecular Biology

CHAPTER 3

Taylor, S., Guo, C., Voronin, G., Golden, T., and Gow, A. The Role of S-nitrosoglutathione Reductase in Macrophage Activation and Phenotype. American Journal of Respiratory Cell and Molecular Biology.

TABLE OF CONTENTS

ABSTRACT OF DISSERTATION ii

DEDICATION iv

ACKNOWLEDGEMENTS v

ACKNOWLEDGEMENTS OF PUBLICATIONS viii

TABLE OF CONTENTS ix

LIST OF TABLES xii

LIST OF FIGURES xiii

CHAPTER 1: GENERAL INTRODUCTION 1

1.1 Nitric Oxide 1

1.2 Phagocytes 2

1.3 Pulmonary Macrophages 4

1.4 Immune Cell Immunophenotyping 5

1.5 Pulmonary Macrophages in Disease 8

1.5.1 Acute Lung Injury 8

1.5.2 Fibrosis 9

1.5.3 Cancer 10

1.6 Regulation of Macrophage Phenotype 11

1.6.1 Epigenetic Regulation 12

1.6.2 Regulation by Noncoding RNA 13

1.6.3 Genetic Regulation 14

1.6.4 Metabolic Regulation 14

1.6.5 Regulation by Cellular Signaling 15

1.6.6 Regulation by S-nitrosylation 16

1.7 Murine Models of Pulmonary Damage 17

1.7.1 Acute Inflammation: Ozone (O_3) Induced Acute Lung Injury 18

1.7.2 Resolution and Repair: Acute Lung Injury and Fibrosis: Intratracheal Instillation of Bleomycin 18

1.7.3 Chronic Inflammation: Lewis Lung Carcinoma (LLC) 20

1.8 Overall Research Hypothesis 20

CHAPTER 2: THE EFFECTS OF SNO DONOR ADMINISTRATION IN OZONE INDUCED ACUTE LUNG INJURY 22

2.1 Abstract 22

2.2 Introduction 22

2.3 Methods 25

2.4 Results 29

2.5 Discussion 44

CHAPTER 3: INCREASED INTRACELLULAR SNO FORMATION IN BLEOMYCIN-INDUCED FIBROSIS AND INFLAMMATION 51

3.1 Abstract 51

3.2 Introduction 51

3.3 Methods 53

3.4 Results 56

3.5 Discussion 67

CHAPTER 4: INHIBITION OF S-NITROSOGLUTATHIONE REDUCTASE IN LEWIS LUNG CARCINOMA 71

4.1 Abstract 71

4.2 Introduction 71

4.3 Methods 72

4.4 Results 75

4.5 Discussion 85

CHAPTER 5: SUMMARY, DISCUSSION, FUTURE DIRECTIONS, CONCLUSIONS, AND SPECULATION 90

5.1 Summary 90

5.2 Discussion 92

5.3 Future Directions 95

5.4 Conclusions and Speculation 96

REFERENCES 98

LIST OF TABLES

1.1 Flow Cytometry Based Macrophage Sorting 6

1.2 Macrophage Pro-inflammatory Markers 6

1.3 Macrophage Anti-inflammatory Markers 7

1.4 Additional Flow Cytometry Based Immunophenotyping 8

2.1 BAL Measures of Lung Injury and Recruitment 30

2.2 Percentage of BAL Macrophages Expressing Ly6C 34

2.3 Markers of Activation in F4/80- Cells in BAL 36

2.4 Percentage of Tissue Macrophages Expressing Ly6C 37

3.1 RT-qPCR of Alveolar Macrophages 59

3.2 FACS Analysis of Bone Marrow Derived Macrophages 61

4.1 BAL Cell Count and Composition 76

4.2 Additional Tissue Populations 82

5.1 Recruitment and Macrophage Activation in Each Model 91

5.2 Effects of Increased S-nitrosylation in Each Model 92

LIST OF FIGURES

1.1 Fates of NO 1

2.1 O_3 Induced Tissue Damage 31

2.2 Cyb5 Immunohistochemical Staining 32

2.3 PCNA Immunohistochemical Staining 33

2.4 Viable, F4/80+ BAL Cell Expression of Cd11c vs Cd11b 35

2.5 Viable, F4/80+ Tissue Expression of Cd11c vs Cd11b 39

2.6 iNOS Immunohistochemical Staining 40

2.7 IL-1β Immunohistochemical Staining 40

2.8 HO-1 Immunohistochemical Staining 41

2.9 Ym1 Immunohistochemical Staining 42

3.1 Increased Collagen Deposition 21 Days Post ITB 57

3.2 Increased Pro-Fibrotic Markers 21 Days Post ITB 58

3.3 Increased Inflammation 8 Days Following ITB 62

3.4 BAL Cell Recruitment 8 Days Following ITB 63

3.5 BAL Cell Size Following ITB 65

3.6 Tissue Macrophage Immunophenotyping 66

3.7 Tissue Expression of STAT3 67

4.1 Lewis Lung Carcinoma Tumors 75

4.2 Alveolar Macrophage Activation Following LLC 78

4.3 Tissue Macrophage Activation Following LLC 79

4.4 Cd11bhi Macrophages Present in Tissue 81

4.5 Tissue Expression of Cd11b and GR1 85

Chapter 1: General Introduction

1.1 NITRIC OXIDE

There are three isoforms of nitric oxide synthase (NOS) that generate nitric oxide (NO) from L-arginine. These are eNOS, nNOS, and iNOS (endothelial, neuronal, and inducible respectively). eNOS is expressed by endothelial cells, nNOS by neuronal cells and iNOS by immune cells including macrophages, thus is the focus of this discussion. iNOS is coded for by the gene *NOS2* and transcription is upregulated following stimulation with pro-inflammatory signals including LPS, and IFN-γ (1). In the C-terminal reductase domain iNOS binds NADPH and the N-terminal domain contains a binding site for heme, arginine, BH4, and calmodulin. iNOS generates the highest levels of NO when compared to other isoforms and is always active when expressed.

The NO molecule is highly reactive and can be found biologically in many different oxidation states. NO is capable of reacting with a plethora of biological targets which may be generally combined into three general categories: oxygen species, metals, and thiols (Figure1).

Figure 1.1

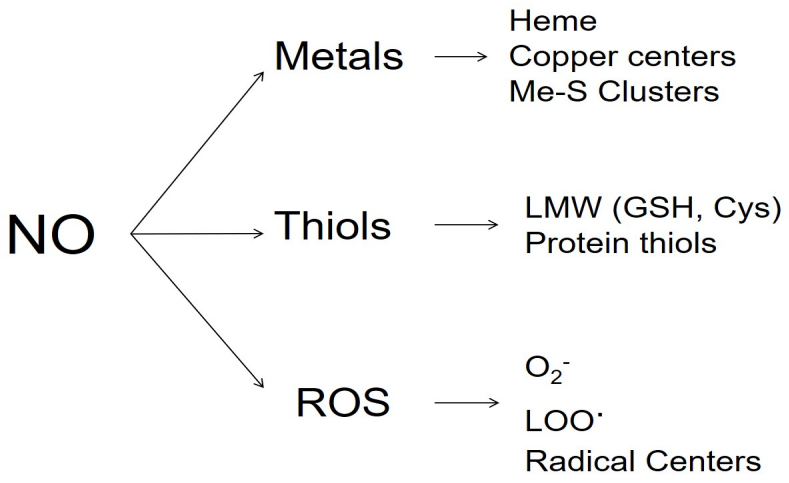

Figure 1.1. Fates of NO. Metabolic fates of NO can be generalized into three categories, ROS, thiols, and metals each having unique physiological consequences.

NO is capable of reacting with superoxide to form peroxynitrite, a reactive species and thus potentially increase cellular damage driven by oxidative stress, or where levels of GSH may have been depleted. This reaction is of special relevance as macrophages produce both superoxide and NO through iNOS and NADPH oxidase (2).

NO's reactivity with thiols allows for NO-derived signaling through post-translational modification of proteins, leading to altered function. While the NO molecule itself has a very short half-life, NO-derived signaling is continued by transfer of the NO+ species in a process known as trans-nitrosylation occurring with thiol containing low molecular weight peptides such as glutathione (GSH) and proteins. Nitrosylated GSH, now GSNO, is a potent and abundant donor of intracellular NO to proteins with S- cysteine residues in thiols. This is of importance as there are several targets that contribute to inflammation and immunosignaling that are substrates for S-nitrosylation. For example, S-nitrosylation NFκ-B reduces its ability to translocate to the nucleus, also allowing iNOS and iNOS-derived NO to serve as a negative feedback regulator of inflammatory signaling (3).

NO's reactivity with redox active metals such as iron is also relevant to inflammatory signaling through the formation of dinitrosyl iron clusters (DNICs) as they may also donate SNO species, thereby nullifying the cytotoxicity of free iron (4, 5). When compared to high molecular weight DNICs, low molecular weight DNICs are more stable, providing longer storage and transfer of NO, even being detected in cells that do not produce NO increasing the pool of thiols for S-nitrosylation. Furthermore, DNIC formation may also be protective from oxidative stress by reducing the availability of NO to react with superoxide.

1.2 PHAGOCYTES

In 1982, Eli Mitchnikof discovered white blood cells with phagocytic capability in the larvae of starfish. He initially termed them “phagocytes” and these are the cells we now know as macrophages (6). Since their discovery the importance of the role of the macrophage in immunity has been continuously highlighted. Macrophages are part of what is classified as the innate immune system and play a significant role in maintaining homeostasis. These cells are responsible for recognizing and destroying invading pathogens through the release of reactive oxygen or nitrogen species (RONS), phagocytosis, efferocytosis, antigen presentation to T cells for an adaptive immune response. Pathogen and damage associated molecular patterns (PAMPS and DAMPS) activate receptors on macrophages leading to their activation, orchestrating an immune response. In response to stimuli, macrophages activate along a spectrum with the pro-inflammatory and pro-reparative phenotypes on opposing ends. With these phenotypes are various functional capabilities, allowing for tailored responses to a wide variety of stimuli (7). Features of the M1/pro-inflammatory macrophage include increased antigen presentation capability and increased production of RONS, thus pro-inflammatory macrophages express higher levels of NADPH Oxidase and inducible nitric oxide synthase (iNOS). Pro-inflammatory macrophages are largely associated with a response that is associated with a Th1 dominant response from the adaptive immune system and are considered “classically activated”. This activation state provides efficient clearing of bacterial and viral pathogens and tumor cells. Conversely, the M2/pro-repair macrophage activation state is referred to as “alternatively activated”. These macrophages are thought to be largely play a role in tissue remodeling, producing high levels of polyamines and are linked to Th2 responses of the adaptive immune system. These pro-reparative macrophages are thought to play a large role in the elimination of helminth infections, and fibrotic responses (8). While the Th1 vs Th2 activation state works well for T cells, macrophage activation has proven to be much more complicated

and has been compared to a color wheel as opposed to a linear spectrum (9). Intermediate phenotypes are frequently observed with macrophages showing features of both activation states (7, 9).

1.3 PULMONARY MACROPHAGES

Because of their key role in protection from damage both foreign and host derived, many organs have a resident population of macrophages that are specialized and are known by specific names (10). These resident cells are derived from the yolk sac or fetal liver, have self-renewing capabilities and have specialized activity specific to the organ. In the lung, these cells are alveolar macrophages where they are tasked with 1) responding appropriately to inhaled microbes and particulate without total pulmonary or systemic inflammation, and 2) successfully resolving the initiated response. Alveolar macrophages reflect the nature of the consistent exposure of lungs to stimuli as they are largely immunosuppressive with reduced phagocytic, antigen presenting and T cell suppressive capabilities (11-13). While alveolar macrophages are the cell type commonly referred to as the resident cell of the lung, macrophages are also found in bronchial airways as well as the interstitium. Interstitial macrophages, like alveolar macrophages have a low turnover rate (however it is unclear whether this rate is higher or lower than that of alveolar macrophages) but are functionally and phenotypically distinct from alveolar macrophages (14, 15). While much remains unknown as they are less frequently studied, interstitial macrophages have demonstrated increased phagocytic ability as well as altered responses to stimuli potentially contributing differently to the pulmonary immune response (14, 16). Both alveolar and interstitial macrophages express CD115, and CD116 (receptors for M-CSF and GM-CSF respectively); however, stimulation with GM-CSF led to increased expression of CD11c in alveolar macrophages, while CD11b was increased in interstitial macrophages (16).

Differences in the responses to these CSFs potentially the observation of interstitial macrophages having reduced proliferative capacity compared to alveolar macrophages as stimulation with both CSFs did not lead to proliferation in interstitial macrophages. These differences in macrophage populations warrants further investigation as preliminary studies suggest they may contribute to inflammation differently (17, 18)

1.4 IMMUNE CELL IMMUNOPHENOTYPING

During homeostasis, resident alveolar macrophages are largely immunosuppressive through a number of mechanisms. For example, in the fluid lining the lung are the pulmonary collectins: surfactant proteins A and D. These collectins interact with alveolar macrophage surface receptors such as TLR4, and SIRPα inhibiting ligand interactions and thus activation (19). During steady state, the lung microenvironment is abundant in IL-10 and TGFβ, both of which lead to a pro-reparative phenotype of alveolar macrophages (20-22). More recently, there has been a greater appreciation for macrophage heterogeneity. It is well documented that resident macrophages are functionally different when compared to “recruited” monocytes that mature into macrophages in the lung as there is now evidence that these macrophages persist in the lung and adopt features consistent with the microenvironment (20, 23-27). With advances in differentiating markers for assessment of macrophages by flow cytometry, it is now possible to distinguish pulmonary macrophage subpopulations, such as resident vs recruited macrophages, and those that reside in the interstitium vs the alveolar space, or upper airways (14, 28), and to determine their contributions to lung function and disease. Table 1.1 shows expression of markers often used to identify pulmonary macrophage subsets.

Table 1.1

	Resting Alveolar	Activated Alveolar	Interstitial	Recruited
CD64	+	+	+	+
CD24	-	-	-	-
F4/80	+	+	+	+/-
CD11c	+	+	-/lo	+/-
CD11b	-/lo	+	+	+
SiglecF	+	+	-	-
CCR2	-	-	-	+
CD115	-	-	-	+
MHCII	+/-	+/-	+	-

Table 1.1 Flow cytometry Based Macrophage Sorting. Macrophage subpopulations can be determined by the presence or absence of surface and/or intracellular markers when assessed by flow cytometry.

Macrophages may also be sorted by markers associated with pro- or anti-inflammatory activation by flow cytometry and/or immunohistochemistry (IHC). As shown in Table 1.2 and 1.3, proteins that are associated with specific activation states that may or may not have any known functional activity.

Table 1.2

Marker	**Technique**
Ly6C	Flow cytometry
iNOS	IHC
IL-1β	IHC
COX-2	IHC

Table 1.2. Macrophage Pro- Inflammatory Markers. Macrophages that are activated and polarized toward a pro-inflammatory phenotype commonly express these markers.

Table 1.3

Marker	Technique
CD206/Mannose Receptor	Flow cytometry, IHC
Ym1	IHC
HO-1	IHC

Table 1.3. Macrophage Pro- Reparative Markers. List of markers commonly expressed by anti-inflammatory markers.

In Table 1.4, additional immune cells and their phenotypic markers are described. Macrophage subpopulations also respond distinctly to stimuli and possess different antigen presenting capabilities (29). There has been considerable research to show that resident macrophages do not alter their phenotype significantly in response to stimuli, and recruited macrophages have more plasticity in their phenotype adoption (20, 23). In the blood, these macrophages are $Ly6C^+$ and home to the lung using the CCL2/CCR2 and CX3CL1/CX3CR1 pathway. Ly6C expression may remain during an inflammatory response, but these macrophages can also contribute to replenishing the resident $Ly6C^-$ macrophage population. It is believed that under homeostatic conditions, only a very small percent of these $Ly6C^+$ monocytes enter the lung, and most return to circulation. However, during an inflammatory response, these monocytes adopt a phenotype based on the pulmonary microenvironment. At the end of the response the ultimate fate of these monocyte-derived macrophages is unclear.

Table 1.4

Cell Type	Surface Markers
Neutrophils (PMNs)	CD11b+Ly6G+SideScatter^{hi}
Immature Recruited Macrophages	F4/80+/-CD11b+/hiLy6C+Ly6G-/lo
Eosinophils (Eos)	F4/80+SiglecF+CD11c-CD11b+Gr1+
Th1 T cell	CD3+CD4+IL-12+Tbet+
Th2 T cell	CD3+CD4+IL-12+GATA3+
Th17 T cell	CD3+CD4+IL-12+IL-17
Cytotoxic T cell	CD3+CD8+IL-2+IFγ
T regulatory cell (Treg)	CD3+CD4+Foxp3+

Table 1.4. Additional Flow Cytometry Based Immunophenotyping. Flow cytometric phenotypes of additional cells of the immune system.

1.5 PULMONARY MACROPHAGES IN DISEASE

Failure of the macrophages to recognize, initiate, and importantly terminate an appropriate immune response to offending agents will inevitably contribute to the etiology and eventual manifestation of pulmonary disease. Often times, pulmonary injury and damage manifests in part, as a result of macrophage dysfunction. However, fully understanding how macrophages contribute to lung pathology is difficult as the lines between how macrophage phenotype determines the pulmonary microenvironment and how the pulmonary microenvironment determines macrophage phenotype is blurry.

1.5.1 Acute Lung Injury

Acute lung injury characterized by tissue damage and destruction has been attributed in part to excessive or exaggerated pro-inflammatory signaling (30-32). During acute inflammation, short lived neutrophils (PMNs), followed by Ly6C+ blood monocytes are recruited to the lung. There, they receive signals that maintain their pro-inflammatory phenotype, releasing increased levels of RONS that eliminates invading pathogens. If necessary, antigen presentation to activate the adaptive immune system also increases. Normally, this response is short-lived. When the threat is neutralized, the microenvironment of the lung switches, and enters a reparative mode (33). When this initial response and necessary repair is proportional and appropriate, there is minimal scarring. However, a pro-inflammatory response that is exaggerated, or lasts too long, this leads to extensive damage to the lung tissue. These damaged epithelial cells will then release additional signaling molecules to further propagate pro-inflammatory signaling, leading to the persistence of Ly6C+ monocyte-derived macrophages in the lung (31). This is further illustrated as loss of alveolar macrophages worsens acute lung injury, and neutrophil persistence during bacterial and viral infections highlighting the contribution of macrophages to cessation of the pro-inflammatory response (34).

1.5.2 Fibrosis

Accumulating evidence suggests that pulmonary fibrosis develops in part because of excessive lung remodeling from an exaggerated pro-reparative macrophage activation, which may or may not have been preceded by prior injury (35-38). Fibrosis may present idiopathically, or be the result of insult from therapeutic intervention (bleomycin, amiodarone, and cyclophosphamide), chronic exposure to irritants (asbestos, and silica) or even chronic infection (39). While tissue remodeling is often a necessary part to the completion of an inflammatory response, damage, lung fibrosis occurs when there is excessive deposition of collagen leading to impaired lung function through increased

resistance to expansion and inefficient gas exchange. Interestingly, during fibrotic processing, it is the recruited macrophages that play a larger and differing role during fibrosis despite the constitutive pro-reparative phenotype of resident macrophages (27, 40). In pro-fibrotic signaling, a network of stromal cells including macrophages, and fibroblasts participate in the remodeling of the extracellular matrix and increase deposition of scar tissue (41). Cytokines such as IL-10, IL-4, IL-13 and TGF-β play a key role in pro-fibrotic signaling. Activation of these receptors on macrophages have been found to lead to the activation of signaling pathways that enhance tissue remodeling through increased secretion of IL-10, IL-4, IL-13, TGF-β, S100A4, chitinases, metalloproteinases, and collagen. Along with factors leading to Th2 activation of the adaptive immune system (CCL1, and CCL22 and CCL4), increased pro-inflammatory cytokines are also observed during fibrosis (42). Surfactant abnormalities including altered metabolism, and Type II cell dysfunction have also been proposed as initiating factors to the pathogenesis of pulmonary fibrosis, potentially indicative of a role of altered lipid metabolism in macrophages as macrophages participate in surfactant recycling (43, 44).

1.5.3 Cancer

Not only do macrophages contribute to pulmonary damage through their responses to stimuli, but also through their failure to do so. Such is the case in lung pathologies characterized by cellular overgrowth. Key to innate immune function is recognition of self vs. non or altered self- a function that fails during tumor development. Tumors avoid immune elimination through a variety of immunosuppressive mechanisms that include evading recognition by immune cells by masquerading as self, as well as hijacking immune cell function to promote tumor progression (45). As cancer cells upregulate markers of self such as CD47, and MHC Class I macrophages fail to adopt a pro-

inflammatory/tumoricidal phenotype; they also fail to activate the adaptive immune system through efficient antigen presentation to CD4+ and CD8+ T cells (46-48). Additionally, the adaptive system also is affected by immune evasion as CD4+ cells fail to recognize “neo-antigens” that would be unique to the tumor, tumors may express checkpoint inhibitor molecules such as CTLA-4 and PDL1, or conversely persistent antigen presentation to CD8+ T cells may lead to exhaustion (49, 50). Pro-inflammatory/Th1 biased responses are normally mounted to eliminate abnormally proliferating cells; however, these cells successfully create an immunosuppressive microenvironment to promote growth, angiogenesis, and dissemination (51-53). This requires persistent and dynamic immunosignaling as the needs of the lesion changes, and this creates a unique phenotypical dysfunction in pulmonary macrophages. Although immune cells isolated from the sites of cellular overgrowth or the surrounding area, should be expressing RONS to eliminate the tumor, in fact, they are in an inactive, and tumor promoting state. These cells are heterogeneous in type (54-60), activation state (61-63) and may be classified based on their location relative to the tumor (64).

Key players in immunosuppression are cells of myeloid origin including myeloid derived suppressor cells, and tumor associated/infiltrating macrophages (MDSCs, TAMs/TILs respectively). Along the MDSC to TAM spectrum are cells that are inappropriately activated in response to abnormally growing cells. Characteristics of this altered activation state include tumor escape of immunosurveillance (65), epithelial-mesenchymal transition to aid angiogenesis and metastasis (66), and suppression of the adaptive immune system (67). In cancer and chronic inflammation (68), both TAMs and MDSCs are found to be heterogenous populations (69, 70). Thus far, TAMs have been identified as differentially activated along the pro- and anti-inflammatory spectrum, while MDSCs have been differentiated based on their monocytic or granulocytic origin (70).

1.6 REGULATION OF MACROPHAGE PHENOTYPE

As macrophages are terminally differentiated cells but are able to mount very different responses to a variety of stimuli, there is much to understand about macrophage activation. There are several mechanisms of regulation of macrophage phenotype at both pre- and post-transcriptional levels. It is interesting to consider how these layers of regulation all work together to co-ordinate the macrophage response to stimuli, and how they are changed during the distinct phases of an inflammatory response.

1.6.1 Epigenetic Regulation

At the epigenetic level, macrophage gene expression is controlled by histone modifying enzymes. Histone demethylase Jmjd3 is upregulated in response to both LPS and IL-4 macrophage stimulation (71, 72). Jmjd3 associates with another histone demethylase KIAA1718 and together they allow for more efficient transcription of inflammatory genes (73). For phenotype specific activation, histone deacetylase 3 (HDAC3) has activity has been found to oppose pro-reparative polarization while favoring pro-inflammatory activation (74). Loss of HDAC3 inhibition creates an exaggerated pro-reparative phenotype in macrophages without stimulation while impairing the effective transcription of pro-inflammatory genes upon stimulation (75). Further regulation of macrophage gene transcription occurs with the variation of enhancers and lineage determining transcription factors (LTDFs). Enhancers and LTDFs are also marked with histone modifications, which determine cell type, and macrophage polarization (76). Recent work has indicated that there are pro-inflammatory specific enhancers termed “de novo” or “latent” enhancers as they have no intrinsic activity; upon TLR4/NFκ-B activation, they gain histone modification marks such as H3K4me1/2 to create active and functional enhancers for increased ease and speed of gene transcription (77, 78). Interestingly, there has been noted diversity in the motifs of the LTDF DNA binding regions leading to

diversity in enhancer selection and thus affecting the polarization potential of macrophages. This is elegantly demonstrated in the analysis of strain specific analysis of LTDF diversity between C57bl/6 and Balb/c mice (79). When C57 SNP's were placed in macrophage and B cell specific LTDF binding regions and p65 binding motifs of Balb/c mice, enhancer activity and p65 binding resembled that of C57bl/6 mice. This epigenetic mechanism of regulation of macrophage phenotype may contribute to the differences of observed immune response in these two strains.

1.6.2 Regulation by Non-coding RNA

There are two primary divisions of non-coding RNA. Short non-coding RNAs are less than 30 nucleotides and includes micro (mi), short interfering (si), and piwi-interacting RNAs (pi). Long non-coding RNAs are greater than 200 nucleotides (lnc). Both short and long noncoding RNAs actively regulate macrophage activation. When short noncoding RNAs are considered, miRNAs (miRs) are the primary subgroup that has been implicated macrophage activation regulation in multiple aspects that determine macrophage activation including phenotype and function. miR-21 is downstream of M-CSF has been found to play critical role in the pro-reparative phenotype of macrophages, as loss of miR-21 led to a more pro-inflammatory macrophage phenotype (80). miR-21 has also been found to be critical to efferocytosis and negative regulation of LPS induced increases in pro-inflammatory signaling indicating a key role in the resolution of inflammation (81). In contrast, miRs-26a and b have both been found to regulate pro-inflammatory macrophage phenotype by increasing the pro-inflammatory response to LPS via NFκ-B (82, 83). Additionally, stimulus dependent miRs have also been observed in macrophage activation following stimuli such as LPS, IL-4, TGF-β and following hypoxic conditions (84, 85). Although findings such as miR-146b's regulation of STAT1 and miR-18a's regulation of STAT3 were discovered outside of macrophages,

given the importance of these transcription factors in macrophage polarization, it is not unreasonable to speculate that these and several others may also regulate macrophage activation (86-89). LncRNAs have also been found to play a role in macrophage activation. A subset of lncRNAs have been found to be immune priming as they remodel chromatin to allow for a more robust response upon re-exposure to a previously encountered stimulus in innate immune cells (90). Additionally, expression of the lncRNA Malat1 increases in macrophages following LPS stimulation in macrophages and is decreased following IL-4 stimulation. Malat1 interacts with genes downstream of NFκ-B (91). Loss of Malat1 was also associated reduced pro-inflammatory signaling leading to decreased acute lung injury but worsened fibrosis. The lncRNAs such as FIRRE, lincRNA-Cox2 and Tnfaip3 has also been found to work downstream of NFκ-B to regulate macrophage phenotype (92-94).

1.6.3 Genetic Regulation

There are several key transcription factors that regulate macrophage phenotype following receptor activation, leading to upregulation of effector molecules that determine macrophage function and activation. Those associated with pro-inflammatory signaling include the STAT family (with the exception of STAT3, and 6) NFκ-B, IRF4 and 5, AP-1, PU.1, and C/EBP-α (95, 96). Translocation and subsequent DNA binding leads to transcription of pro-inflammatory genes such that code for IFNγ, iNOS, IL-1β, TNFα, and IL-12 leading to pro-inflammatory macrophage function. In contrast, STAT3, STAT6, HIF family, Nrf2, miRNAs, C/EBPβ and PPARγ either suppress transcription of pro-inflammatory genes or lead to the transcription of anti-inflammatory genes coding for Arginase I, IL-4, HO-1, and NQO1 (97).

1.6.4 Metabolic Regulation

Glucose metabolism represents another means of control of macrophage activation as pro-inflammatory macrophages shift toward anaerobic glycolysis in addition to upregulation of the pentose phosphate pathway when compared to resting or pro-reparative macrophages (98). Pro-inflammatory macrophages express the PFK2 isoform of 6-Phosphofructo-2-kinase which is more active than the liver-type L-PFK2 isoform, increasing fructose-2,6 biphosphate levels, further increasing the shift toward glycolysis. Following stimulation with LPS, CARKL (carbohydrate kinase-like protein) is downregulated, promoting glycolysis, and loss of CARKL increases pro-inflammatory activation in macrophages without stimulus (99). Interestingly, a similar upregulation in glycolysis occurs during phagocytosis, a function associated with a subtype of M2 macrophages. In M2 macrophages, oxidative phosphorylation predominates, and is also associated with increased mitochondrial content (100). Resting and M2 macrophages also have normal TCA cycles while M1 macrophages display TCA disruption as succinate, citrate, and itaconate are all increased following stimulation with LPS and IFNγ stimulation (101). These increases in citrate in M1 macrophages also leads to altered lipid metabolism as citrate is used for fatty acid synthesis seen in M1 macrophages whereas beta oxidation predominates in M2 macrophages. Metabolism of arginine also plays a key role in determining macrophage phenotype. L-arginine for is the substrate for iNOS and Arginase I. Pro-inflammatory macrophages express higher levels of iNOS producing NO promoting killing effector function while pro-reparative macrophages express higher levels or Arginase I producing higher levels of ornithine promoting wound repair effector function (98).

1.6.5 Regulation by Cellular Signaling

Control of macrophage phenotype is also regulated in part by multiple families of signaling cascades induced by phosphorylation leading to translocation of transcription

factors involved in macrophage polarization. The PI3K/Akt signaling pathway has been implicated in both pro-inflammatory and pro-reparative macrophage phenotypes (102). Akt2 is associated with pro-inflammatory activation while Akt1 is associated pro-reparative signaling as loss of each led to a switch of the opposing phenotype. Loss of Akt2 led to increased C/EBP-β induced expression of Arginase 1 and IL-10 following LPS exposure while loss of Akt1 led to increased expression of iNOS and TNFα. The Jak family of kinases are upstream of the STAT transcription factors and different stimuli leads to phosphorylation of a cascade of kinases followed by translocation of different members of the STAT family, leading to M1 or M2 activation in macrophages. Following exposure to IFN-γ, STAT1 is activated following Jak1/2 phosphorylation leading to increased transcription of key genes associated with pro-inflammatory activation. Additionally, SOCS3 inhibits STAT1 activation further limiting M1 activation (103). The large family of mitogen- activated protein (MAP) kinases are also play a key role in macrophage activation with ERK-1 and 2, JNK-1 and 2, and p38 all being upregulated following stimulation with LPS and IFN-γ (104). Conversely, the MKP-1 phosphatase also serves to limit pro-inflammatory activation following stimulus induced phosphorylation of the MAP kinases (105).

1.6.6 Regulation by S-nitrsoylation

The importance and complexity of S-nitrosylation in cellular signaling has been highlighted in the immune response to various stimuli including cancer and inflammation as the activity of iNOS and abundance of NO plays a key role in determining macrophage phenotype and function outside of NO's effects as a RNS. As previously described, in S-nitrosylation a molecule of NO is transferred to a thiol containing protein, altering its function or stability. Such proteins that a relevant to macrophage phenotype include HIF-1α, Keap-1, Surfactant Protein D (SP-D), GAPDH, and NF-κB (106). The

pools of targets for S-nitrosylation are dependent on a variety of factors including cellular redox status, the type of SNO donor, target availability and stability of the nitrosothiol bond as dictated by the local microenvironment (107, 108). Since NO and S-nitrosylation levels are easily manipulated through inhibition of iNOS, administration of SNO donors or inhibition of SNO degradation, the effects of signaling on macrophage function can be assessed during the pathogenesis of lung injury models.

1.7 MURINE MODELS OF PULMONARY INFLAMMATION

Mouse models have been instrumental in understanding immune signaling, and macrophage phenotype. There currently exists a multitude of models to study inflammatory signaling. In this work we attempt to better understand the diverse immunosignaling mechanisms as well as the effects of S-nitrosylation in acute lung injury, resolution and repair and chronic inflammatory signaling as illustrated below.

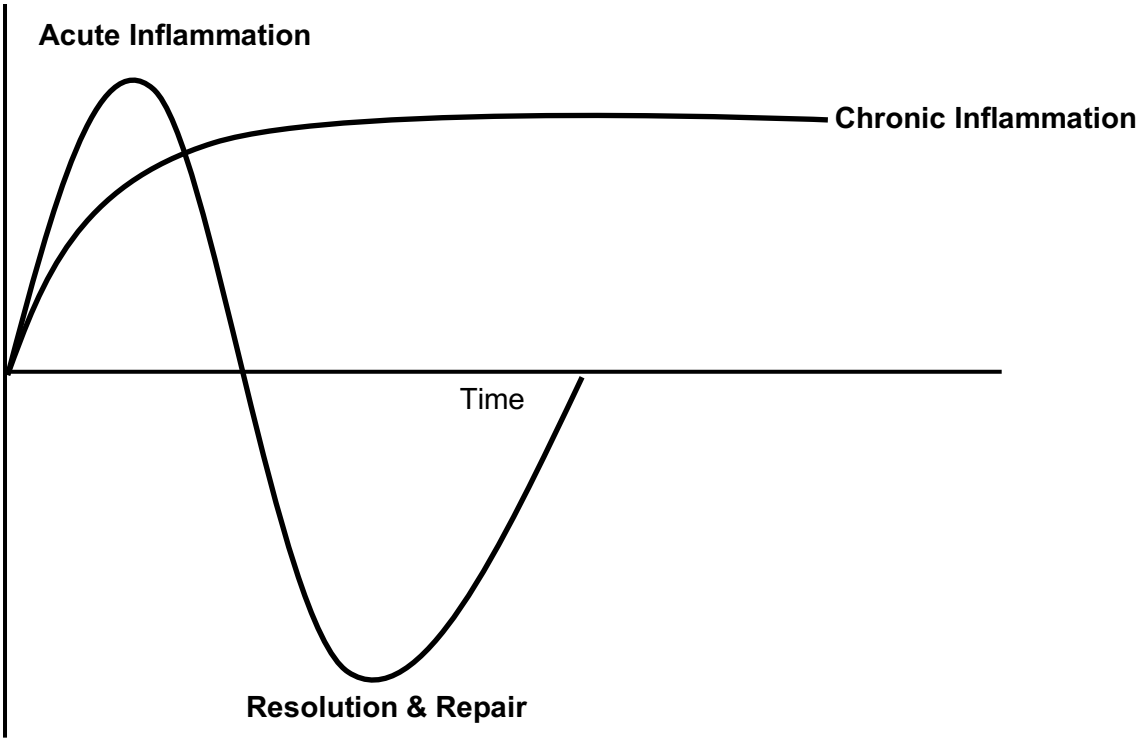

1.7.1 Acute Inflammation: Ozone (O_3) Induced Acute Lung Injury

O_3 is formed through the reaction of higher order nitrogen species and volatile organic chemicals generated from vehicle and factory emission (109). Acute O_3 exposure has been found to negatively affect respiratory function, especially in susceptible populations such as children, asthmatics, and those that work outdoors in urban areas. Effects include difficulty breathing/wheezing, and coughing. O_3 causes oxidative stress induced cellular damage in pulmonary epithelial cells (110). This leads to an immune response including neutrophilia and subsequent macrophage activation, possibly further adding to tissue damage (111). However, with O_3 exposure, an inflammatory response is not correlated with changes in lung function (112). There are various models of O_3 that include both high and low doses as well as acute and chronic exposures (113-115). Following acute exposure to ozone an inflammatory response is observed 24-72 hrs following exposure (33). There is an increase in cellular recruitment as total BAL cell counts and increased numbers of neutrophils and macrophages are observed. Pro-inflammatory macrophages are observed 24-48 hours post-exposure, and pro-reparative macrophages are observed 48-72 hours. Loss of pro-inflammatory macrophages through decreased recruitment, or loss of iNOS reduces measures of lung injury including BAL protein concentrations, and reduced measures of oxidative stress, highlighting the contribution of the pro-inflammatory macrophage to O_3 induced injury (116, 117).

1.7.2 Resolution and Repair: Acute Lung Injury and Fibrosis: Intratracheal Instillation of Bleomycin

Bleomycin is an effective antitumor agent used to treat variety of solid tumors (118). Its mechanism of action of this therapeutic includes the degradation of both DNA and RNA, and possibly inhibition of thymidine incorporation (119, 120). Administration of bleomycin has been associated with interstitial pneumonitis, and/or pulmonary fibrosis, creating a dose-limiting effect (121). Bleomycin has been utilized model of pulmonary fibrosis *in vivo.* In mice there are two predominant models of bleomycin-induced lung injury and fibrosis: systemic and intratracheal administration. In the former, bleomycin is administered via Alzet osmotic pump (122). This means of administration has also been used to model systemic sclerosis (123).

The intratracheal instillation model consists of a single dose of the chemotherapeutic bleomycin (ITB) which leads to the development of fibrosis ~21 days later. This fibrotic phase is preceded by an acute inflammatory response seen at day 3, the peak of inflammation is observed at day 8 and resolution of the inflammation is seen at day 15 (124). In this model, as inflammatory signaling progresses and recruitment continues, there is a phenotypical switch observed in macrophages (125). While cellular recruitment remains active throughout, during the “inflammatory” portion of the model, macrophages are in a pro-inflammatory activation state. This pro-inflammatory phenotype contributes to the observed histological damage to alveoli during this first phase. Loss of iNOS in ITB leads to reduced lung damage as assessed by pathological scoring; however, late phase fibrosis is worsened revealing the necessity of iNOS derived NO in the resolution of the inflammatory response (126). While these phases are more distinct, and occur over a longer period in ITB as compared to O_3, both models are oxidative stress dependent and recapitulate the three phases in the initiation and termination of an acute

inflammatory response with pro-inflammatory responses being followed by a period of resolution that precedes reparative signaling.

1.7.3 Chronic Inflammation: *Lewis Lung Carcinoma (LLC)*

Use of the Lewis Lung Carcinoma (LLC or 3LL) model allows for study of the effect of chronic, and dynamic inflammation on macrophages, and how they contribute to the microenvironment as well. The LLC model is especially useful as it is a syngeneic model and allows us to understand how these macrophages affect the adaptive immune system as well (127). These cells were discovered by Dr. Margaret Lewis from a spontaneous carcinoma in a C57bl/6 mouse (128). The development of this model allowed for the study of lung carcinomas, metastasis, and chemotherapeutics in a fully immunocompetent model. While this model has primarily been used to study therapeutic efficacy and metastasis, this syngeneic model is being used more to understand the tumor immune microenvironment (129-131). A growing body of work has implicated M2-like, tumor-promoting, immunosuppressive macrophages in the LLC model of non-small cell lung cancer (132-135).

1.8 OVERALL RESEARCH HYPOTHESIS

The importance of iNOS and iNOS derived NO as an effector molecule in inflammation and in macrophage function is well established. More recently, the role of in signal transduction through SNO formation has received considerable attention. The overall goal of these studies is to elucidate the contribution of NO's thiol-based effects on macrophage activation and overall immunosignaling. As key inflammatory signaling molecules such as NFκ-B, SP-D, HIF-1α, and Keap1 are dysregulated by SNO formation, we speculated that increased SNO formation would alter macrophage

activation. More specifically, it is our hypothesis that increased S-nitrosylation causes changes in macrophage phenotype during pulmonary inflammatory responses, leading to improved resolution of inflammation, and an overall change in inflammatory signaling. To test this hypothesis, the contribution of SNO dependent changes in macrophage activation and inflammatory signaling were assessed in models of acute lung injury, pulmonary fibrosis, and the development of cancer.

CHAPTER 2: THE EFFECTS OF SNO DONORS ON OZONE INDUCED ACUTE LUNG INJURY

2.1 Abstract

Acute exposure to Ozone (O_3) has been found to adversely affect lung function and induce an inflammatory response in humans. The mechanism by which O_3 exerts its pathologic effects involve oxidative stress and pro-inflammatory macrophage activation. Increased levels of iNOS and NO have been observed 24-48 hr following exposure (ref). Moreover, loss of iNOS is associated with reduced ozone toxicity (xxx). In these studies we sought to understand and the role of iNOS derived NO in inflammatory signaling following O3, focusing on NO's interaction with thiols. Thiol modification by NO leads to formation S-nitrosothiols (SNOs), conferring altered protein function and activity through a variety of biochemical mechanisms. Several key players in the general inflammatory signaling process, as well as those that are key regulators of macrophage activation are regulated in part by SNO formation. However, SNO formation is highly regulated by a number of mechanisms including thiol accessibility and biochemical permissibility. In these studies, we administered three distinct SNO donors to determine how SNO donation would affect O_3 induced lung injury, and to determine which thiol subsets play a dominant role in macrophage phenotype following O_3. All three SNO donors reduced O_3 induced lung injury; however, the general SNO donor ethyl nitrite (ENO) and intracellular SNO donor SNO-propanamide (SNOPPM) were the most effective at reducing pro-inflammatory macrophage activation following exposure to O_3.

2.1 Introduction

Ozone (O_3), a common pollutant and a component of smog, is a known toxicant as it has been found to adversely affect lung function and induce inflammation in healthy adults(136, 137). These effects become of special concern to susceptible populations including those residing in areas where ozone levels are not compliant with the current Clean Air Act, children, the elderly, and those with preexisting lung disease(136, 138, 139). For example, O_3 has been found to exacerbate inflammation in asthmatics(140). Exposure to O_3 leads to oxidative stress in pulmonary epithelial cells and the lipid components of lung lining fluid, inducing an inflammatory response that is characterized by neutrophilia and macrophage activation(141-145). Pulmonary macrophages adopt a pro-inflammatory phenotype 24-48hrs following acute ozone exposure, while reparative/anti-inflammatory macrophages are seen 48-72hrs following exposure(145). During the early phase macrophages recovered from the lung express high levels of inducible nitric oxide synthase (iNOS). In macrophages, iNOS expression is associated with pro-inflammatory activation, producing increased levels of nitric oxide (NO). iNOS derived nitric oxide (NO) not only serves as a source of reactive nitrogen species (RNS), capable of reacting not only with O_3 and resulting ROS's, but also with products of O_3 induced oxidation, increasing oxidative stress by forming products such as peroxynitrite and higher nitrogen oxides capable of tyrosine nitration(144, 146-148). Despite these potential harmful reactions, iNOS derived NO is critical to the inflammatory process as loss of iNOS dysregulates proper resolution of inflammatory

signaling(126). This may be due in part to NO's capability to react with targets beyond ROS(149).

NO is capable of reacting with thiols in both low molecular weight peptides, such as glutathione (GSH), and proteins to form S-nitrosothiols (SNOs). As post translational modification, SNO formation has been found to regulate the function of a wide range of proteins (150). Like other forms of post-translational modification, SNO formation is remarkably specific, and reversible. However, unlike other forms, SNO formation is largely dictated by physiological chemistry. Investigation into the mechanism of SNO formation has revealed specific motifs in SNO formation creating unique thiol subset (151, 152). The hydrophobicity, surface accessibility, pKA, and location of the thiol (including surrounding amino acids of the cysteine) as well as the type SNO donor all dictate SNO formation(107, 152, 153). Stated simply, the physicochemical properties of individual thiol moieties will determine their propensity to be modified by different SNO donor compounds.

Importantly, SNO formation serves as another point of regulation of inflammatory signaling as S-nitrosylation can increase or decrease activity proteins, and transcription factors in signal cascades that control the expression of inflammatory signals(154). For example, S-nitrosylation of the p65 and p50 subunits of NF-κB reduces translocational and DNA binding capability, thus decreasing gene transcription(3). Additional regulatory activity can be found in several inflammatory signaling pathways as STAT-3, HIF-1α, SP-D (Surfactant

Protein D), and GADPH all contain thiols that are capable of being S-nitrosylated, conferring altered activity (106).

As O_3's mechanism of action includes epithelial cell and macrophage inflammatory signaling, and inflammatory targets of S-nitrosylation are found in both cell types, often opposing pro-inflammatory activation,

we questioned how increased SNO levels would affect inflammatory signaling following O_3 exposure. To this end we investigated the effects of SNO donors following exposure to O_3.

In the present study, we administer three chemically distinct SNO donors that would target different SNO subsets and observed their effects on O_3 induced injury and inflammation. We found that administration of SNO donors led to a reduction in measures of injury and inflammation. Additionally, SNO donor administration led to a reduction in markers associated with pro-inflammatory macrophage activation. These studies demonstrate the influence of S-nitrosylation on inflammatory signaling and show that altering the levels of S-nitrosylation may be a point of intervention in diseases where pro-inflammatory macrophages contribute to etiology.

2.3 Methods

SNO Compounds

Mice received SNO donors intranasally in 50μL of vehicle.

0.0125% Ethyl Nitrite (Millipore Sigma 309923) was degassed and dissolved in 50% ethanol.

25mM SNO-Propanamide was prepared from N-mehyl-3-sulfanylpropanamide (Enamine EN300-127389), sodium nitrate (Millipore Sigma S5506250G), and 0.5M Hydrochloric acid in sterile 1X PBS.

25mM S-nitrosyl N-acetylcysteine was prepared from N-acetylcysteine (Millipore Sigma A7250) and sodium nitrate in sterile 1X PBS.

Animals

Female C57Bl/6/J mice (7 week old) were obtained from the Jackson Laboratories (Bar Harbor, Maine). Mice were exposed to air or 0.8 ppm of ozone for 3 hrs in whole body Plexiglas chambers. Ozone was generated by UV ozone generator (Gilmont Instruments, Barrington, Illinois) and mixed with air. Ozone concentrations were measured inside the chamber by photometric ozone analyzer (Teledyne Instruments, Thousand Oaks, California). One hour following exposure, mice were administered ENO, SNAC, or SNO-PPM. Mice were sacrificed 48 hrs later. All animal procedures were approved by the Rutgers University Institutional Animal Care and Use Committee and done in accordance to the National Institute of Health's Guide for the Care and Use of Laboratory Animals.

Histology

Left lungs were inflation fixed with 3% paraformaldehyde, stored overnight at 4°C, and then transferred into 70% ethanol. Paraffin embedded tissue were cut into 5 μm sections, and deparaffinized in xylenes, and rehydrated by decreased

alcohol concentrations (100%-50%) then washed in deionized water. Following citrate antigen retrieval (10.2 mM sodium citrate, pH 6.0), endogenous peroxidase activity was quenched in 10% H_2O_2 in methanol. Tissue sections were then blocked with 10% normal goat serum for all antibodies with the exception of cytochrome b5 (25%). Tissues were incubated overnight at 4°C with IgG controls or the following primary antibodies: iNOS (Ab15323), IL-1β (Ab9722), Cytochrome b5 (Cyb5) (Ab69801), Ym1 (Stem Cell Technologies 1404), HO-1 (Enzo Life Sciences ADI-SPA-896). Sections were subsequently incubated with 1:2000 or 1:5000 dilutions of biotinylated secondary antibody (Vector Labs, BA-1000). Slides were developed using DAB peroxidase kit (Vector Labs, SK-4100).

Inflammatory Scoring

H&E stained lung sections were scored on a 5 point scale (0-4) and scoring criteria that included normal alveolar structure, the presence of inflammatory cells, septal thickening and, normal bronchial structure. Scores were determined by a blinded independent observer.

Bronchoalveolar Lavage

Following perfusion with heparinized PBS, bronchoalveolar lavage fluid and cells were collected. A 20G cannula was inserted into the trachea. Using a 1mL syringe, PBS was slowly instilled and withdrawn from the lung a total of 5 times through a 20G cannula that was inserted in the trachea.

The fluid was then centrifuged at 300g x 10 min at 4ºC. The resulting supernatant was collected and stored. Cells were resuspended in PBS and counted using a Beckman Coulter Cell Counter and then processed for flow cytometry (see below).

BAL fluid protein content was determined by Pierce BCA Protein Assay Kit (Thermo Fisher Scientific 23225). BAL IgM levels were determined by ELISA (Bethyl Laboratories, E99-101).

Lung Digestion and Magnetic Associated Cell Selection

Right lung lobes were enzymatically digested in 5 mL of 2 mg/mL collagenase IV (Miilipore Sigma C5138) in RPMI 1640 Medium (Thermo Fisher 11875119) with 5 % heat inactivated FBS (S11550) and 37°C for 30 min with shaking. A single cell suspension was then generated using a 70 µm strainer. Following RBC lysis for 5 min at RT (Millipore Sigma R775), F4/80-PE conjugated cells were then positively selected as per Stem Cell Easy Eight Mouse PE Positive Selection kit protocol. Cells were then stained for flow cytometric analysis.

Flow Cytometric Analysis

BAL and tissue associated cells were Fc blocked for 10min 4°C or 5min RT respectively. Cells were then incubated with the following antibodies (1:100) and respective conjugates for 30min at 4°C. As tissue associated macrophages were selected based on F4/80 positivity, these cells were stained with all antibodies F4/80-PE (Stem Cell 60027PE clone BM8).

Cd11c- Af700 (Biolegend 117320, clone N48)

Cd11b- FITC (Biolegend 101206, clone M1/70)

Ly6G- Alexa Fluor 647 (Biolegend 127610, clone 1A8)

Ly6C- PerCp5.5 (Biolegend 128012, clone HK1.4)

Viability 780 (Thermo Fisher 65-0865-14, eBiosciences Fixable Viability)

Gating Strategy

Following the exclusion of doublets, in the BAL viable cells were selected based on expression of F4/80 and CD11c. Cells double positive for F4/80 and CD11c were then analyzed for expression of CD11b, followed by the exclusion of Ly6G followed by the expression of Ly6C. In magnetically selected F4/80 positive cells, following the exclusion of doublets, viable cells were analyzed based on expression of CD11b followed by the exclusion of Ly6G. Cells were then analyzed for expression of CD11c and Ly6C.

Statistical Analysis

Data were analyzed using Graphpad Prism software. Parametric data was analyzed by two-way ANOVA and Tukey's post-hoc tests. Median histological scores were analyzed by Kruskal-Wallis Test. All p values ≤ 0.05. For each treatment group, $n \geq 4$.

2.4 Results

Administration of ENO Reduces Ozone Induced Lung Injury

Initially, we determined whether administration of ENO, the general SNO donor, reduced ozone-induced pulmonary injury. We first measured total proteins in the BAL; consistent with previous findings (33), ozone exposure was found to result in increases in BAL protein. Administration of ENO significantly reduced total protein levels in BAL. Ozone also caused an increase in concentrations of IgM in BAL, a response also reduced following ENO administration. (Table 2.1).

Table 2.1

	[Protein] (ug/mL)	**[IgM] (ng/mL)**	**Cell Count (*10^4 cells/mL)**
Air	120.3 ± 17.8	8.4 ± 3.1	13.5 ± 1.3
Air + ENO	156.7 ± 24.3	9.1 ± 3.8	24.1 ± 6.1
Air + SNAC	185.7 ± 12.3	57.9 ± 18.0	15.3 ± 2.1
Air + SNOPPM	**90.4 ± 16.0**	17.2 ± 5.2	18.5 ± 0.6
O_3	**245.6 ± 31.2**	130.0 ± 38.0	17.2 ± 2.1
O_3 + ENO	**179.4 ± 32.9 ***	69.0 ± 5.0	21.61 ± 6.3
O_3 + SNAC	**193.5 ± 12.3**	29.6 ± 19	**26.1 ± 1.0**
O_3 + SNOPPM	**98.2 ± 16.0 ***	13.2 ± 12	21.88 ± 2.7

Table 2.1 BAL Measures of Lung Injury and Recruitment. Lungs were lavaged with sterile PBS and fluid separated from cellular components. O_3 led to increases in total protein, IgM and cell counts. SNO compounds decreased O_3 induced increases in protein and IgM,

and increased cell counts. $p \leq 0.05$ 2-way ANOVA, Tukey's post-hoc test. **Bold**- significant to Air *- significant to O_3 , # - significant to O_3 + ENO.

Treatment of mice with ozone led to an increased inflammatory response and tissue damage, as assessed in histologic sections. Based on scoring criteria the lungs of ozone treated mice had a median score of 2 compared to that of 0 in air controls. The pulmonary response to ozone was characterized by damage to the alveolar tissue, the presence of macrophages in the alveolar space. Additionally, there was immune cell recruitment near the respiratory bronchioles. ENO reduced tissue damage and inflammation surrounding the bronchioles (Figure 2.1).

Figure 2.1

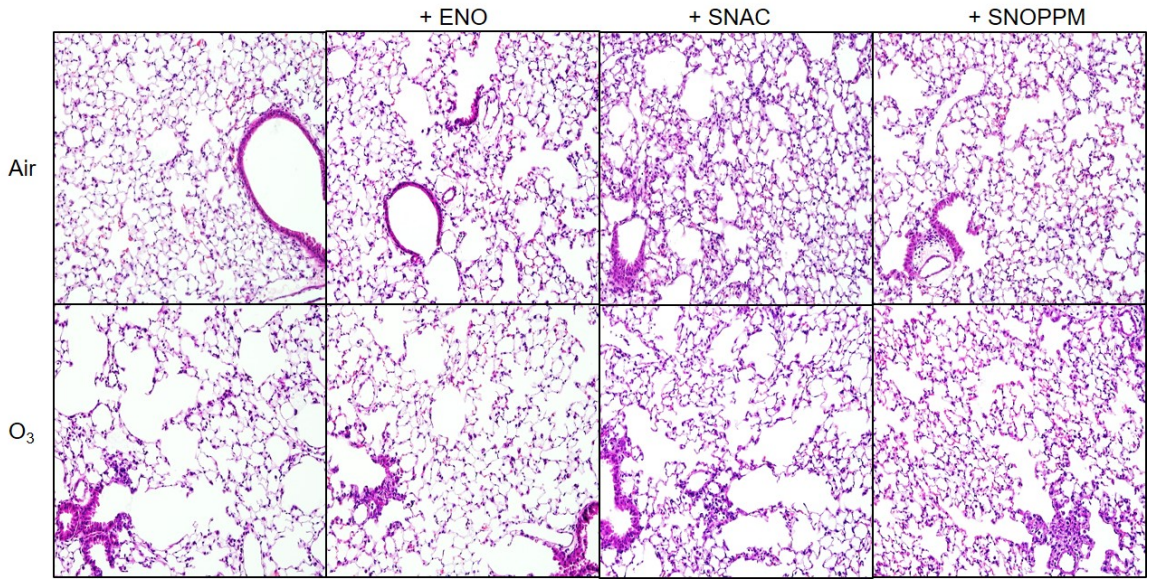

Figure 2.1 O_3 Induced Tissue Damage. Left lungs were inflation fixed and paraffin-embedded. H&E staining reveals characteristic peribronchial and perivascular inflammation and damage to lung parenchyma which is reduced by administration of SNO compounds, with SNAC being the least effective.

We next examined expression of biochemical markers of oxidative stress and injury. We found that ozone increased expression of the oxidative stress marker, Cyb5 (Figure 2.2) in the airway epithelium and alveolar epithelium. Administration of ENO reduced alveolar epithelial staining; conversely Cyb5 staining of macrophages increased. Re-epithelialization is part of the response to lung injury (155); this can be assessed by PCNA staining. We observed that PCNA staining of epithelial cells was increased after ozone primarily in the airways, but also in type II cells (Figure 2.3). ENO reduced the number of PCNA positive cells in the lung.

Figure 2.2

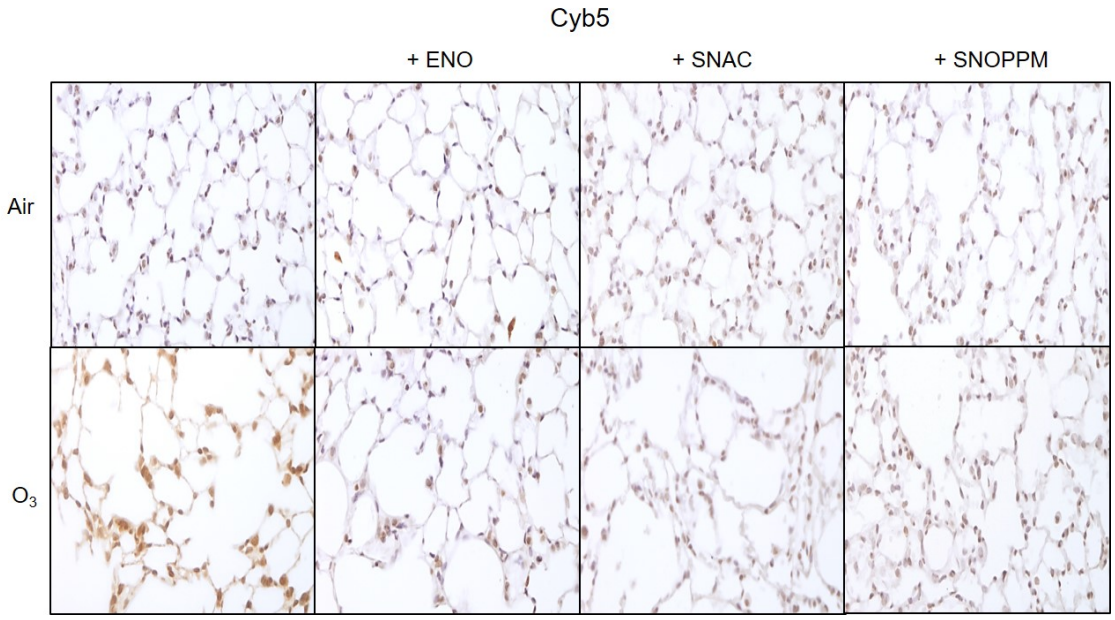

Figure 2.2. Cyb5 Immunohistochemical Staining. Left lungs were inflation fixed and paraffin-embedded. IHC staining reveals increased Cyb5 staining following O_3 reduced by SNO compounds.

Figure 2.3

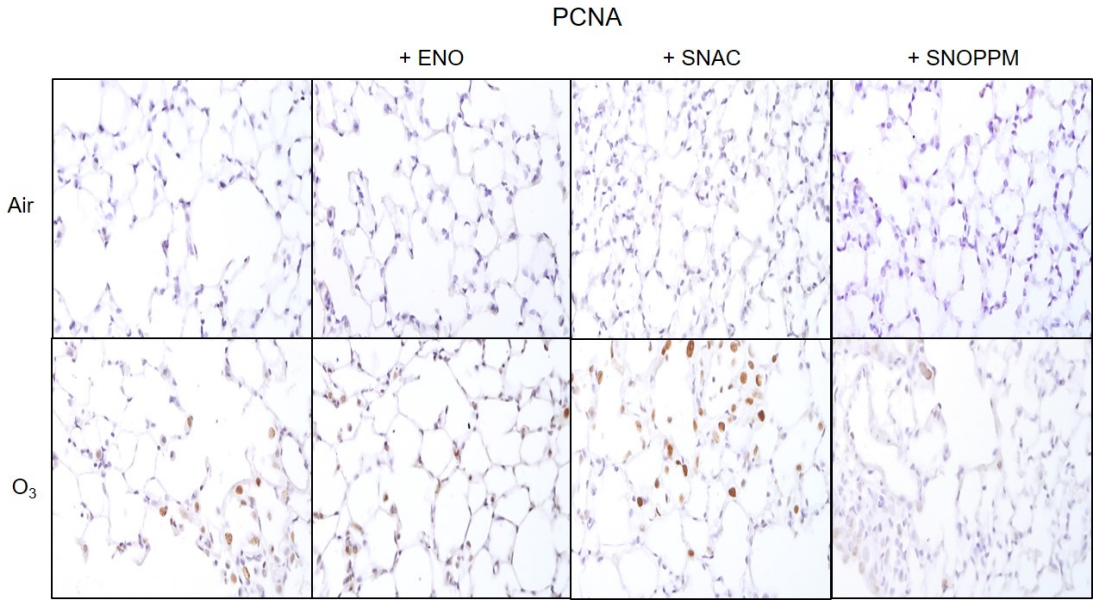

Figure 2.3 PCNA Immunohistochemical Staining. Left lungs were inflation fixed and paraffin-embedded. IHC staining reveals increased PCNA staining following O_3 reduced by SNO compounds with the exception of SNAC.

Effects of ENO on Ozone-induced Alterations in the Phenotype of Lung Macrophages

As the inflammatory response plays a key role in the response to ozone, we sought to understand if this was altered by ENO administration. We found that both ozone exposure was associated with increased numbers of inflammatory cells recovered in BAL; this was not altered by ENO (Table 2.2). The total BAL cell population was analyzed by flow cytometry, using a pre-defined gating strategy. Pulmonary macrophages were defined within the population of viable cells as cells expressing F4/80 but not Ly6G, which is expressed by granulocytes. F4/80+Ly6G- cells were almost exclusively mature, resident tissue macrophages (Cd11c+Cd11b-) (Fig. 2.4). Treatment of mice with ozone led to an increase in the percentage of cells expressing Cd11b, a marker of migratory cells. Cd11c+Cd11b+ macrophages (11.3 ± 1.3% versus

2.7 ± 0.19% in air treated mice). Interestingly, in mice treated with ENO a novel population of macrophages was identified that are Cd11c-Cd11b+. This population was 16.5 ± 8.4% of pulmonary macrophages in air exposed controls but reduced to 10.7 ± 3.8% of F4/80+ cells after ozone exposure. We next analyzed the activation state of the macrophages by assessing Ly6C expression. While there is no current function associated with this protein, expression of Ly6C is associated with activated proinflammatory monocytes and macrophages. In all 4 treatment groups (air, ozone, air + ENO and ozone + ENO), Cd11c+Cd11b- pulmonary macrophages remained Ly6C-, indicating a lack of activation (Table 2.2). Conversely a subset of Cd11c+Cd11cb+ macrophages were positive for Ly6C. Ly6C+ macrophages from ozone exposed mice were 27.9 ± 3.1% of Cd11c+Cd11b+ cells. This population was reduced to 6.8 ± 2.1% following ENO treatment.

Table 2.2

	Alveolar Macrophages	**Mature Recruited Macrophages**	**Immature Recruited Macrophages**
Air	0.2 ± 0.02	49.5 ± 1.6	13.75 ± 3.6
Air + ENO	0.4 ± 0.1	24.7 ± 6.0	24.2 ± 14.7
Air + SNAC	0.1 ± 0.03	4.6 ± 1.1	9.75 ± 3.8
Air + SNOPPM	0.1 ± 0.02	2.0 ± 0.9	13.63 ± 3.0
O_3	0.2 ± 0.09	27.9 ± 3.1	9.14 ± 3.0
O_3 + ENO	0.7 ± 0.07	25.0 ± 3.6	7.6 ± 2.8
O_3 + SNAC	0.1 ± 0.02	9.9 ± 4.3$^{*\#}$	7.63 ± 1.9

O_3 + SNOPPM	0.5 ± 0.1	6.4 ± 1.9$^{*\#}$	8.13 ± 2.8

Table 2.2 Percentage of BAL Macrophages Expressing Ly6C. Ly6C expression was measured of each macrophage population found in lung lavage. SNO donors reduced O_3 induced increases in Ly6C expression. Percentages are expressed as % of indicated population. p ≤ 0.05 2-way ANOVA, Tukey's post-hoc test. **Bold**- significant to Air *- significant to O_3 # - significant to O_3 + ENO

Figure 2.4

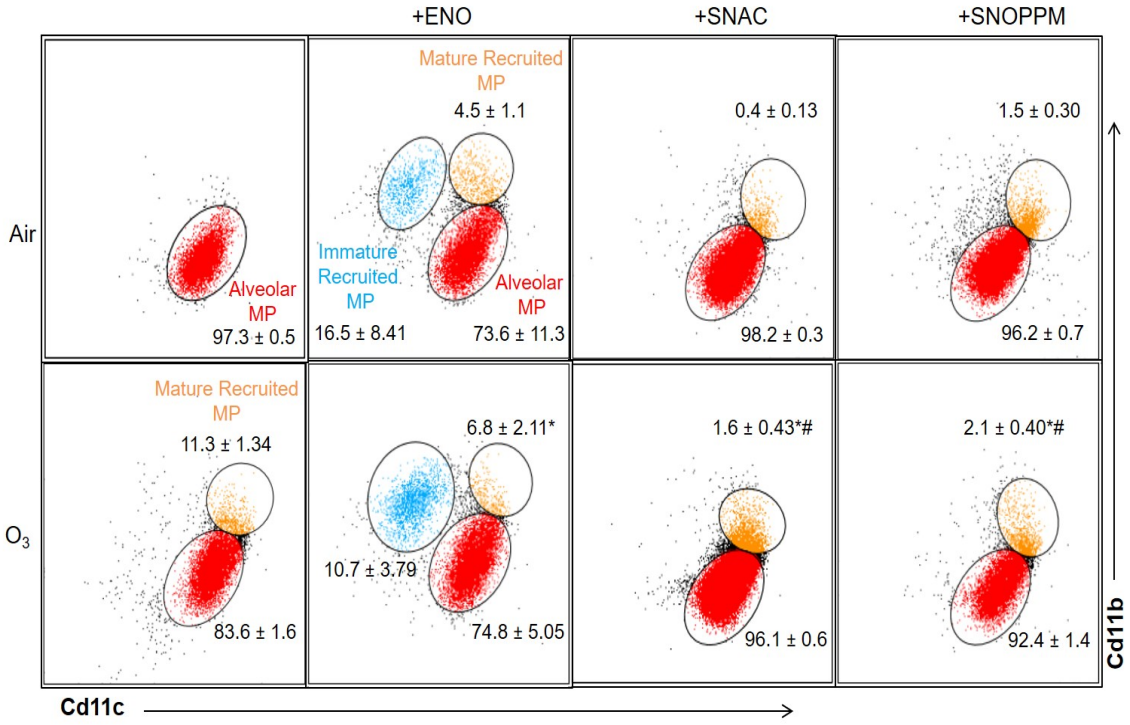

Figure 2.4 Viable, F4/80+ BAL Cell Expression of Cd11c vs Cd11b. Flow cytometric analysis of cell recovered from lung lavage shows distinct populations of macrophages recovered from the alveolar space. Exposure to O_3 and SNO donors led to recruitment of novel populations to the BAL. Percentages are expressed as % of F4/80+ cells. MP = Macrophage. p ≤ 0.05 2-way ANOVA, Tukey's post-hoc test. **Bold**- significant to Air *- significant to O_3 # - significant to O_3 + ENO

Table 2.3

	%F4/80-Cd11b+	%Ly6G-Ly6C+	% Ly6G+Ly6C-	% Ly6G+Ly6C+
Air	1.4 ± 0.5	0 ± 0	0 ± 0	0 ± 0
Air + ENO	**51.5 ± 6.8$^{\#}$**	0.3 ± 0.1$^{\#}$	**26.2 ± 11.3**	0 ± 0$^{\#}$
Air + SNAC	0 ± 0	0 ± 0	0 ± 0	0 ± 0
Air + SNOPPM	0 ± 0	0 ± 0	0 ± 0	0 ± 0
O_3	**7.1 ± 1.3**	0 ± 0	**20.88 ± 1.8**	0 ± 0
O_3 + ENO	**24.31 ± 8.0 ***	**4.4 ± 1.4***	**24.81 ± 9.2**	**6.0 ± 5.7***
O_3 + SNAC	**14.1 ± 2.4**	0.1 ± 0.1$^{\#}$	**55.6 ± 2.6**	**25.8 ± 1.7$^{\#*}$**
O_3 + SNOPPM	**5.2 ± 1.1***	2.0 ± 1.6	**38.9 ± 4.9**	**27.5 ± 3.9$^{\#*}$**

Table 2.3 Markers of Activation in F4/80 Negative Cells in the BAL. Expression of Ly6G and Ly6C in F4/80-Cd11c-Cd11b+ cells reveal O_3 and SNO dependent recruitment of immature macrophages and PMNs. F4/80-Cd11b+ percentage expressed as % of F4/80- cells. Activation markers expressed as percentage as F4/80-Cd11b+ cells. $p \leq 0.05$ 2-way ANOVA, Tukey's post-hoc test. **Bold**- significant to Air *- significant to O_3 # - significant to O_3 + ENO

Effects of Ozone on Cellular Recruitment

We analyzed cell phenotype within the F4/80- population. In O_3 treated mice, 9.3 ± 1.8% of F4/80- cells were Cd11b+ (Table 2.3). Within this Cd11b+ population, exposure to O_3 led to increased neutrophils characterized by expression of Ly6G and side scatter fluorescence. Neutrophils comprised 20.8% ± 1.8% of F4/80-Cd11b+ cells in O_3 exposed mice. Treatment with ENO also resulted in an increase in the Cd11b+

population to 15.5 ± 6.3% and 29.9 ± 6.4% in air and O_3 exposed mice, respectively. Of the F4/80-Cd11b+ population, neutrophils were 26.2 ± 11.3% in air control mice treated with ENO and 24.39 ± 9.2% in O_3 exposed mice, demonstrating that ENO exposure led to neutrophil infiltration independently of each O_3. We also analyzed expression of Ly6C in these cells, as cells that are F4/80-Cd11b+Ly6C+ are pro-inflammatory, recently recruited macrophages. Interestingly, this population was only present in ENO treated mice.

Table 2.4

	Tissue Resident Macrophages	**Recruited Macrophages**	**Interstitial Macrophages**
Air	8.1 ± 1.6	21.9 ± 3.6	8.7 ± 2.1
Air + ENO	19.8 ± 2.1	21.4 ± 5.9	18.7 ± 4.9
Air + SNAC	19.0 ± 3.4	37.0 ± 4.9	30.3 ± 6.3
Air + SNOPPM	12.6 ± 1.8	34.9 ± 1.4	9.1 ± 0.6
O_3	18.7 ± 2.4	25.4 ± 3.5	25.6 ± 7.4
O_3 + ENO	15.5 ± 2.6	16.2 ± 3.3	14.5 ± 1.9*
O_3 + SNAC	17.3 ± 2.1	44.6 ± 1.9$^{\#}$	24.0 ± 3.1
O_3 + SNOPPM	14.3 ± 1.0	47.8 ± 1.5$^{\#}$	15.5 ± 1.2*

Table 2.4 Percentage of Tissue Macrophages Expressing Ly6C. Ly6C expression was measured of each macrophage population found in lung tissue. SNO donors reduced O_3 induced increases in Ly6C expression. Percentages are expressed as % of indicated population. $p \leq 0.05$ 2-way ANOVA, Tukey's post-hoc test. **Bold**- significant to Air *- significant to O_3 # - significant to O_3 + ENO

Effects of ENO on Ozone-induced Alterations of the Phenotype of Tissue Associated Macrophages in the Lung

In order to examine changes in the tissue associated macrophages in response to zone and ENO we used a tissue digest approach. In control mice 67.3 ± 3.6% of viable F4/80+ cells were Cd11c+Cd11b-, while 17.0 % ± 4.3 were Cd11c+Cd11b+ (Figure 2.5). The interstitial macrophages (Cd11c-Cd11b+) compromised 9.7 ± 1.4% of tissue associated macrophages. Ozone increased the recruited Cd11c+Cd11b+ population to 24.7 ± 5.8% of the tissue population. Administration of ENO resulted in a small population change with Cd11c+Cd11b- cells contributing 55.9 ± 4.1% compared to 67% in controls, the recruited cells comprised 31.2 ± 4.7% of F4/80+ tissue associated macrophages, while interstitial macrophages were unchanged. Treatment of ozone exposed mice with ENO resulted in 61.1 ± 51% of tissue associated macrophages as Cd11c+Cd11b-, 16.5 ± 2.6% were Cd11c+Cd11b+, while 16.2 ± 3.3% were Cd11c-Cd11b+. When we evaluated pro-inflammatory activity, 8.1 ± 1.6% of tissue resident macrophages were Ly6C+ (Table 2.4). Ly6C+ recruited macrophages contributed 21.9 ± 3.6% of Cd11c+Cd11b+ macrophages while Ly6C+ interstitial macrophages were 8.7 ± 2.1%. Acutely activated Ly6C+ cells comprised 18.7 ± 2.4%, 25.4 ± 3.5%, and 25.6 ± 7.4% in ozone treated mice in resident, recruited, and interstitial populations respectively while mice administration of ENO following O_3, Ly6C+ populations were reduced to 15.5 ± 2.6%, 16.2 ± 3.3%, and 14.5 ± 1.9%.

Figure 2.5

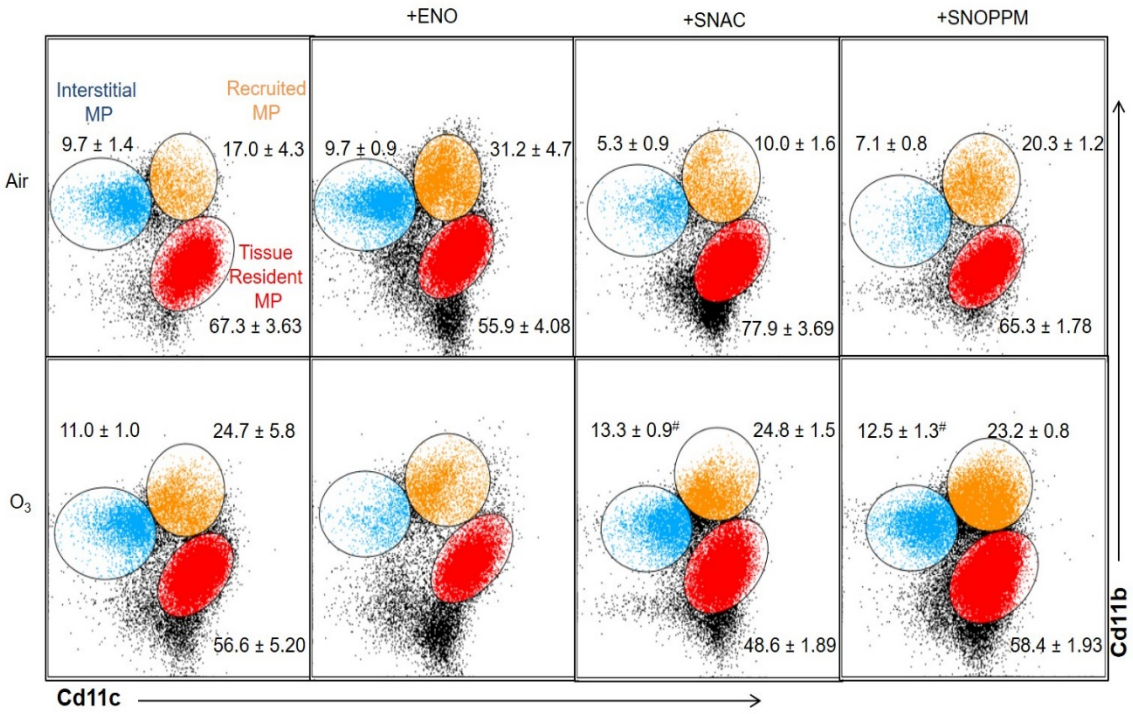

Figure 2.5 Viable, F4/80+ Tissue Expression of Cd11c vs Cd11b. Flow cytometric analysis of cell recovered from lung tissue following enzymatic digestion, and MACS selection, shows three distinct populations of macrophages. Exposure to O_3 and SNO donors led to alterations of tissue populations. Percentages are expressed as % of F4/80+ cells. $p \leq 0.05$ 2-way ANOVA, Tukey's post-hoc test. **Bold**- significant to Air *- significant to O_3 # - significant to O_3 + ENO

ENO Reduces Ozone-induced Markers of Pro-inflammatory Signaling and Activation. The reduced expression of Ly6C in F4/80+ macrophages observed in ENO treated mice prompted us to look at expression of the classic pro-inflammatory makers: iNOS and IL-1β. Following O_3 exposure, expression of iNOS and IL-1β was increased in both epithelial cells and macrophages (Figures 2.6 and 2.7). This was reduced in ENO treated mice.

Figure 2.6

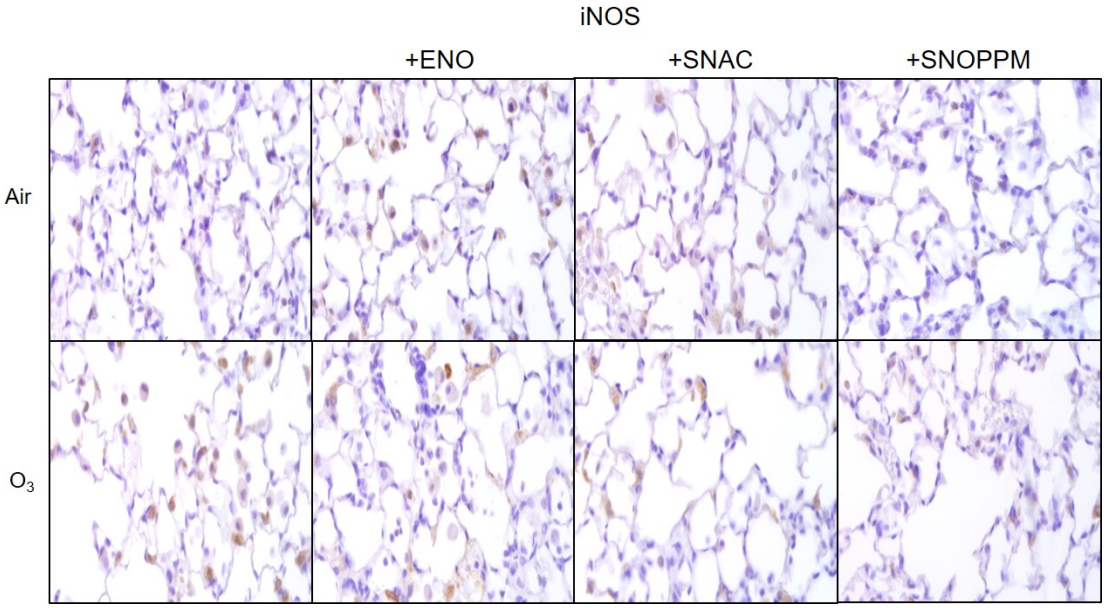

Figure 2.6 iNOS Immunohistochemical Staining. Left lungs were inflation fixed and paraffin-embedded. IHC staining reveals increased iNOS staining following O_3 which was reduced by SNO donor administration.

Figure 2.7

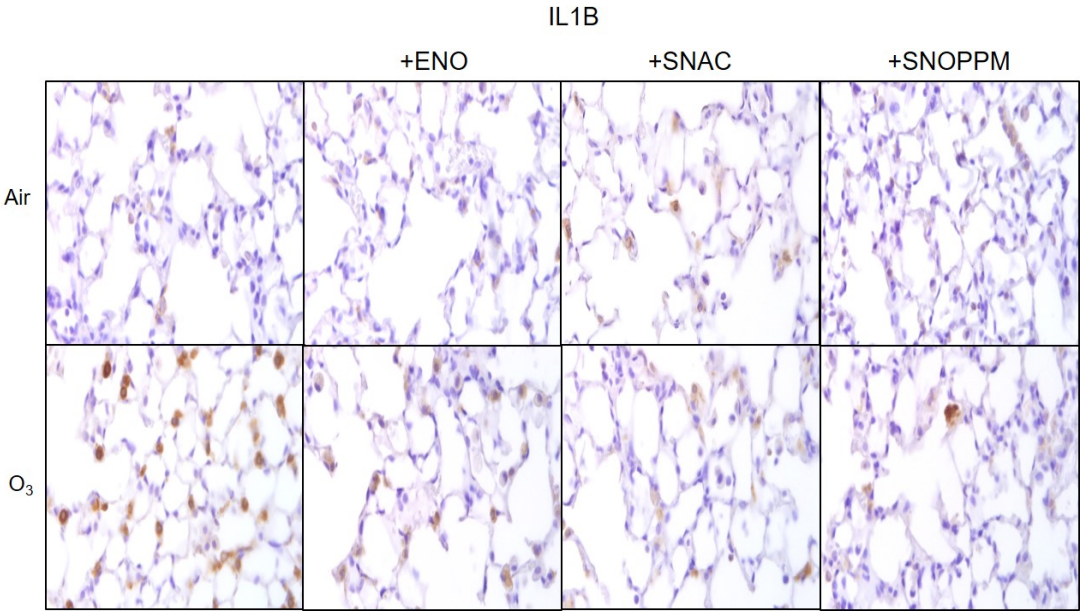

Figure 2.7 IL-1β Immunohistochemical Staining. Left lungs were inflation fixed and paraffin-embedded. IHC staining reveals increased IL-1β staining following O_3 which was reduced by SNO donor administration.

ENO Reduces Ozone-Induced Increases in Anti-Inflammatory Signaling and Activation

In response to ozone, expression of HO-1 was increased in both epithelial cells and pulmonary macrophages (Figure 2.8). ENO reduced this response in epithelial cells but not macrophages. Ym1 is a characteristic of pro-reparative macrophages. An increase in numbers of Ym1+ macrophages was observed in the lung following ozone exposure. This was reduced by administration of ENO, potentially indicative of a dampened reparative and anti-inflammatory response as a result of an ENO mediated reduction in ozone induced lung injury (Figure 2.9).

Figure 2.8

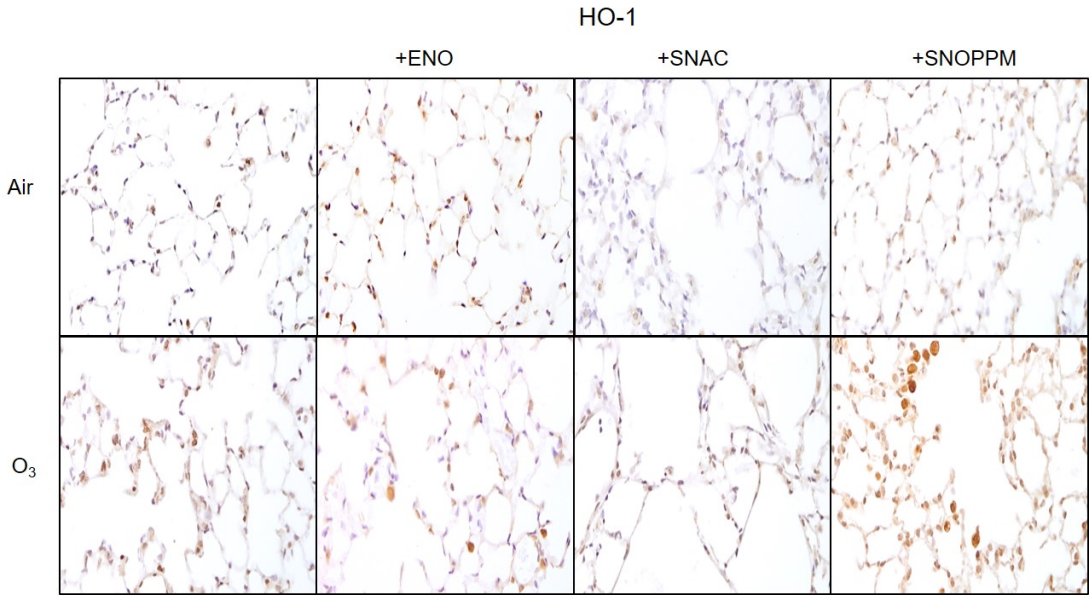

Figure 2.8 HO-1 Immunohistochemical Staining. Left lungs were inflation fixed and paraffin-embedded. IHC staining reveals increased HO-1 staining following O_3 and SNO donor administration.

Figure 2.9

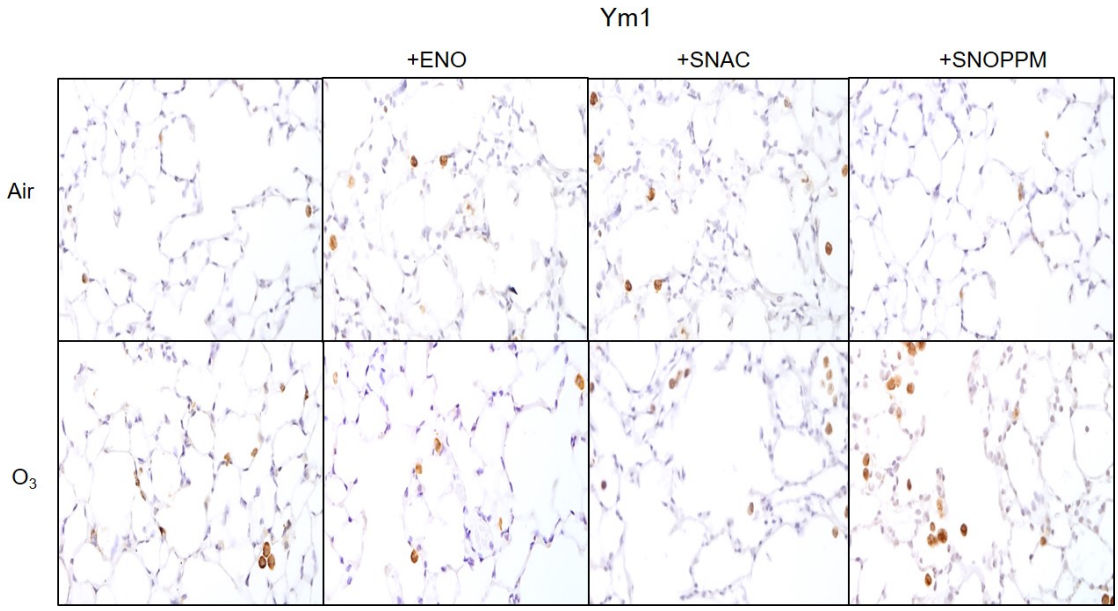

Figure 2.9 Ym1 Immunohistochemical Staining. Left lungs were inflation fixed and paraffin-embedded. IHC staining reveals altered expression of Ym1 staining following O_3 and SNO donor administration.

Targeting Unique Thiol Subsets Effectively Reduces Ozone Induced Inflammation.

In our next series of studies, we focused on better understanding of which S-nitrosylated thiol subsets were responsible for the observed effects of ENO. In these experiments we treated mice with SNO donors that target distinct thiol groups as opposed to the general donation by ENO. SNAC targets thiols that are easily accessible as they are found near the protein surface and have a low pKA. Thiols of this nature are found in proteins such as STAT-3, p50 subunit of NFκB, and chloride intracellular calcium 4 (153). Furthermore, as SNAC is rapidly hydrolyzed and thus is unlikely to enter the cell, we assumed that SNAC would not only target thiols that follow the acid-base motif, but also primarily extracellular targets. The second compound, SNO-PPM targets thiols that are hydrophobic, or surrounded by basic residues such as T complex protein 1, Keap1 and

HMGB1. Based on the biochemical properties of SNOPPM, SNO formation by SNOPPM will primarily be found within the intracellular region. Both SNAC and SNOPPM reduced BAL and tissue markers of injury and inflammation induced by ozone exposure. Mice treated with SNOPPM had the lowest concentrations of both protein and IgM in BAL (Table 2.1). Histologic scoring confirmed that SNOPPM was also more effective in reducing injury when compared to SNAC (Figure 2.1). SNOPPM also showed the greatest reduction in positive staining for markers of injury and cell proliferation, Cyb5 and PCNA (Figures 2.2 and 2.3).

SNOPPM is Most Effective in Reducing Ly6C Expression in Cd11c+Cd11b+ BAL Macrophages

In contrast to ENO, neither SNOPPM or SNAC caused the recruitment of Cd11c-interstitial macrophages into the lung. As compared to ozone treated mice, which showed Cd11c+Cd11b+ cells were 11.3% of cells, they comprised 1.6 ± 0.4% following treatment with SNAC and 2.1 ± 0.4% with SNOPPM (Figure 2.5). Both compounds were effective in reducing the Cd11c+Cd11b+Ly6C+ macrophages. When ozone exposed mice were treated with SNAC, Ly6C+ cells were 9.9 ± 4.3% of the Cd11c+Cd11b+ population, while SNOPPM reduced the population to 6.4 ± 1.9% (Table 2.2).

SNAC and SNOPPM Increase the Percentage of F4/80-Cd11b+Ly6C+Ly6G+ Macrophages in the Lung Following Ozone Exposure

In contrast to ENO, administration of SNAC and SNOPPM to air control mice had no effect on Ly6G+ neutrophils (Table 2.3). O_3 induced neutrophilia was reduced with administration of both compounds. Pro-inflammatory Ly6C macrophages were also decreased in both SNAC and SNOPPM treated mice that were exposed to O_3; however, a novel population of Ly6G+Ly6C+ macrophages was observed in response to O_3.

SNOPPM but not SNAP Reduces Ly6C Expression in Interstitial Cd11c-Cd11b+ Macrophages

We next investigated Ly6C expression in the two populations of tissue macrophages that were responsive to ozone and ENO (Cd11c+Cd11b+ and Cd11c-Cd11b+). Neither SNAC nor SNOPPM reduced the Ly6C+ population of Cd11c+Cd11b+ cells following ozone; however, SNOPPM, but not SNAP effectively reduced Cd11c-Cd11b+Ly6C+ cells to 8.1 ± 2.8% of the total tissue associated macrophages (Table 2.4).

Both SNAC and SNOPPM Reduce Pro-inflammatory Signaling Following Ozone Exposure

Consistent with the findings of reduced inflammation and injury, both SNAC and SNOPPM reduced the ozone induced increased expression of iNOS and IL-1β in both macrophages and epithelial cells (Figure 2.6 and 2.7).

SNOPPM Increases Anti-inflammatory Signaling Following Ozone Exposure

SNOPPM appeared to have similar effects on HO-1 expression following ozone as ENO. Administration of SNOPPM increased HO-1 expression in macrophages with reduced positive staining found in the tissue (Figure 2.8 and Figure 2.9). In contrast, SNAC administration reduced positive HO-1 staining in primarily macrophages with HO-1 expression still found in pulmonary epithelial cells. Both SNAC and SNOPPM reduced the ozone induced increase of Ym1 positive macrophages.

2.5 Discussion

Inappropriate or dysregulated activation of macrophages and excessive pro-inflammatory signaling lead to diseases characterized by tissue injury resulting from high levels of RONS production, while excess anti-inflammatory signaling leads to diseases characterized by excess tissue remodeling (34, 41, 143). Studies have shown that macrophages adopt a pro-inflammatory activation state 24-48 hours following ozone (145). iNOS expression and activity has been long associated with macrophage pro-inflammatory activation. Nitric oxide can have effects through multiple mechanisms, however, there has been a growing acknowledgement of S-nitrosylation as a mechanism of NO-mediated signaling (3, 106, 156). Therefore, we investigated the effects of increased S-nitrosylation on macrophage activation and lung injury following exposure to O_3. Using ENO as a general SNO donor, and SNAC and SNOPPM to target extracellular and intracellular thiols respectively, we found that administration of all three compounds reduced markers of oxidative stress, epithelial cell proliferation following insult, and indicators of lung leakage in the BAL. We also observed reduced pro-inflammatory macrophage activation in distinct subsets following SNO donor administration, with different subsets targeted by each donor.

The contribution of iNOS derived NO to the post-ozone inflammatory response has been unclear as studies using O_3 exposed $iNOS^{-/-}$ mice show opposing results (117, 157). NO's dual and complicated role in inflammatory signaling is further demonstrated in other models of inflammation such as bleomycin where $iNOS^{-/-}$ mice show improved inflammation but worsened fibrosis 8 and 21 days following the intratracheal instillation of bleomycin (126). This is

likely due in part to NO's reactivity to a wide variety of targets including thiols, and the importance of NO's activity for the proper resolution of an initiated inflammatory response. Loss of iNOS derived NO undoubtedly leads to dysregulation of inflammatory signaling as seen in the altered response in models of iNOS inhibition and ablation (158-160). In the current studies we the effects of increasing NO's propensity to react with thiols, reducing the potential for the formation of nitrosyl metals, and higher order nitrogen oxides.

We first sought to determine whether increased SNO formation would decrease the markers of injury that are upregulated following ozone exposure. We found that administration of all three SNO donors reduced ozone-induced markers of oxidative stress, epithelial cell proliferation following insult, and indicators of lung leakage in the BAL. These finding demonstrate that increased SNO formation reduced O_3 induced lung inflammation.

We next assessed potential mechanisms underlying the ability of SNO donor administration mediated decreases in O_3-induced lung injury. It is our proposal that SNO-mediated reduction of lung injury is mediated, at least in part, via reduced inflammatory activation of macrophages. Consistent with previous studies, we found that O_3 increased the presence of Cd11b+ macrophages recovered from the BAL and increased the expression of Ly6C in this population of cells. Administration of SNO donors reduced the population of Ly6C+ cells retrieved from the BAL following O_3. These findings were consistent in Cd11b+ macrophages found in lung tissue as well, with the most pronounced effect on the interstitial macrophages that were Cd11c-. We found these changes also led to reduced expression of both classical markers of pro-inflammatory signaling

and markers associated with reparative signaling. Treatment with all three SNO compounds reduced expression of iNOS, IL-1β, YM-1 and HO-1 with the reduction in reparative signaling likely being a consequence of SNO induced reduction in injury.

In this study we used three chemically distinct SNO donors to observe their effects on the response to O_3. ENO is a general SNO donor, that preferentially donates a nitrosonium ion to thiols as compared to additional available targets. There is currently no literature to suggest that ENO displays any unique thiol specificity or potentially has its own biochemical mechanism of SNO formation, thus SNO donation by ENO would only be bound by biochemical permissibility. Interestingly, ENO administration led to increased cellular recruitment into the alveolar space. Both air controls and O_3 exposed mice that received ENO had a novel population of Cd11c-Cd11b+ cells in the BAL. Based on the cell populations recovered from the tissue it is presumable that these are interstitial macrophages that entered the alveolar space in response to ENO as these populations were reduced in the tissue. These macrophages also failed to gain Cd11c expression despite being in the alveolar space, potentially suggesting that ENO directed SNO formation may regulate macrophage maturity. This cellular recruitment was not only limited to macrophages, but also led to the recruitment of F4/80-Cd11b+Ly6G+SShi neutrophils. The ENO-mediated neutrophilia was comparable to that of, and unaffected by O_3 exposure. And while administration of ENO reduced markers of injury, and pro-inflammatory

macrophage activation following O_3, in air controls ENO led to increased expression of markers of pro-reparative macrophages (Ym1, HO-1) but not markers of injury and/or oxidative stress (BAL measures and tissue Cyb5 and PCNA). Taken together, these findings indicate that under homeostatic conditions, increased SNO formation through ENO administration alters inflammatory signaling, leading to increased recruitment to the lung.

To better understand our observations following ENO we sought to target specific thiol subsets with the two SNO donors SNAC and SNOPPM. SNO motifs place thiols in specific subsets based on a variety of factors including location and biochemical properties of the cysteine and its surroundings. SNAC quickly donates nitrosonium ions to potential targets including thiols. Because of its short half-life and rapid hydrolyzation, it is unlikely that SNAC would enter the cell thus primarily targeting extracellular thiols. In contrast, based on its hydrophobicity, SNOPPM should be capable of crossing the cell membrane, and has a longer half-life than that of SNAC, thus would be more effective at targeting intracellular thiols than SNAC. As well as the differential ability to enter the cell, SNOPPM is more reactive with thiol residues in hydrophobic regions of the target proteins, while SNAC is more reactive with charged surface accessible thiols.

While both compounds effectively reproduced ENO's effects on ozone-induced inflammation and macrophage activation, the mechanism by which they achieved this is unlikely the same. Some effects that were seen in ENO were observable uniquely in SNAC or SNOPPM treated mice. We observed increased HO-1 staining at baseline with ENO and SNOPPM but not with SNAC. This

further supports our hypothesis that SNOPPM would preferentially target intracellular targets. There are a number of targets that may explain this finding. One that seems especially relevant is Keap1. It is proposed that upon SNO formation, Keap1 is unable to inhibit Nrf2, allowing for increased nuclear translocation, and HO-1 expression is regulated in part by Nrf2.

Based on our findings, it would appear that thiols targeted by SNOPPM may be the most effective at reducing acute lung injury, followed by those altered by ENO administration which has already proven beneficial in clinical settings. While much still needs to be understood about the regulation and site directed specificity of SNO formation, these findings add to previous studies that demonstrate that macrophage phenotype, and NO metabolism in part mediate the pulmonary inflammatory response (41, 117, 126). Discovering the specific SNO dependent inflammatory pathways that have been altered by each of these compounds in response to O_3 is certainly a plausible next step. There exists a plethora tools to aid in this analysis including, investigating these pathways in the specific macrophage populations that are altered in response to O_3 and SNO compounds, as opposed to the entire population in which these minor changes may be lost.

Using three distinct SNO donors, we have found that increased SNO formation reduced O_3 induced lung injury as well as reduced pro-inflammatory macrophage activation 48 hours following exposure. SNOPPM was the most effective at reducing markers of injury, followed by ENO. Furthermore, we found that each SNO donor had distinct effects on macrophage populations with

reductions in pro-inflammatory macrophage activations occurring in a compound dependent manner. ENO reduced Ly6C expression in tissue associated macrophages, while SNAC and SNOPPM reduced Ly6C expression in macrophages from both the tissue and alveolar compartments. Overall these data demonstrate that increased S-nitrosylation effectively reduces pro-inflammatory macrophage activation and lung injury following O_3 exposure.

Chapter 3: Increased Intracellular SNO Formation in Bleomycyin Induced Fibrosis and Inflammation

3.1 Abstract

In this study we examined how inhibition of GSNOR altered pulmonary fibrosis and acute lung injury as a result of intratracheal bleomycin (ITB) administration, a model known to be modulated by iNOS function. In the absence of iNOS, acute injury is reduced but long-term fibrosis is exacerbated, likely due to failure to resolve the preceding inflammation. A number of pro-inflammatory targets involved in the inflammatory process are inhibited by SNO formation such as NF-κB, while protective mechanisms such as Keap-1, are activated. Thus, we hypothesized that inhibition of GSNOR would reduce fibrosis and inflammation in ITB through increased SNO formation. 8-12 week old, male C57BL6/J mice were administered 3 U/kg ITB or saline. Mice received the GSNOR inhibitor N6022 (or saline) every 48hrs from days 8-21 (fibrotic endpoint) by i.p injection, or daily from days 0-8 (at the peak of inflammation). RT-qPCR analysis of cells from broncho-alveolar lavage fluid revealed altered inflammatory signaling 21 days post ITB. N6022 administration reduced expression of inflammatory genes with the exception of *Arg1*, which remained unchanged compared to saline treatment. However, analysis of histology, and additional fibrotic markers revealed no reduction in fibrosis as a result of N6022 administration. At day 8, N6022 treated animals that received ITB had a reduced median inflammatory score compared to their saline controls indicating that increased SNO formation reduced the injury response. Taken together, it appears that increased GSNO reduces inflammation without affecting fibrosis in the ITB model.

3.2 Introduction

Intratracheal bleomycin (ITB) has been used extensively as a model of acute pulmonary injury and consequent fibrosis. It has been shown that NO generated from the iducible isoform of nitric oxide synthase (iNOS) is a critical component of the inflammation that results from ITB. Recent work from this laboratory has established that iNOS derived NO is not only critical to the inflammation that results from ITB but also plays a role in its resolution. Thus iNOS inhibition reduces inflammation but exacerbates fibrosis (126). However, the molecular mechanisms by which iNOS-derived NO can have these opposing functions are unknown. NO is capable of modifying a range of biomolecules including both proteins and lipids. A key modification is the nitrosylation of cysteine thiols to produce a S-nitrosothiol (SNO). One of the principle mediators of protein SNO-formation is S-nitrosoglutathione (GSNO), whose intracellular concentration is regulated by GSNO reductase (GSNOR). Within the pro-inflammatory signaling pathways of macrophages there are a number of proteins that are known targets of S-nitrosylation and whose function is inhibited by SNO formation, including NF-kB. We have chosen to investigate our proposal by examining the effects of administration of a GSNOR inhibitor, N6022 on ITB responses, in general inflammatory and macrophage specific gene expression. Our specific research hypothesis is that GSNOR inhibition aids in resolution from injury reducing fibrosis and reduces acute inflammatory activation in response to ITB. It is the goal of this research to investigate how the role of NO, and its associated protein modifications, regulates macrophage and inflammatory signaling in response to bleomycin-induced injury. Macrophages are activated along a spectrum of phenotypes ranging from pro-inflammatory to pro-reparative. Balance between both activation states is a key aspect to regulating the response of airway macrophages to stimulation such that an appropriate response is initiated and ultimately terminated. iNOS and INOS-derived NO are critical determinants of macrophage activation. Expression of iNOS is used as a marker of pro-inflammatory activation; however, it is also possible that iNOS is

critical to maintaining the balance between the two phenotypes. A key component of iNOS signaling is the formation of SNOs and this study examines how altering the SNO pool alters macrophage activation, fibrosis and inflammation subsequent to ITB administration.

3.3 Methods

ITB Model and N6022 Administration

Male, 8 week old C57bl/6 mice were obtained from Jackson laboratories and housed in the Animal Care Facility of Rutgers University under standard conditions with food and water given *ab libitum*. Mice received either sterile, lipopolysaccharide (LPS)-free saline or 3.0 units of Bleomycin sulfate dissolved in 50uL of saline intratracheally. This protocol was approved by the Rutgers University Institutional Animal Care and Use Committee (IACUC) and conducted in accordance with the recommendations in the Guide for the Care and Use of Laboratory Animals of the National Institutes of Health.

Fibrotic Signaling

Mice began receiving 0.5-1.2mg/kg of the S-nitrosoglutathione Reducatase (GSNOR) inhibitor N6022 (Cayman Chemicals) in DMSO on day 0 (day of administration) by i.p injection in 50μL of saline every 48hrs 8 days post-ITB and were sacrificed on day 21.

Inflammatory Signaling

Mice began receiving 1.8mg/kg of the S-nitrosoglutathione Reducatase (GSNOR) inhibitor N6022 (Cayman Chemicals) in DMSO on day 0 (day of administration) of by i.p injection in 50μL of saline every 24hr. Mice were sacrificed on day 8 post-ITB.

Histopathology

Left lung lobes were inflation fixed with 1mL of 3% paraformaldehyde and 2% sucrose and processed for paraffin embedding. Sections were stained with Hematoxylin and Eosin, and Masson's trichrome stain to assess fibrosis. Inflammation was assessed on severity and area of involvement and given an overall score ranging from 0-4. Area of involvement was calculated using ImageJ software. Inflammation was assessed by criteria that included the severity of the inflammation (based on criteria that included cellular infiltrate, airway hypertrophy, septal thickening, and loss of pulmonary acini) as well as how much of the lung was affected by inflammation relative to the total lung area. Severity of fibrosis was assessed by the same criteria with the addition of collagen deposition.

Histochemistry

Tissue protein expression was also analyzed by immunohistochemistry. Paraffin embedded sections were deparaffinized with xylene and rehydrated with ethanol. Heated sodium citrate was used for antigen retrieval followed by endogenous peroxidase quench. Sections were blocked in 10% goat serum in PBS and incubated in primary antibody overnight in 10% serum in PBS. Slides were washed with 0.1-0.5% Tween20 in PBS and incubated in rabbit IgG secondary antibody for an hour, followed by washing. Sections were visualized using DAB.

BAL

Lungs were washed 5 times using the 1+4 method to recover BAL fluid and cells. Cells were counted by Beckman Coulter cell counter and 30,000 cells obtained from BALF were spun onto slides using the Thermo Shandon Cytospin-4 at 800rpm for 3 minutes and cells stained for identification with Kwik-Diff solutions. Cell differentials were obtained by counting 5 fields at 20X magnification. Cell counts and mean cell diameters were obtained using the Beckman Coulter particle counter. BAL protein concentration

was measured using the Bio-Rad Bradford Assay as described in manufacturer's instructions.

RNA Extraction, and RT-qPCR

RNA was extracted rom alveolar immune cells obtained from broncho-alveolar lavage fluid from control and N6022 treated mice through Trizol and chloroform extraction. The aqueous phase was separated and precipitated with 2-propanolol and washed with 75% ethanol. RNA was then dissolved in Ultrapure RNAse and DNAse free water and converted to cDNA with Taqman Reverse Transcription Reagent kit. RT-qPCR was performed with the ABI Prism 7300 Sequence Detection System for the following target genes: *Il-1β* (Mm00434228_pro-inflammatory), *Arg1* (Mm00475988_pro-inflammatory), *Nos2* (Mm00475988_pro-inflammatory), *Il-6* (Mm00475988_pro-inflammatory), *Il-10* (Mm01288386_pro-inflammatory), and *Ccl2* (Mm00441242_pro-inflammatory) with β-actin (Mm02619580_g1) as a control. Fold changes were calculated using the ΔΔCt method.

Western Blot

Tissue homogenate was generated and protein content measured as previously described. 20μg of homogenates were run on 4–12% Novex Bis-Tris gels (Invitrogen, San Diego, CA) and then transferred onto nitrocellulose membranes. Nonspecific binding was blocked by incubation of the blots with 5% non-fat dry milk in Tris-buffered saline/Tween-20 (20 mM Tris Base, pH 7.6, 137 mM sodium chloride, and 0.1% Tween 20) for 1hr RT. Membranes were incubated overnight at 4°C with primary antibodies (1:1000) in 1% non-fat dry milk in 0.5% Tris-buffered saline/Tween-20, washed three times, and then incubated for 1hr at RT with HRP-conjugated secondary antibody (1:5000), diluted in1% non-fat dry milk in 0.5% Tris-buffered saline/Tween-20. Bands were developed using an ECL detection system (GE Healthcare Biosciences, Piscataway, NJ). Densitometry was analyzed using ImageJ Software.

Bone Marrow Derived Macrophages

BMDMs were harvested from the tibias and fibulas from mature C57bl/6 mice. Cells were plated at a density of $1*10^6$ cells/mL. Cells were grown in 20ng/mL of M-CSF for 5 days before exposure. BMDMs were treated with 5μM of N6022, 100ngmL of LPS or a combination of both treatments.

Statistical Analysis

Non-parametrical data was analyzed by Krusal-Wallis testing with Wilcoxon Rank Sum *post-hoc* analysis. Parametrical data was analyzed by ANOVA.

3.4 Results

N6022 Does Not Reduce Bleomycin Induced Fibrosis

Histological analysis of Masson Trichrome stains from mice receiving 0.5mg/kg or 0.75mg/kg of N6022 every 48hrs 8-21 days post ITB did not reveal any marked difference in the levels of collagen deposition based on the presence of blue stain 21 days following intratracheal instillation of bleomycin (Figure 3.1). Panel a. shows no discernable differences in the deposition of collagen with N6022 treatment. In Panel b, levels of hydroxyproline confirmed histological findings, with no statistically significant differences in collagen content. Immunohistochemical staining for markers associated with collagen deposition, and fibroblast activation revealed no differences in the quantity of the positive stain observed, there were some qualitative differences observed with the administration of N6022.

Figure 3.1

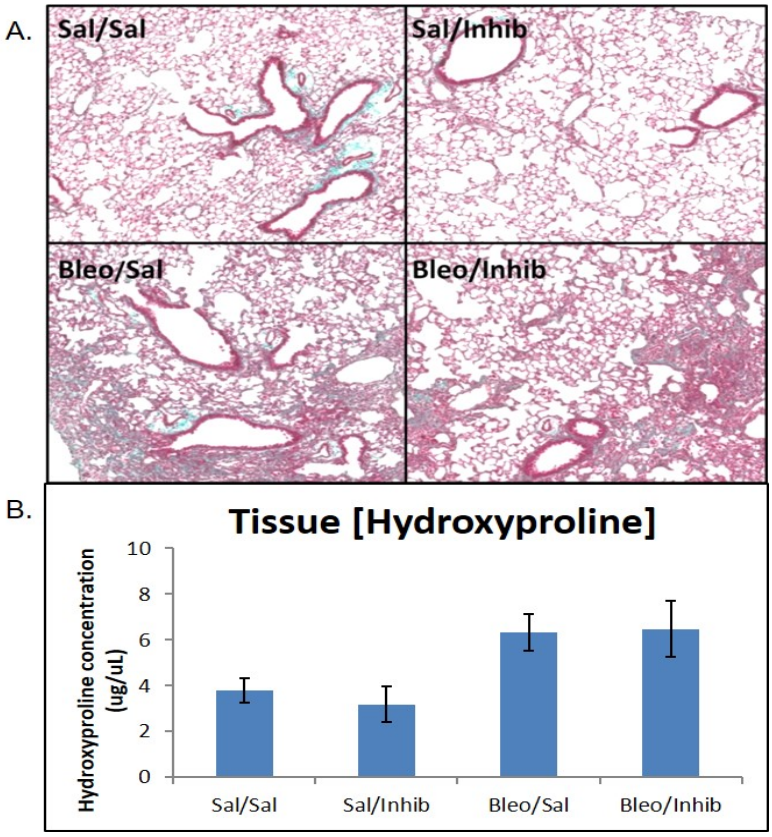

Figure 3.1. Increased Collagen Deposition 21 Days Post ITB. Left lungs were inflation fixed and paraffin-embedded. Masson's Trichrome staining reveals characteristic peribronchial and perivascular inflammation as well increased collagen deposition. Panel B. shows tissue hydroxyproline concentrations. Both measures of fibrosis indicate no change with N6022 administration. Mice received 0.5mg/kg or 0.75mg/kg of N6022 every 48 hours on days 8-21 post ITB.

Both treated and untreated mice showed positive TGF-β staining in macrophages and in the parenchyma (top panel, Figure 3.2). N6022 treated mice showed increased epithelial

staining in the alveolar space, while untreated mice showed reduced epithelial staining, with increased positive signal in areas of collagen deposition. Similarly, the expression of vimentin was altered by N6022. N6022 treated mice showed reduced vimentin positive fibroblasts and reduced vimentin staining in areas of collagen deposition as seen in the lower panel. Mice from both groups showed vimentin positive macrophages. These qualitative differences in N6022 treated mice pointed toward altered inflammatory signaling following inhibition of GSNOR 21 days following bleomycin.

Figure 3.2

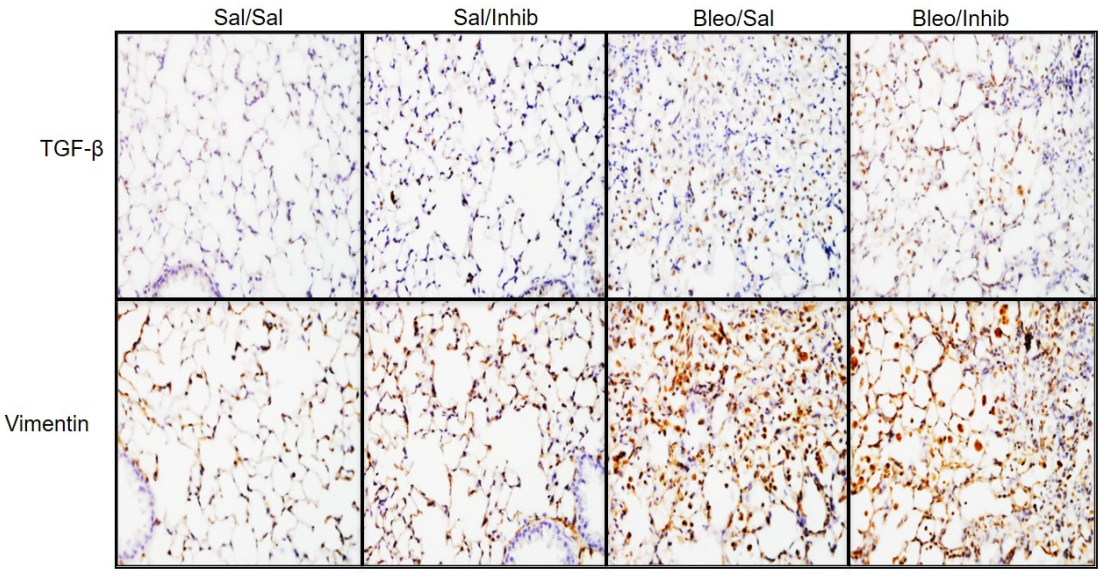

Figure 3.2 Increased Pro-Fibrotic Markers 21 Days Post ITB. Left lungs were inflation fixed and paraffin-embedded. IHC staining reveals increased TGF-β and Vimentin signaling 21 days post-ITB. N6022 administration leads to altered TGF-β staining pattern.

Inhibition of GSNOR Alters Inflammatory Signaling in Alveolar Macrophages

Analysis of inflammatory signaling by RT-qPCR revealed that N6022's inhibition of GSNOR altered signaling in these cells (Table 3.1). Macrophage phenotype may be inferred in part by expression of two key enzymes iNOS and Arginase. Both of these enzymes utilize arginine to generate their final products. Pro-inflammatory macrophages

express higher levels of iNOS when compared to Arginase while anti-inflammatory macrophages express higher levels of Arginase as opposed to iNOS. As anticipated during the fibrotic phase 21 days following bleomycin in both untreated and N6022 treated mice, expression of *Arg1*, the gene which encodes for Arginase I was highly upregulated as compared to both control groups (88, and 82 fold respectively). Expression of *Nos2*, was slightly upregulated 21 days post-ITB (1-fold); however, this increase was reduced in N6022 treated mice (0.5- fold). Expression of the gene encoding the chemoattractant ligand to the receptor CCR2 *Ccl2* was increased 5-fold over controls following bleomycin but this upregulation was not affected by N6022 administration. Gene transcription levels of key inflammatory signaling proteins *Il-6* and *Il-1β* were induced by bleomycin but reduced in N6022 treated mice. Bleomycin led to a 4-fold increase in *Il-6*, which was reduced to a 2-fold increase with administration of N6022. Inhibition of GSNOR also reduced the 7-fold bleomycin-induced increase in *Il-1β* expression to 0.3-fold. This reduction in general inflammatory signaling genes such as *Il-6*, coupled with the reduction in *Il-1β and Nos2* in N6022 treated mice 21 days following bleomycin suggests that these alveolar macrophages are further polarized toward a pro-reparative phenotype.

Table 3.1

	Sal/Inhib	**Bleo/Sal**	**Bleo/Inhib**
iNOS	0.72 ± 0.49	1.12 ±0.35	0.46 ± 0.23
Arginase 1	1.5 ±0.6	87.56 ±0.88*	82.23 ±0.88*
Il-6	1 ±0.4	4.03 ± 1.0	**1.89 ±0.91**
Ccl2	0.5 ± 0.13	5.15 ± 0.95	4.47 ±0.98

Il-1β	1.5 ± 0.7	6.67 ±0.88	**0.27 ±0.38**

Table 3.1 RT-qPCR of Alveolar Macrophages. Macrophages recovered from alveolar space were phenotyped by RT-qPCR. Fold change calculated by ΔΔCt method to Sal/Sal controls. $p \leq 0.05$ 1-way ANOVA, Bon Ferroni post-hoc test. *- significant to Sal/Sal **Bold**- significant to Bleo/Sal.

Inhibition of GSNOR Reduces Pro-inflammatory Macrophage Activation In Vitro

BMDMs were harvested from the tibias and femurs of 8-12-week-old C57bl/6 mice. Cells were matured into a macrophage phenotype with M-CSF and exposed to 100ng/mL of LPS or vehicle with or without 5μM of N6022. BMDMs were analyzed by flow cytometry first based on their expression of F4/80 and CD11b (Table 3.2).

Without treatment, 76.9 ± 7.8% were mature, F4/80+ macrophages with 96.6 ± 0.7% of F4/80+ cells expressing CD11b. The majority of these cells were not activated as only 16.3 ± 3.1% were positive for the pro-inflammatory marker Ly6C, and 9.0 ± 3.1% were positive for pro-reparative marker CD206. Administration of N6022 led to an increase of mature macrophages as 84.5 ± 1.8% were F4/80+ and 97.9 ± 0.4% of these were CD11b+. Administration of N6022 to BMDMs led to a modest reduction of expression of Ly6C as 13.9 ± 4.5% were positive for Ly6C while expression of CD206 remained consistent at 9.3 ± 0.9%. LPS increased the maturity of BMDMs as now 88.3 ± 2.6% were F4/80+ but LPS reduced the expression of CD11b present in mature F4/80+ macrophages to 88.3 ± 2.8%. After exposure to LPS, Ly6C expression increased as 19.3 ± 1.1% of macrophages were activated, while CD206 expression also increased to 12.6 ± 1.8%. Administration of N6022 following stimulation with LPS led to the highest increase in maturity as 91.2 ± 0.4% of BMDMs were F4/80+. N6022 administration increased CD11b expression of F4/80/+ cells compared to both control and LPS

exposed cells, with 98.0 ± 0.5% of mature macrophages expressing CD11b. While, N6022 did not alter expression of CD206 (13.5 ± 0.9%), expression of Ly6C was reduced in response to LPS with N6022 as 12.9 ± 1.1% of F4/80+CD11b+ BMDMs demonstrated pro-inflammatory activation in response to LPS compared to 19% in untreated cells. Coupled with the previous 21 day findings, this reduction in Ly6C expression was indicative that inhibition of GSNOR would potentially be effective in reducing bleomycin-induced acute lung inflammation.

Table 3.2

	% F4/80+	**% F4/80+CD11b+**	**%F4/80+CD11b+ Ly6C+**	**%F4/80+CD11b+ CD206+**
Untreated	76.9 ± 7.8	96.6 ± 0.7	16.3 ± 3.1	9.0 ± 3.1
+ N6022	84.5 ± 1.8	97.9 ± 0.4	13.9 ± 4.5	9.3 ± 0.9
+ LPS	88.3 ± 2.6	88.3 ± 2.8	19.4 ± 1.1	12.6 ± 1.8
+ LPS and N6022	91.2 ± 0.4	98.0 ± 0.5	12.9 ± 1.1	13.5 ± 0.9

Table 3.2 FACS Analysis of Bone Marrow Derived Macrophages. Macrophages were matured in 20ng/mL M-CSF and exposed to 100 ng/mL LPS and/or 5μM N6022. Expression of F4/80, CD11b, Ly6C and CD206 were analyzed.

Inhibition of GSNOR Reduces Histological Inflammatory Scores 8 Days Post-ITB

Based on the findings of N6022's effects on alveolar macrophages, we hypothesized that these changes may be beneficial during the pro-inflammatory signaling phase of bleomycin. Thus, we gave 1.2mg/kg of N6022 every 24hrs starting on the day of instillation. Histopathological assessment of H&E stained sections revealed reduced inflammation in the lungs of N6022 treated mice. The median inflammatory scores for

mice receiving saline following bleomycin administration was 15 with a range of 6-20 while N6022 treated mice had a median score of 9 with a range of 1-21, N6022 reduced the characteristic peribronchial and perivascular inflammatory cell infiltration that is typically observed 8 days following bleomycin (Figure 3.3). As shown in the lower right panel of Figure 3.3, N6022 administration led to a modest reduction in the concentration of total protein measured in the BAL, from 390 ± 45µg/mL to 334 ± 52µg/mL.

Figure 3.3

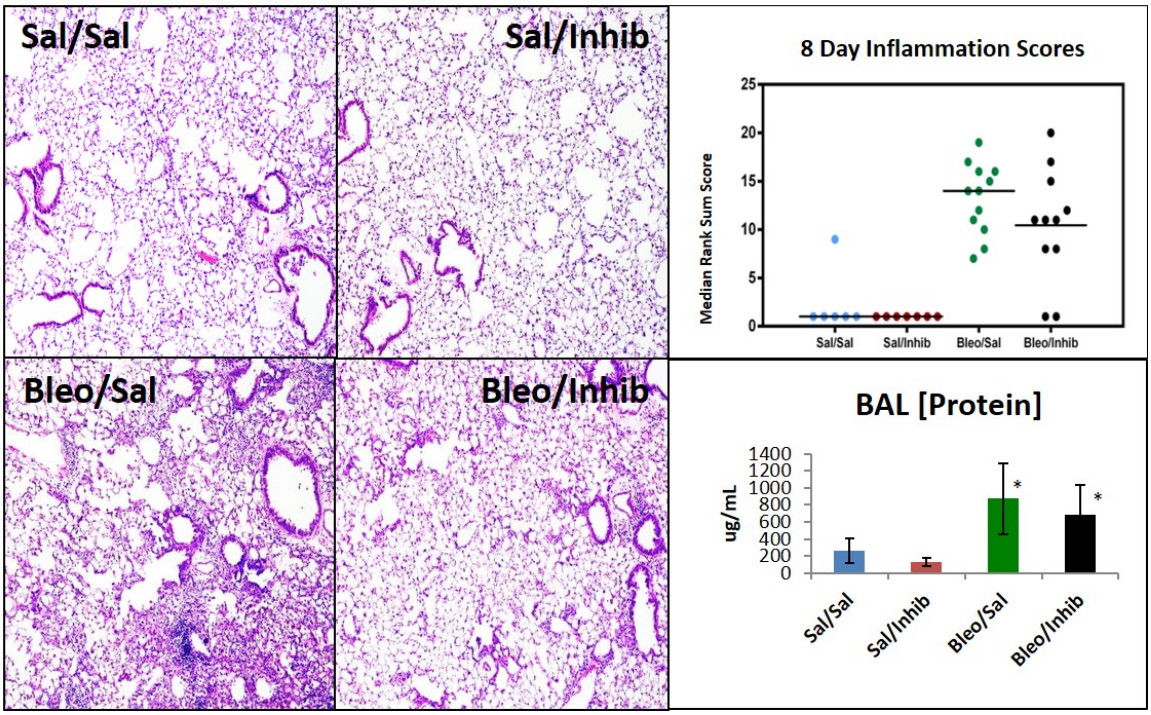

Figure 3.3 Increased Inflammation 8 Days Following ITB. Left lungs were inflation fixed and paraffin-embedded. A and B. H&E staining reveals increased perivascular and peribronchiolar inflammation 8 days post-ITB. C. Total BAL protein concentration was also increased. $p \leq 0.05$ 1-way ANOVA, Bon Ferroni post-hoc test. ***- significant to Sal/Sal **Bold**- significant to Bleo/Sal

N6022 Administration Does Not Alter Inflammatory Cell Recruitment

Bleomycin-induced increases in cell counts were not affected by administration of N6022 8 days post-ITB (Figure 3.4). Also, administration of N6022 did not alter cell differentials as assessed by cytospins (lower left panel, Figure 3.4). The lack of N6022 dependent alteration of cellular recruitment was confirmed by expression of CD11b, a surface integrin associated with chemotaxis and activation, N6022 did not affect the bleomycin-induced increase in CD11b expression.

Figure 3.4

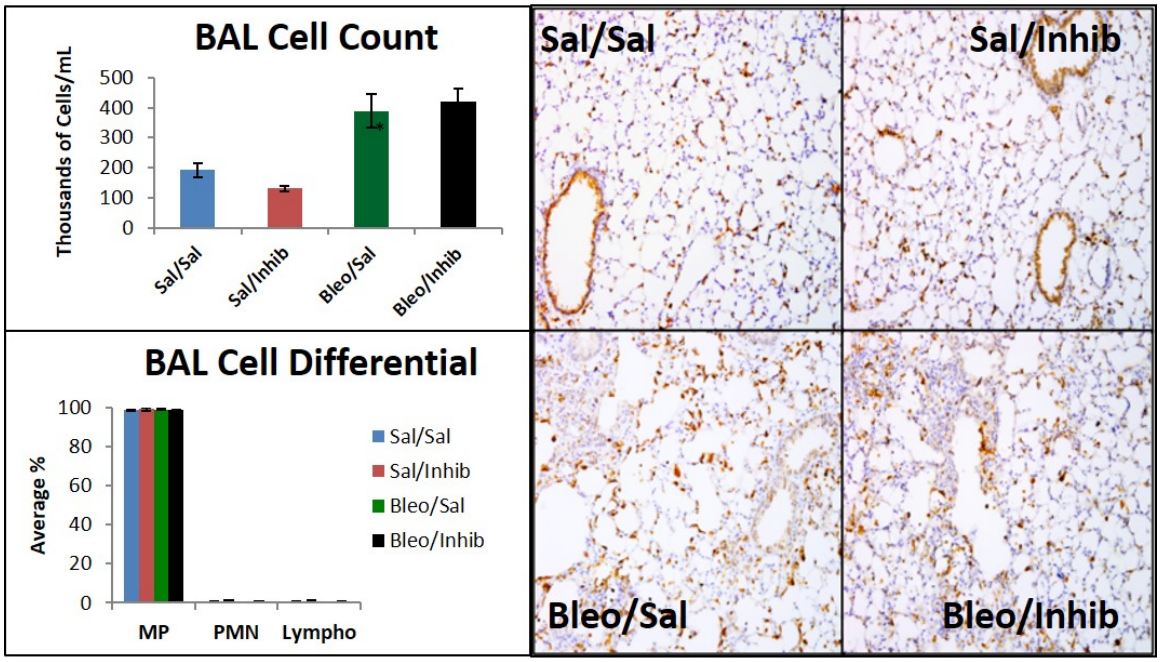

Figure 3.4 BAL Cell Recruitment 8 days Following ITB. Lungs were lavaged and cells recovered. Upper and lower left panels show cell counts by Beckman Coulter and cell differentials by cytospins respectively. Paraffin-embedded left lungs were stained by IHC for CD11b expression showing unchanged recruitment into the alveolar space and tissue by N6022.

N6022 Alters Macrophage Activation in Response to Bleomycin Eight Days Post-ITB

Macrophage size is a good indicator of activation. As anticipated and viewed in the left panel of Figure 3.5, administration of bleomycin led to the induction of a larger population of cells with a diameter of 4-10μm as assessed by Beckman Coulter Cell Counter where macrophages are experimentally observed in the 4-20μm range based on this machine. The average mean cell diameter (MCD) of bleomycin mice receiving saline was 6μm. Administration of N6022 to mice receiving bleomycin caused a leftward shift in cell diameter, with the average MCD being reduced to 5.8μm. Also worth noting, N6022 led to an increase in the macrophage population with a 4-5μm diameter. In N6022 treated mice, the population count for this macrophage population was increased to $15*10^6$ cells/mL as compared to $5*10^6$ cells/mL in saline treated mice following bleomycin. Based on the finding that cell recruitment to the alveolar space was unaltered, but activation was decreased, we looked at inflammatory signaling in the lung tissue. When pro-inflammatory markers were observed, N6022 led to a reduction of the bleomycin-induced increase of iNOS and IL-1β found in both epithelial cells as well as macrophages (Figure 3.7). We also found that increased levels of GSNO reduced the presence of COX-2 positive macrophages in both saline and bleomycin treated mice. In contrast, we found that N6022 did not alter the expression of the anti-inflammatory macrophage marker Ym1.

Figure 3.5

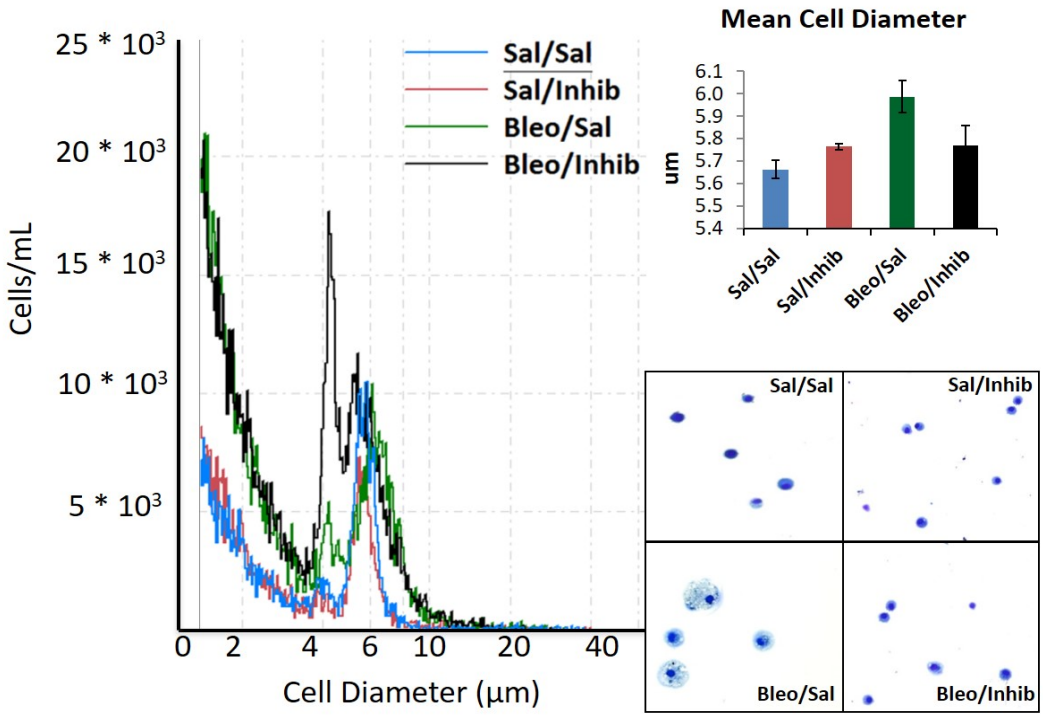

Figure 3.5 BAL Cell Size Following ITB. Lungs were lavaged and cells recovered. Left panel shows cell size and count by Beckman Coulter Counter with a novel population present following N6022 administration. Right panel shows mean cell diameters of alveolar macrophages, with additional sizing by cytospin.

Figure 3.6

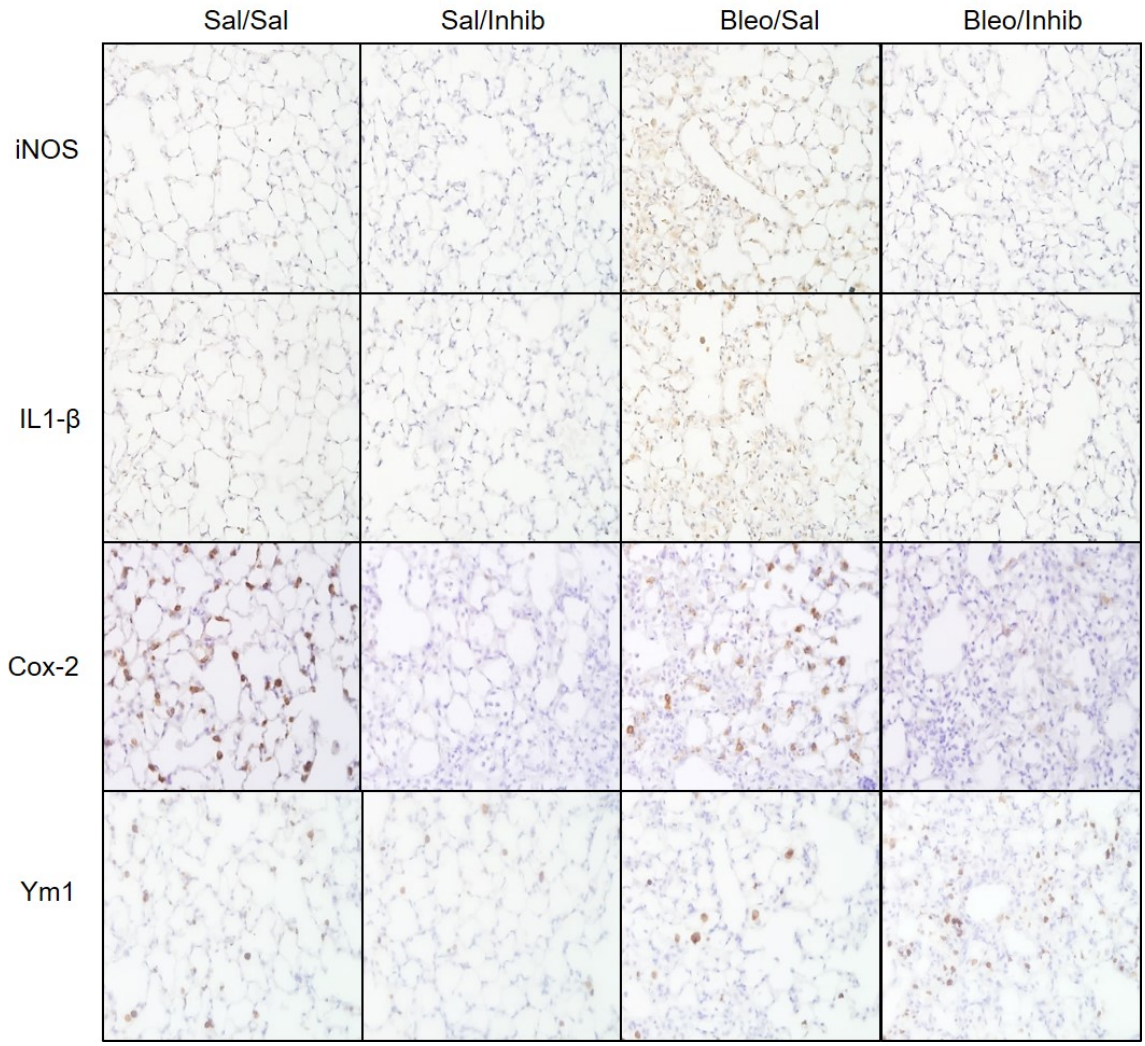

Figure 3.6 Tissue Macrophage Immunophenotyping. IHC expression of pro- and anti-inflammatory macrophage markers. N6022 reduced pro-inflammatory markers while keeping levels of Ym1 unchanged in response to bleomycin.

STAT3 Activation Is Reduced in N6022 Treated Mice

Based on the reduction of *Il-6* previously found we explored activation of the IL-6/STAT3 pathway. STAT3 is also a substrate for S-nitrosylation, and S-nitrosylation of STAT3 opposes activation by phosphorylation (156). Lung tissue lysate was probed by western blot for Phospho-STAT3 expression (Figure 3.8). We found that administration of bleomycin increased Phospho-STAT3 expression indicative of increased activation. This increase was reduced by the presence of N6022. We confirmed that N6022 did not alter overall STAT3 expression.

Figure 3.7

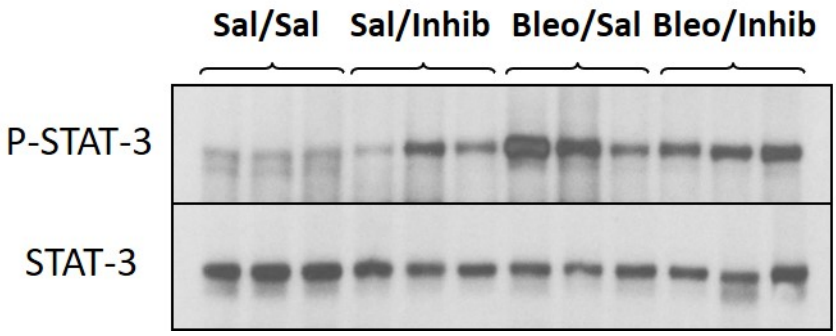

Figure 3.7 Tissue Expression of STAT3. Western Blot of tissue homogenates probed for the activated, phosphorylated form of STAT3 as well as total STAT3. Bleomycin increased levels of P-STAT3 which was reduced by N6022 administration.

3.5 Discussion

ITB has long served as a model of inflammation and fibrosis. We previously used this model to understand the role of iNOS and iNOS derived NO in ITB. Using $iNOS^{-/-}$ mice we found that loss of iNOS led to improved inflammation 8 days following bleomycin; however, the fibrosis is ultimately worsened (126). Based on these findings, we hypothesized that iNOS derived NO was key to the successful resolution of inflammation and highly relevant to fibrotic signaling. Thus, we hypothesized that the worsened fibrosis was due to a loss of S-nitrosylation, especially as levels of NO are reduced

during the fibrotic phase as opposed to the preceding inflammatory phase. Therefore we sought to improve ITB induced fibrosis through increasing S-nitrosylation by inhibiting degradation of GSNO.

Observed changes in macrophage phenotype induced by increased levels of GSNO 21 days post ITB were not accompanied by changes in collagen deposition. These results on the effects GSNOR inhibition on bleomycin induced fibrosis are in contrast with the currently published and similarly designed study (161). Despite the similarities in experimental model, we found opposing results. First this study uses a different inhibitor of GSNOR named SPL-334, which may have an ADME profile distinct from N6022. Additionally, Luzina and colleagues administered a standard dose of 0.075U of bleomycin to 8-12 week old mice while we dosed based on current body weight for a dose of 3U/kg. The use of standard dosing in this study may have led to animals of lower mass receiving higher doses of bleomycin. In our model, we typically do not see changes in animal body weight following the cessation of the acute inflammatory response to ITB while this study reports body weight loss that is improved by inhibition of GSNOR. Another indication that our findings may be due to model differences can be found in the cell differentials. Cells recovered from BAL 21 days following bleomycin are still predominantly macrophages while Luzina and colleagues recover fewer cells, and observe the presence of lymphocytes while we find that lymphocytes remain in the tissue and are observable in histological sections only.

Twenty-one days following bleomycin, macrophages were polarized toward an pro-reparative phenotype consistent with pro-fibrotic signaling. Bleomycin also induced expression of genes downstream from key regulators of inflammatory signaling (*Il-1β* and *Il-6*). Increased levels of GSNO reduced these changes, but interestingly did not alter the recruitment as assessed by the type or number of cells recruited into the alveolar space. As N6022's effects on macrophage activation were skewed toward pro-

reparative activation, it was surprising that this shift in activation did not worsen bleomycin-induced fibrosis.

We surmised that these effects would be beneficial during the peak of inflammation 8 days following bleomycin. Eight days post-ITB, N6022 reduced macrophage activation when assessed by size, and expression of pro-inflammatory markers iNOS, COX-2, and IL-1β. These changes in macrophage phenotype potentially contributed to the decrease in the observed overall inflammation. These findings were consistent with previous findings with that inhibition of GSNOR leads to down-regulation of pro-inflammatory genes (162). This study also found an upregulation in Nrf2 dependent antioxidant signaling; however, we did not explore this avenue especially as overall Ym1 pro-inflammatory expression, a marker typically expressed on anti-inflammatory macrophages remained unchanged.

The effects of inhibiting GSNOR are distinct from the changes induced by genetic ablation of GSNOR. Our own lab has found that loss of GSNOR alters the SNO proteome, as $GSNOR^{-/-}$ mice have a unique population of SNO-ed proteins not found in wild type or $iNOS^{-/-}$ mice (unpublished data). These changes in the SNO proteome may potentially explain some of the observed phenotypes such as spontaneous liver carcinoma (163), and the increased susceptibility of $GSNOR^{-/-}$ mice to LPS toxicity (164). The phenotypes associated with GSNOR deficiency as opposed to inhibition further demonstrate the importance and complexity of S-nitrosylation.

The exact pathways that may contribute to our observed findings have yet to be explored. The relevant pathways to each phase of signaling in ITB, as well as in additional models that are altered by inhibition of GSNOR/ increased S-nitrosylation are certainly avenues worth exploring as it is unlikely that they all contribute equally to each disease state. The significance of differences in signaling during the progression of the inflammatory response is partially demonstrated by our own findings as macrophage

size remained unchanged in the fibrotic phase following ITB; however, it was reduced during the inflammatory phase. Additionally, fibrosis is typically associated with M2/Th2 biased inflammatory response, yet we found no change in collagen deposition with N6022 administration despite increasing M2-likeness in macrophages. However, inhibition of GSNOR with various compounds including N6022 has been found to reduce asthmatic and allergen responses in the mouse lung and these disease states are also associated with a Th2 biased response, again demonstrating the need for understanding of specific signaling mechanisms (165-167).

To summarize, our findings demonstrate that S-nitrosylation has a role in regulation inflammatory signals that also affect macrophage phenotype. Macrophage activation has long been an appreciated target for disease intervention. GSNO mediated S-nitrosylation presents an additional avenue through which macrophage activation and inflammatory signaling may be altered. Inhibition of GSNOR allows for the potentiation of NO dependent signaling without changing overall levels of NO. Our macrophage specific findings are consistent with currently published data, and further lend to the exploration of which specific pathways would contribute to our findings.

Chapter 4: Inhibition of S-nitrosoglutathione Reductase in Lewis Lung Carcinoma

4.1 Abstract

The Lewis Lung Carcinoma (LLC) model allows for study of tumor progression in an immunocompetent model.

Tumor development requires suppression of the immune system and is achieved in part by altering macrophage phenotype. The pathways by which the tumor microenvironment alters macrophage phenotype are targets for S-nitrosylation such as NFk-B, STAT3, and HIF-1α. Thus, we sought to determine if increased intracellular S-nitrosylation would oppose LLC induced changes on macrophage phenotype. To achieve this, we increased levels of GSNO through inhibition of GSNOR with N60222. Daily treatment with N6022 following injection of LLC cells, led to reduced tumor size when compared to untreated mice. In mice treated with N6022, recruitment of additional immune cell types was altered included immature macrophages, eosinophils, and neutrophils. Activation state of recruited and resident lung populations was also altered by LLC cells, and subsequently changed by administration of N6022.

4.2 Introduction

The effects of the tumor microenvironment on the immune response are two-fold and are immunosuppressive by two primary mechanisms: evasive to avoid detection by the immune system or permissive by exploiting cellular functions that are conducive for tumor growth (168). In response to tumor growth, macrophages adopt unique phenotypes and have been termed tumor associated and/or infiltrating macrophages (TAMs and TILs), and myeloid derived suppressor cells (MDSCs). As inflammatory signaling progresses, additional cell types are recruited to the tumor microenvironment, and adopt a phenotype of the microenvironment (169, 170). Despite the pro-inflammatory/ pro-reparative spectrum, macrophages in the tumor microenvironment

have their own unique phenotype that does not fall on either end of the spectrum (171). In general, TAMs and TILs phenotypically resemble M2-like macrophages, while MDSCs resemble pro-inflammatory macrophages phenotypically but functionally suppress T cell function. The Lewis Lung Carcinoma model allows for study of the immune response in an immunocompetent mouse model. As we are aware that much of iNOS' and NO's physiological effects are through S-nitrosylation and have identified key pathways through which SNO formation regulates inflammatory signaling, we sought to determine whether increased intracellular S-nitrosylation through increased levels of GSNO would oppose LLC induced alteration of macrophage phenotype, and to determine if these alterations would lead to reduced tumor growth.

4.3 Methods

Animals

8-12 week old mixed sex mice were injected with $1*10^6$ LLC cells by tail vein injection 72 hours following pump implantation surgery. Mice were sacrificed 23-25 days following injection based on morbidity as assessed by body weight and behavior.

Alzet Pump Preparation and Implantation

2004 28-day mini osmotic pumps were prepared sterilely according to manufacturer's instructions. Pumps were filled with either sterile PBS or filtered N6022 for a dose of 1.2mg/kg every 24 hours. Pumps were then subcutaneously implanted into mice using the "No touch/Tip only" technique. In brief, mice were sedated under 5% isoflurane, and surgery performed under 3%. Following the incision, a pocket was made under the skin and pumps were implanted and closed with 7mm clips. Mice received both systemic and local anesthetics and were monitored daily for 14 days.

Bronchoalveolar Lavage

Following perfusion with heparinized PBS, bronchoalveolar lavage fluid and cells were retrieved with four total washes with sterile PBS. A 20G cannula was inserted into the trachea. Using a 1mL syringe, lungs were slowly filled and emptied using the 1+3 method. The collected fluid was then spun at 300g x 10min at 4ºC to separate cellular and fluid components. The resulting supernatant was collected and stored. Cells were resuspended in PBS and counted by Beckman Coulter and processed for flow cytometry.

Lung Digestion and Magnetic Associated Cell Selection

Right lung lobes were enzymatically digested in 5mL of 2mg/mL collagenase IV (Miilipore Sigma C5138) in RPMI 1640 Medium (Thermo Fisher 11875119) with 5% Heat Inactivated FBS (S11550) and 37°C for 30min with shaking. A single cell suspension was then created using a 70µm strainer. Following RBC lysis for 5min at RT (Millipore Sigma R775), CD45-APC conjugated cells were then positively selected as per Stem Cell Easy Eight Mouse APC Positive Selection kit protocol. Cells were then stained for flow cytometric analysis.

Flow Cytometric Analysis

BAL and tissue associated cells were Fc blocked for 10min 4°C or 5min RT respectively. Cells were then incubated with the following antibodies (1:100) and respective conjugates for 30min at 4°C.

BAL

F4/80-PE (Stem Cell 60027PE clone BM8)

SiglecF-PerCPCy5.5 (BD Biosciences 552125, clone E502440)

CD11c- PeCy7 (Biolegend 117320, clone N48)

CD11b- APC (Biolegend 101206, clone M1/70)

Ly6C- PE Cf594 (Biolegend 128012, clone HK1.4)

CD206/MR- FITC (Biologened 141703, clone C068C2)

Viability 780 (Thermo Fisher 65-0865-14, eBiosciences Fixable Viability)

Tissue

Macrophages

CD45- APC (Biolegend 103101, clone 30-F11)

F4/80-PE (Stem Cell 60027PE, clone BM8)

SiglecF-PerCPCy5.5 (BD Biosciences 552125, clone E502440)

CD11c- PeCy7 (Biolegend 117320, clone N48)

CD11b- e450 (Biolegend 101206, clone M1/70)

Ly6G- PE (Biolegend 127610, clone 1A8)

Viability 780 (Thermo Fisher 65-0865-14, eBiosciences Fixable Viability)

T Cells

CD45- APC (Biolegend 103101, clone 30-F11)

CD3-Af700 (Biolegend 100212, clone 17A2)

CD8- FITC (Biolegend 100726, clone 53-6.7)

CD4- PeCf594 (Biolegend 100425, clone GK1.5)

CD69- PE (Biolegend 104516, clone H1.2F3)

CD25- PECy7 (Biolegend 102018, clone PC61)

CD196- BV421 (BD Biosciences 557976, clone 140706)

Viability 780 (Thermo Fisher 65-0865-14, eBiosciences Fixable Viability)

Immunohistochemistry

IHC protocol was performed as previously described using anti CD11b (ab133357), and Gr1 (MAB1037) antibodies. Paraffin embedded sections were deparaffinized with xylene and rehydrated with ethanol. Heated sodium citrate was used for antigen retrieval followed by endogenous peroxidase quench. Sections were blocked in 10% goat serum in 1xPBS and incubated in primary antibody overnight in 10% serum in PBS. Slides were

washed with 0.1-0.5% Tween20 in PBS and incubated in rabbit IgG secondary antibody for an hour, followed by washing. Sections were visualized using DAB.

4.4 Results

Inhibition of GSNOR with N6022 Reduces LLC Tumor Size

Tumor bearing mice receiving N6022 via Alzet Osmotic Pump showed reduced tumor size 25 days following injection with $1*10^6$ LLC cells via tail vein injection. Mice that were treated with PBS had tumors that affected 26.3 ± 12.1% of the lung. When compared to mice that received 1.2mg/kg of N6022, tumor size was reduced to only affecting 2.6 ± 1.8% of the lung (Figure 4.1). LLC tumors were associated with pleural edge of the lungs and were mixed histologically with both solid and acinar patterns observable. N6022 administration led to a reduction in the acinar structures present within the tumors with areas of necrosis present. Airway epithelial cells were also altered in response to LLC, becoming stratified/ pseudostratified. Tumors in N6022 treated mice were also less invasive and were better encapsulated when compared to untreated mice. This observable reduction in tumor size led us to investigate the effects of inhibition of GSNOR on the inflammatory process in response to adenocarcinoma. This reduction in tumor size was accompanied by a reduction in the number of mitotic figures.

Figure 4.1

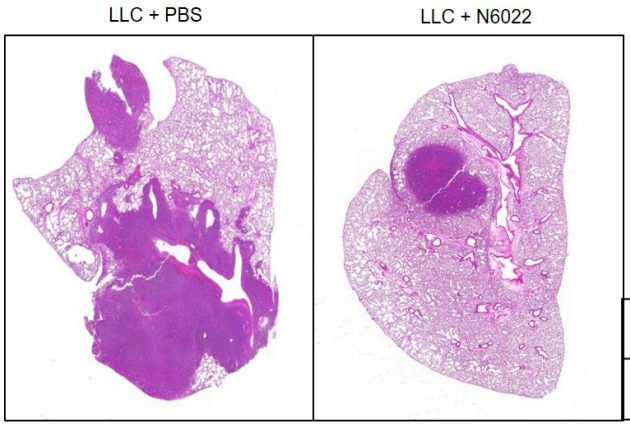

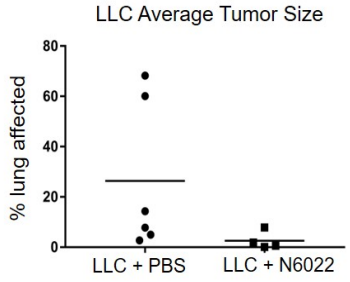

	LLC + PBS	LLC + N6022
Mitotic figures/ field	23.0± 2.0	13 ± 3.0

Figure 4.1. Lewis Lung Carcinoma Tumors. Left lungs were inflation fixed and paraffin-embedded. H&E staining reveals characteristic pleural associated neoplasms of the LLC model. Right panel shows distribution of tumor sizes as well as the average number of mitotic figures counted in 5 randomly selected areas.

N6022 Marginally Alters the Cellular Composition of Cells Recovered from the BAL in Response to LLC

Cells recovered the BAL of naïve mice are typically ≥ 98.0% macrophages, and approximately 0.1-0.2 * 10^6 cells/mL are recovered by lavage from the 1+3 method. After inoculation with LLC cells, average cell counts recovered from the BAL were unchanged at 0.09 *10^6 ± 2.0 cells/mL (Table 4.1). Administration of slightly N6022 increased this number to 0.15*10^6 ± 5.5 cells/mL. The macrophage population was reduced to 88.3 ± 2.3%, as neutrophils now comprised 4.0 ± 1.3% of the population. Lymphocytes were 3.6 ± 1.6%, and eosinophils were 1.2 ± 0.4%. N6022 again, led a modest modification as macrophages comprised 91.1 ± 3.3%. Neutrophilia and eosinophilia were unaffected, as lymphocytes were reduced to 1.2 ± 0.5% of the population as determined by Kwik Diff stained cytospins.

Table 4.1

	Cell Count (*10^4 cells/mL)	**% Macrophages**	**% Neutrophils**	**% Eosinophils**	**% Lymphocytes**
LLC + PBS	9.9 ± 2.0	88.3 ± 2.3	4.0 ± 1.3	1.2 ± 0.4	3.6 ± 1.6
LLC + N6022	15.0 ± 5.5	91.1 ± 3.3	4.1 ± 0.5	0.7 ± 0.5	1.2 ± 0.5

Table 4.1 BAL Cell Count and Composition. Cells recovered from alveolar lavage fluid were counted by hemocytometer and analyzed by cytopsin.

When cells from the BAL were analyzed by flow cytometry, we found that LLC led to the recruitment of immune cells to the alveolar space. Of cells recovered from the BAL ≥ 97.0% are mature, resting, alveolar macrophages. These cells are F4/80+SiglecF+CD11c+CD11b- and negative for markers of granulocity (Ly6G) and activation (Ly6C). LLC mice had a general reduction in the population of F4/80+ cells likely due to increased recruitment of immune cells to the alveolar space. Of these F4/80+ cells, 66.8 ± 6.7% were resting, mature macrophages (F4/80+SiglecF+CD11c+CD11b-). 5.9 ± 2.1% of mature macrophages (F4/80+SiglecF+CD11c+) now expressed CD11b in response to LLC and 10.0 ± 3.2% of these CD11b+ mature macrophages were acutely activated based on Ly6C expression (Figure 4.2). Administration of N6022 led to modest changes in these populations. 69.1 ± 16.6% of macrophages were resting mature macrophages of cells recovered from the BAL. In N6022 treated mice, 3.3 ± 2.0% of F4/80+SiglecF+CD11c+ cells were CD11b+ and as with untreated mice, 9.6 ± 2.0% were Ly6C+. This was indicative that treatment with N6022 reduced activation of the mature alveolar macrophage population in response to LLC as the % of CD11b+ cells were slightly reduced. As anticipated, unrelated to their expression based on CD11b, these cells were positive for CD206, and expression was not affected by N6022 administration.

Figure 4.2

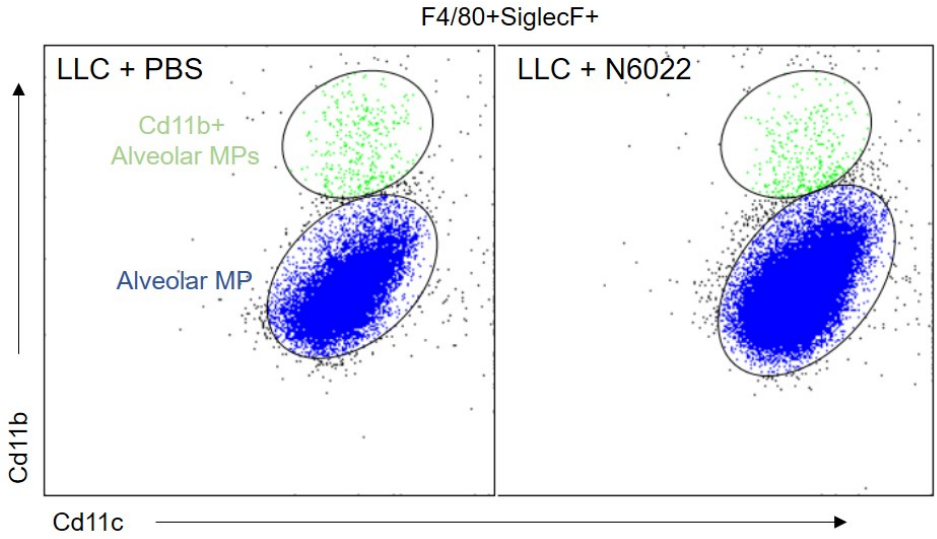

	% Alveolar Macrophage	% Cd11b+ Alveolar Macrophages	% Cd11b+Ly6C+ Alveolar Macrophages
LLC + PBS	66.8 ± 6.7	5.9 ± 2.1	10.0 ± 3.2
LLC + N6022	69.1 ± 16.6	3.3 ± 2.0	9.6 ± 2.0

Figure 4.2 Alveolar Macrophage Activation Following LLC. Cells recovered from alveolar lavage fluid were analyzed by FACS for expression of CD11c, CD11b, and Ly6C and Ly6G. Percentages shown are % gated of indicated population. Inhibition of GSNOR by N6022 reduced the population of CD11b+ alveolar macrophages.

N6022 Reduces Tissue Resident Macrophage Population and Activation

We then sought to understand the effects of adenocarcinoma on tissue-associated macrophages, and how N6022 administration affected these changes. We found that inoculation with LLC cells reduced the F4/80+ population overall, and that this loss was potentiated by the administration of N6022. The tissue resident macrophage population of SiglecF+CD11c+CD11b- cells represented 6.8 ± 14.9% of the F4/80+ cells, which was reduced by N6022 administration, as this population contributed 3.4 ± 13.5% (Figure

4.3). Although this is a typically stable population, expression of the pro-inflammatory activation marker Ly6C was increased to 5.2 ± 2.5%. N6022 reduced this pro-inflammatory activation as the population of Ly6C+ cells was reduced to 3.7 ± 3.2%. Over 90% of mature macrophages were negative for Ly6C as compared to the untreated population of just over 70%. Interestingly, LLC led to increased expression of Ly6G, a marker of granulocyticity typically found on neutrophils, immature monocytes and myeloid derived suppressor cells. Of these mature, tissue resident cells, 20.8 ± 12.3% were Ly6G+, while N6022 reduced this LLC associated phenotype to 6.1± 4.2%.

Figure 4.3

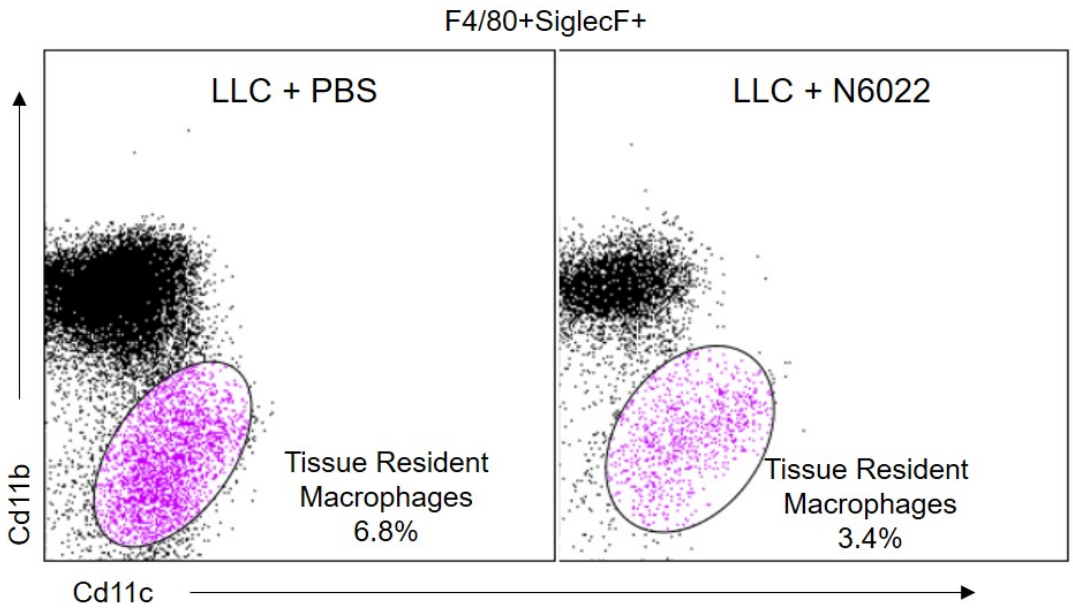

Tissue Resident Macrophages		
	% Ly6C+	% Ly6G+
LLC + PBS	5.2 ± 2.5	20.8 ± 12.3
LLC + N6022	3.7 ± 3.2	6.1± 4.2

Figure 4.3. Tissue Macrophage Activation Following LLC. SiglecF+ cells recovered from digested lung tissue were analyzed by FACS for expression of CD11c, CD11b, and Ly6C.

Percentages shown are % gated of indicated population. N6022 reduced expression of both Ly6C and G in resident macrophages.

LLC Induces F4/80+SiglecF-CD11bhi Tissue Macrophage Population

Following observation of tissue resident cells, we then proceeded to observe the F4/80+SiglecF- macrophage population. Selecting for those cells with positive CD11b expression in this population allows for observation of interstitial macrophages (IMs) and newly recruited macrophages that are negative for CD11c. Naïve mice, typically have a singular population of IMs that are CD11b+; however, mice with LLC tumors had two distinct populations of CD11b+ cells. The first population expressed CD11b at levels comparable to those typically associated with IMs. Because the novel population expressed higher levels of CD11b than the IMs, IMs were termed CD11blo and the novel population, presumably recently recruited macrophages were termed CD11bhi (Figure 4.4). In mice that were treated with PBS IMs were 9.1 ± 2.6% of SiglecF- cells, while the CD11bhi population was 17.4 ± 13.0%. N6022 reduced these populations to 6.1 ± 7.1% and 13.9 ± 16.7% respectively.

Figure 4.4

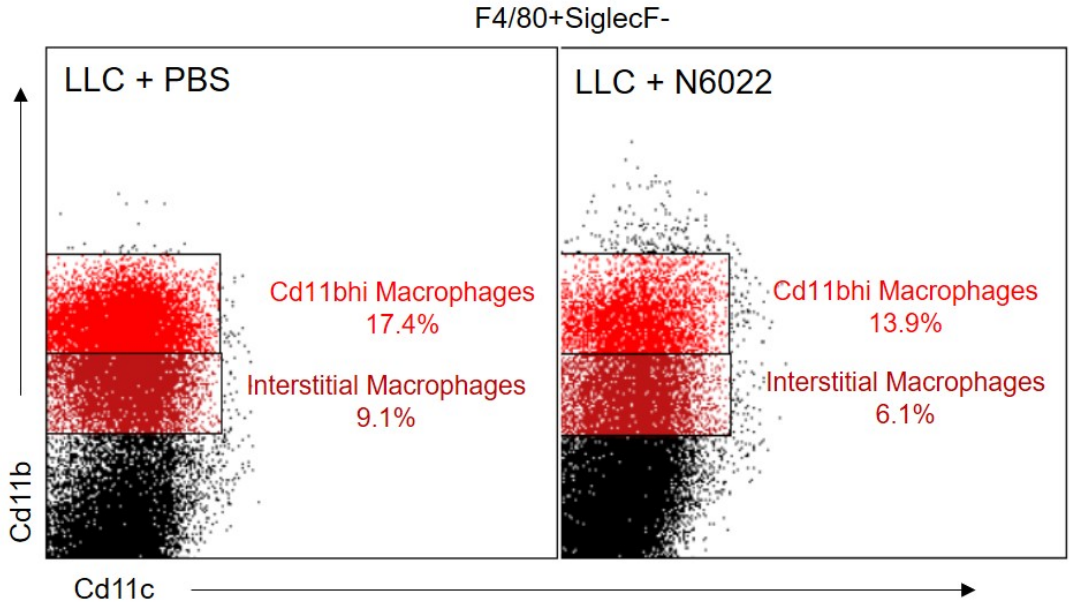

Cd11bhi Macrophages		
	% Ly6C+	% Ly6C+Ly6G+
LLC + PBS	61.0 ± 3.2	20.8 ± 12.3
LLC + N6022	6.5 ± 3.2	2.0 ± 1.8

Figure 4.4. Cd11bhi Macrophages Present in Tissue. SiglecF- cells recovered from digested lung tissue were analyzed by FACS for expression of Cd11c, Cd11b, and Ly6C. Percentages shown are % gated of indicated population. Administration of N6022 reduced markers of activation.

N6022 Alters Expression of Activation Markers in CD11bhi Tissue Population

We then sought to determine if N6022 altered the activation of this cell subset in response to LLC. We found that in response to LLC, 61.0 ± 3.2% of CD11bhi cells were Ly6C+, and 65.4 ± 8.4% in N6022 treated mice. When the population of cells that were double positive for both Ly6G and Ly6C were considered, we found that administration of N6022 reduced this population from 6.5 ± 3.2% to 2.0 ± 1.8%.

Effects on N6022 on Various Immune Cell Subsets

Eosinophils

Eosinophils are characterized by expression of F4/80, SiglecF, CD11b, Gr1 and the absence of CD11c. As eosinophilia has been implicated in several lung diseases including the LLC model of adenocarcinoma, we first sought to determine whether these cells were observable by FACS in our model. LLC mice had an overall increase in eosinophils, as 67.5 ± 10.6% of F4/80+SiglecF+CD11b+CD11c- cells were Gr1+ in untreated mice (Table 4.2). This population was reduced to 56.93 ± 9.9% by N6022. Because we used Ly6G and C separately as opposed to Gr1, we were able to distinguish two eosinophil subsets based on expression of Ly6G. Ly6G+ eosinophils were Ly6C+/-, while Ly6G- eosinophils were Ly6C+. Furthermore, we found that administration of N6022 affected each of these subsets differently. While N6022 decreased Ly6G+ eosinophils from 62.9 ± 24.3% to 55.0 ± 19.5%, Ly6C+ eosinophils were increased from 10.6 ± 1.8% to 20.5 ± 12.2%.

Table 4.2

	F4/80+SiglecF+Cd11c-Cd11b+		F4/80-SiglecF-Cd11c-Cd11b+			Cd3+	
	%Ly6G+Ly6C+/- Eosinophils	%Ly6G- Eosinophils	%Ly6G+ PMNs	%Ly6C+ Immature Macrophages	%Ly6G+Ly6C+ Immature Macrophages	Cd4 T Cell	Cd8 T Cell
LLC + PBS	62.9 ± 24.3	10.6 ± 1.8	23.3 ± 8.2	57.1 ± 19.8	1.06 ± 0.5	55.9 ± 2.3	27.7 ± 4.3
LLC + N6022	55.0 ± 19.5	20.5 ± 12.2	0.89 ± 0.9	73.2 ± 12.0	0.01 ± 0.01	49.6 ± 1.5	31.8 ± 3.4

Table 4.2. Additional Tissue Populations. Cells recovered from lung tissue were assessed based on expression of F4/80, SiglecF, Cd11b, Ly6G, and Ly6C. T lymphocytes were assessed based on expression of CD3. CD4, and CD8.

Neutrophils and Ly6C+ Immature Macrophages

Administration of N6022 led to an increase in the presence of F4/80- cells in the lung tissue. F4/80- cells are a diverse cell population and may be neutrophils, splenic/lymphoid macrophages, and myeloid derived suppressor cells. Overall, we found that N6022 increased this mixed population of cells. Of the total CD45+ cells recovered from the lung tissue, 25.8 ± 21.4% were F4/80- as opposed to the 52.3 ± 24.1% in N6022 treated mice (Table 4.2). We then found that N6022 also altered the cellular composition of this population. The first step in better defining this population, cells were analyzed based on positive expression of CD11b as well as the exclusion of CD11c and SiglecF positive cells. Neutrophils are typically distinguished by their expression of Ly6G, as well as their lack of Ly6C. We found that there was a signification PMN population in untreated mice that was not found in N6022 treated mice. 23.3 ± 8.2% of CD11b+ were Ly6G+Ly6C- as opposed to the minimal 0.89 ± 0.9%. We then observed an immature macrophage population that was Ly6G-Ly6C+ in our F4/80-SiglecF-CD11c-CD11b+ and found that this population was increased by N6022 from 57.1 ± 19.8% in untreated mice to 73.2 ± 12.0% in N6022 treated mice. We also observed that N6022 decreased the small population of cells that were double positive for Ly6G and Ly6C from 1.06 ± 0.5% to 0.01 ± 0.01%.

Lymphocytes

When we observed the CD3+ T lymphocyte population, we found that LLC cells led to a modest decrease in CD4+T cells, as the population of CD8+ T cells increased. This shift

in T cell population was enhanced by administration of N6022, as CD8+ T cells were marginally increased to 31.8 ± 3.4% of CD3+ cells as opposed to untreated mice, where CD8+ T cells were 27.7 ± 4.3% of CD3+ cells (Table 4.2). Activation of T cells as assessed by CD69 expression was unaltered. Surprisingly, expression of Th17 and Treg subsets of CD4+ cells were not induced in by LLC cells.

N6022 Alters Tissue Expression of Gr1

Immunohistochemical staining of left lung sections revealed minimal changes of CD11b staining in treated vs untreated mice; however, there was an overall alteration in the expression pattern of Gr1 in the same areas. In untreated mice, Gr1 staining was less intense than N6022 treated mice (Figure 4.5). The general staining patter however was more diffuse in untreated mice with areas of specific staining; whereas N6022 treated mice displayed only specific positive staining. When H&E stained slides were assessed in the same areas, we found altered immune cell populations. This was most notable in areas of necrosis within the tumor. In untreated mice, eosinophils and neutrophils were found in areas of necrosis. These cell populations were markedly reduced in N6022 mice, with macrophages being the primary observable immune cell present.

Figure 4.5

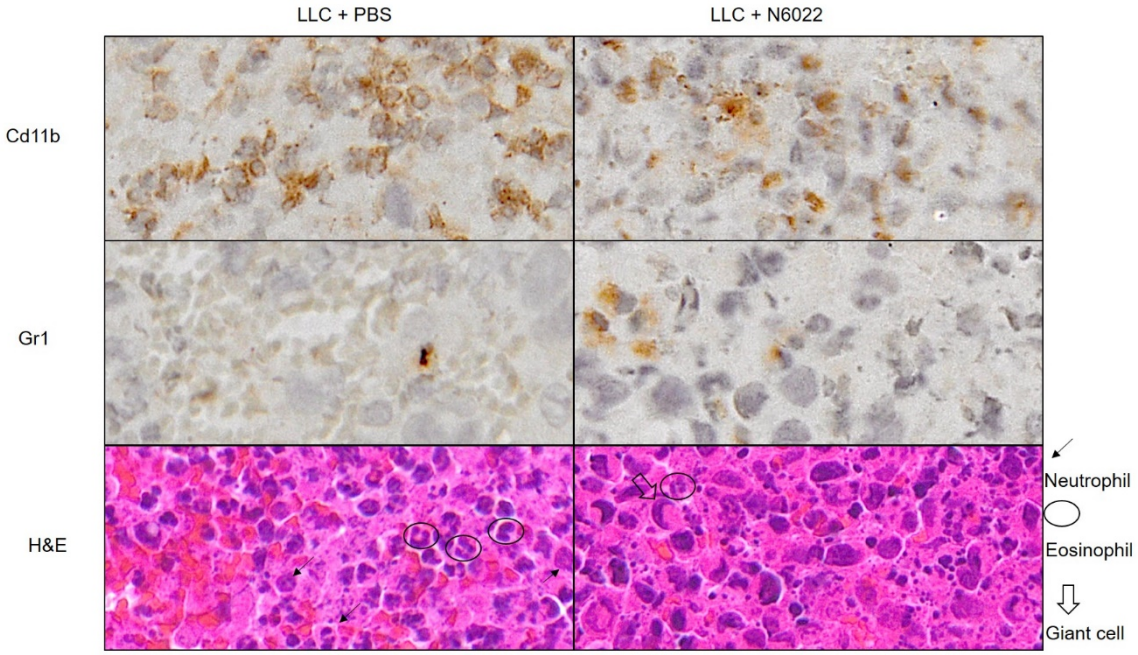

Figure 4.5. Tissue Expression of Cd11b and GR1. Left lungs were inflation fixed and paraffin-embedded. IHC staining of Cd11b and GR1 expression in necrotic areas of LLC tumors reveal altered staining patters. H&E sections of corresponding region for immune cell identification also demonstrate N6022 dependent changes in immune cell populations.

4.5 Discussion

In this study we use an established immunocompetent model of adenocarcinoma to observe chronic inflammatory signaling, and the contribution of primarily intracellular S-nitrosylation to this process. In this model, we observe the effects of inhibition of GSNOR on LLC tumor-based macrophage activation. N6022- induced immune cell composition and macrophage activation in both the alveolar and tissue and cellular compartments in response to the tumor microenvironment were accompanied by reduced tumor size in N6022 treated mice. While the development of LLC tumors did not lead to increased recruitment of macrophages to the alveolar space, we found that LLC derived signaling led to the recruitment of additional inflammatory cells types recovered from BAL fluid

including macrophages, neutrophils, eosinophils, and lymphocytes. N6022 administration led to a decreased pro-inflammatory response in alveolar macrophages but increased the presence mature F4/80+SiglecF- non-alveolar macrophages to the alveolar space. This observation was accompanied by a decrease in the immature F4/80-SiglecF- macrophage population. Interestingly, N6022 increased the expression of CD206 only in the latter population while leaving Ly6C expression unaltered in both populations. These is the first observations in this model that macrophage heterogeneity also leads to a heterogeneous response to inhibition of GSNOR.

This macrophage heterogeneity is further appreciated as the tissue associated cells were assessed. LLC led to the improper activation of the tissue resident population, as well the recruitment of pro-inflammatory macrophages. Surprisingly, N6022 either reduced or did not affect LLC dependent pro-inflammatory activation in the macrophage populations native to the lung when we consider the SiglecF+ tissue resident and SiglecF- IMs respectively. However, N6022 increased the pro-inflammatory recruited macrophage population. This suggests a potential mechanism by which N6022 may lead to reduced tumor development and brings macrophage diversity to light. Loss of pro-inflammatory activation of macrophages is a key mechanism of immunosuppression; but studies have often described the diversity of activation states found in the tumor microenvironment (171). It is possible, that the pro-inflammatory activation of these two populations contribute differently to tumor development and signaling. This is in accordance with previously published data describing not only distinct macrophage subpopulations, but also how these populations respond differently to LLC tumor development (171).

Observation of non-macrophage populations also revealed N6022 dependent changes on the recruitment of these cells. The recruitment of eosinophils in various lung diseases including cancer has long been observed and has gained greater appreciation (172-

174). However, the contribution and function of eosinophils to the development of lung disease has not yet been elucidated. Eosinophil heterogeneity has been documented in asthmatic models (175). One group uses GR1 and found two eosinophil subsets to be Gr1+ and Gr1- (176). As Gr1 is a combination of Ly6G and C, it is possible that our Ly6C+Ly6G- and Ly6G+ subsets are analogous, or eosinophil expression of Ly6C may eosinophils, their exact role in tumor suppression and tumor progression is unclear (177). In our model, reduction of neutrophils was observed with N6022 administration and reduced tumor growth. Delineation of both eosinophil and neutrophil subsets may provide clarity on these opposing effects.

The complexity of the immunosignaling and cellular heterogeneity highlights a significant limitation of this study. We have completed the first step in observing the immune response to LLC and its modifications by inhibition of GSNOR. However, none of these changes have been correlated with altered function and their distinct contributions and responses to the tumor microenvironment remain unknown. Our flow cytometric analysis of macrophages and neutrophils show populations expressing phenotypic markers typically associated with myeloid derived suppressor cells (178); however, these cells cannot be classified as such without confirmation of T cell suppressive activity on either effector function or proliferation. This is also of special interest as N6022 increased this subpopulation of macrophages. Basic flow cytometric analysis of the T cell population in LLC show modest modification in CD4 and CD8+ T cells, which was slightly altered with N6022. It is possible that N6022 altered the balance of Th1 vs Th2 CD4+ T cells however as this was not covered by our analysis, and eosinophilia is typically associated with Th2 CD4+ T cells. Ex vivo functional analysis of specific cell populations may go a long way in revealing the mechanisms by which these cells contribute to tumor progression.

Analysis of functional activity of obtained cells from the tumor microenvironment, while useful, still leaves an additional key aspect of the complexity of cancer immunosignaling unexplored. In this study, we were able to observe distinct cellular responses to different regions of the tumor. When we observed the tumor associated immune cells, N6022 reduced CD11b and Gr1 expression. As we moved into the tumor region and observed CD11b and Gr1 expression of infiltrating cells, we found that CD11b and Gr1 expression was not changed with N6022 administration. N6022's alteration of the immune response was most clear when the necrotic areas of the tumors were observed. In untreated mice, eosinophils and neutrophils were observed in this area, confirming previously published data on eosinophilia and neutrophilia to necrotic areas. Following administration of N6022, macrophages were the primary cells observed and they were smaller in size with some noticeable giant cells. This was especially interesting as areas of necrosis are typically hypoxic and HIF-1α is a key substrate of S-nitrosylation dependent signaling. Furthermore, hypoxia has been implicated in epithelial mesenchymal transition (179, 180). This process has been described and contributed to lung diseases characterized by tissue remodeling including cancer and fibrosis. The crosstalk between the immune system and the EMT process has recently gained traction as both have been found to be key events in cancer progression and metastasis.

In our model, we typically do not observe metastatic events, or multiple tumors per lung lobe. However, we observed a singular metastatic event to the kidney in an untreated mouse. In contrast, we also observed an unusually large tumor burden in an N6022 treated mouse. As NO-dependent signaling and S-nitrosylation has been implicated in reduction of EMT, it lends to the thought if metastatic pathways were downregulated by N6022, leading to an increased tumor burden. Additionally, as metastasis is dependent on the preconditioning of the metastatic niche as described in the seed and soil method

by the immune system, it is possible N6022 dependent inhibition of GSNOR altered immune function, inhibiting metastatic niche preconditioning (181).

In closing, this study further confirmed the importance of SNO dependent inflammatory signaling in chronic inflammation. The tumor microenvironment is extremely diverse, complex, and dynamic. We provide evidence that increased levels of GSNO is an effective mechanism to alter the tumor driven immunosignaling in the LLC model of adenocarcinoma. Importantly, these changes were associated with decreased tumor size. This study also presented additional evidence for immune cell heterogeneity within and across cell types. Better understanding of how these subpopulations respond to and interact with the tumor microenvironment, other immune cells, and which SNO pathways are relevant in their activation are all feasible next steps to understand the mechanism by which N6022 reduces tumor size.

Chapter 5: Summary, Discussion, Future Directions, Conclusion and Speculation

5.1 Summary

Macrophage activation is a key factor in maintenance of pulmonary homeostasis and normal lung function. Thus, inappropriate macrophage activation is implicated in lung disease. Inflammation is a requirement for preservation of the steady state in the lung as we constantly inhale stimuli such as particles and microbes; however, dysregulation of inflammatory signaling or improper activation in response to non-noxious stimuli adversely affects pulmonary function. iNOS function and iNOS derived NO is extremely critical to inflammatory signaling and macrophage activation both as an effector molecule, and signal transduction agent. In these studies, we focus on the latter role of NO in macrophage activation and immune signaling; observing the role of increased NO-based thiol modification in murine models of acute lung injury, fibrosis, and cancer. With techniques such as IHC, RT-qPCR, and flow cytometry we were able to perform immunophenotyping of pulmonary macrophage while observing the effects of SNO dependent signaling on overall disease outcome. Increased SNO signaling altered model-induced changes in macrophage activation, often times ultimately altering overall outcome. We utilized three models of pulmonary inflammation to assess inflammatory signaling in acute lung injury, resolution and repair, and chronic inflammatory signaling using O_3, ITB, and LLC respectively. In these studies we focused on model- induced changes in macrophage activation and subsequent changes to this phenotype induced by S-nitrosylation.

In all 3 models, changes to the pulmonary microenvironment led to changes in cellular recruitment to the BAL and/or tissue and altered macrophage activation (Table 5.1).

Table 5.1

	O_3	ITB- D.21 -fibrosis	ITB- D.8 -inflammation	LLC
Recruitment to alveolar space	Neutrophils, macrophages	Macrophages	Macrophages	Neutrophils, macrophages, eosinophils, lymphocytes
Recruitment to tissue	Neutrophils, macrophages	Macrophages, lymphocytes, fibroblasts	Macrophages	Neutrophils, macrophages, eosinophils, lymphocytes
Increased pro-inflammatory macrophage activation	Alveolar, interstitial macrophages	None observed	Alveolar, interstitial macrophages	Alveolar, tissue resident macrophages
Increased pro-reparative macrophage activation	Interstitial macrophages	Alveolar, interstitial macrophages	None observed	Not measured

Table 5.1. Recruitment and Macrophage Activation in Each Model. During acute inflammation, resolution and repair and chronic inflammatory signaling, similarities and differences in cellular recruitment and macrophages are observed.

We then observed the effects of increased S-nitrosylation on macrophage activation in these models. Along with our observations on macrophage phenotype, we used various markers of disease progression to determine if SNO driven changes in macrophage phenotype were associated with improved disease outcome. As summarized in Table 5.2, we observed that increased S-nitrosylation altered macrophage phenotype in all

models of pulmonary inflammation and improved overall pathology in both models of acute lung injury and tumor progression but not in ITB-induced fibrosis.

Table 5.2

	O_3	ITB- D.21	ITB- D.8	LLC
Changes to total recruitment	None observed	None observed	None observed	None observed
Changes in recruited cell types	Reduced neutrophilia	None observed	None observed	Reduced eosinophils, and lymphocytes
Changes to macrophage phenotype	Reduced pro-inflammatory activation, increased pro-reparative activation	Reduced pro-inflammatory activation, increased pro-reparative activation	Reduced pro-inflammatory activation	Reduced pro-inflammatory activation
Changes to overall pathology	Reduced epithelial damage, and oxidative stress	No change observed	Reduced epithelial damage	Reduced tumor progression

Table 5.2. Effects of Increased S-nitrosylation in Each Model. In all models, increased S-nitrosylation altered model-induced change in macrophages. With the exception of ITB-induced fibrosis, these changes were accompanied by improvements in measures of disease outcome.

5.2 Discussion

The importance of NO has long been appreciated in physiology and inflammatory signaling, primarily as an effector molecule. In the immune system, iNOS is the primary

source of NO, expressed in macrophages and neutrophils. iNOS and iNOS-derived NO are especially relevant to macrophage activation as increased expression of iNOS has been associated with pro-inflammatory and Th1 biased immune responses. In contrast, pro-reparative macrophages have lower levels of iNOS in comparison to Arginase and are associated with Th2 biased responses. As a biomolecule, NO's reactivity outside of RONS has recently come to greater appreciation as NO's reactivity with thiols in the formation of SNOs has emerged as an additional mechanism of immune signaling regulation. Several key transcription factors and enzymes that play a role in immune signaling and macrophage activation have altered function upon S-nitrosylation. In chapters 2-4, we observe that increased SNO signaling is capable of altering inflammatory signaling, macrophage activation with or without improvement to the overall disease outcome.

In all three models, we observe that in response to dysregulation, increased SNO formation limits expression of pro-inflammatory macrophage activation. Based on the current literature we can speculate ont a few potential mechanisms that may contribute to these observations as this was not investigated in the scope of this work. S-nitrosylation of the both the p50 and p65 subunits of NFκB have been associated with decreased activity and thus downregulation of NFκB-dependent gene signaling. This pathway is first relevant directly to macrophage activation as key pro-inflammatory protein are genetically regulated by NFκ-B including iNOS, IL-1β , IL-6, IFN, TNFα and several chemokines such as CCL1, eotaxin, and CCL5 (3, 182-187). Enhanced SNO donation capitalizes on increased nitrosothiol signaling without requiring increased levels of NO, reducing undesired NO based reactivity with non-thiol targets. Support of this concept is provided by the use of inhaled ENO as opposed to inhaled NO in clinical settings, as NO's reactivity with non-thiols often contribute to off target effects and pathology (188). Additionally, NFκ-B activity in pulmonary epithelial cells has been

associated with increased inflammatory signaling in models of asthmatic inflammation, as well as ozone induced acute lung injury (189-191). SNO dependent reduction of NFκ-B has been found to affect the nature of cancer cells, decreasing proliferation, and enhancing responsiveness to chemotherapeutics (192). As the interaction between the pulmonary microenvironment and macrophage activation are bidirectional, SNO-dependent reduction of NFκ-B signaling may not only contribute to reduced macrophage activation but also improve disease outcome through alteration of signaling of the lung microenvironment itself.

SNO-dependent downregulation of the IL-6/STAT3 signaling pathway may also contribute to our observations. Not only is IL-6 a NFκ-B -controlled gene, but STAT3 is also a substrate for S-nitrosylation, opposing activation by phosphorylation (156, 192). Our findings of reduced IL-6 mRNA as well as reduced Phospho-STAT3 following increased levels of GSNO in response to bleomycin certainly support that this is may be a relevant pathway in the nitrosothiol based regulation of macrophage inflammatory signaling. This pathway likely holds more relevance in our model of adenocarcinoma, as opposed to our models of ozone induced acute lung injury, and bleomycin induced inflammation, and subsequent fibrosis. STAT3 dependent inflammatory signaling has been associated with pro-tumorigenic/pro-reparative/pro-fibrotic macrophage polarization, often antagonizing the pro-inflammatory/tumoricidal response of the immune system (193). N6022 reduced LLC tumor size, decreased resident macrophage pro-inflammatory activation, while increasing pro-inflammatory activation of select macrophage subsets.

Through advances in immunophenotyping by flow cytometry, allowing for better definition of macrophage and additional immune cell subsets, we were able to observe differential effects of increased SNO formation in macrophage subsets, and noted SNO mediated effects on additional cell types in tumorigenic signaling. This is certainly in

correspondence with previous findings in our own lab as well as published literature detailing pulmonary macrophage heterogeneity and iNOS function based on origin and location (27, 116, 194).

Interestingly, despite the relevance of SNO-dependent pro-reparative signaling through pathways such as HIF-1α and Nrf2, our data provided very little evidence that increased SNO donation leads to increased pro-reparative signaling. Outside of SNOPPM's and ENO's increase in HO-1 and Ym1 staining, all SNO donors did not modify additional markers of M2 macrophages such as Ym1 and expression of CD206. This however may be a consequence of our selection of markers for M2 markers and pro-reparative signaling. The M2 macrophage signaling spectrum is incredibly broad, and it is possible that we did not select markers to adequately assess the effects of increased SNO donation on this population (195).

Taken together, these data demonstrate the complexity, and stimulus dependent nature of inflammatory signaling in the lung, both across and within cell types as well as the complexity of S-nitrosylation. However, our endpoints of macrophage activation, as well as overall disease outcome provided further evidence that SNO formation plays a key role in regulation of immunosignaling and macrophage phenotype, and thus represents a viable target for therapeutic intervention in lung disease.

5.3 Future Directions

We utilized multiple models of lung inflammation to observe disease induced alterations in macrophage phenotype, and SNO based opposition of these changes. As SNO donors successfully modified immunosignaling in all three models, investigation of the specific SNO-modified pathways involved in each model, and how these changes contributed to changes in macrophage activation and/or the pulmonary microenvironment would be an informative follow-up. This would potentially allow for

tailoring of SNO donors to specific diseases based on pathology and contributions of the immune system, while reducing off target effects. The presented work also delves into macrophage phenotype and subpopulations in various models of lung disease. However, it is unclear how these specific populations contribute to the disease pathology, as well as how their SNO-dependent alterations played a role in improved disease outcome. A logical and informative next step would be to correlate these phenotypic based subpopulations with functional activity. Assessment of macrophage activity, their interactions with the pulmonary microenvironment, as well as other immune cell types to further distinguish subpopulations, and their contributions to disease would capitalize upon previous findings. This would be especially relevant for diseases such as cancer and fibrosis where the microenvironment is complex, dynamic, and heterogeneous.

5.4 Conclusions and Speculation

Pulmonary macrophages are a diverse cell population, tasked with maintenance of homeostasis. Dysregulation of inflammation leads to inappropriate macrophage activation which may further contribute to disease pathology as opposed to improving it. The crosstalk between the lung microenvironment and macrophages often presents a “chicken and egg” paradox, thus creating necessity for understanding of disease pathology and etiology. There are several mechanisms by which immune signaling is regulated, and S-nitrosylation has recently gained traction as a highly relevant mechanism, especially as iNOS activity and expression has proven to be critical to immunity, macrophage function and has been implicated in disease pathology. In pathologically distinct models of inflammatory signaling, increased SNO formation altered macrophage phenotype in response to disease, leading to improved overall outcome with the exception of bleomycin induced fibrosis. Our findings demonstrate that

macrophage activation may potentially be an effective therapeutic target in pulmonary disease, as well as demonstrate that SNO donation is a feasible mechanism to alter inflammatory signaling and macrophage phenotype, as well as the lung microenvironment; however, these effects are dependent on disease mechanism.

References

1. Lowenstein CJ, Padalko E. iNOS (NOS2) at a glance. J Cell Sci. 2004;117(Pt 14):2865-7. Epub 2004/06/16. doi: 10.1242/jcs.01166. PubMed PMID: 15197240.
2. Cathcart MK. Regulation of superoxide anion production by NADPH oxidase in monocytes/macrophages: contributions to atherosclerosis. Arterioscler Thromb Vasc Biol. 2004;24(1):23-8. Epub 2003/10/04. doi: 10.1161/01.ATV.0000097769.47306.12. PubMed PMID: 14525794.
3. Marshall HE, Hess DT, Stamler JS. S-nitrosylation: physiological regulation of NF-kappaB. Proc Natl Acad Sci U S A. 2004;101(24):8841-2. doi: 10.1073/pnas.0403034101. PubMed PMID: 15187230; PMCID: PMC428432.
4. Drapier JC, Pellat C, Henry Y. Generation of EPR-detectable nitrosyl-iron complexes in tumor target cells cocultured with activated macrophages. J Biol Chem. 1991;266(16):10162-7. Epub 1991/06/05. PubMed PMID: 1645341.
5. Li Q, Li C, Mahtani HK, Du J, Patel AR, Lancaster JR, Jr. Nitrosothiol formation and protection against Fenton chemistry by nitric oxide-induced dinitrosyliron complex formation from anoxia-initiated cellular chelatable iron increase. J Biol Chem. 2014;289(29):19917-27. Epub 2014/06/04. doi: 10.1074/jbc.M114.569764. PubMed PMID: 24891512; PMCID: PMC4106312.
6. Gordon S. Elie Metchnikoff: father of natural immunity. Eur J Immunol. 2008;38(12):3257-64. Epub 2008/11/29. doi: 10.1002/eji.200838855. PubMed PMID: 19039772.
7. Martinez FO, Gordon S. The M1 and M2 paradigm of macrophage activation: time for reassessment. F1000Prime Rep. 2014;6:13. Epub 2014/03/29. doi: 10.12703/P6-13. PubMed PMID: 24669294; PMCID: PMC3944738.
8. Mantovani A, Biswas SK, Galdiero MR, Sica A, Locati M. Macrophage plasticity and polarization in tissue repair and remodelling. J Pathol. 2013;229(2):176-85. Epub 2012/10/26. doi: 10.1002/path.4133. PubMed PMID: 23096265.
9. Mosser DM, Edwards JP. Exploring the full spectrum of macrophage activation. Nat Rev Immunol. 2008;8(12):958-69. Epub 2008/11/26. doi: 10.1038/nri2448. PubMed PMID: 19029990; PMCID: PMC2724991.
10. Epelman S, Lavine KJ, Randolph GJ. Origin and functions of tissue macrophages. Immunity. 2014;41(1):21-35. Epub 2014/07/19. doi: 10.1016/j.immuni.2014.06.013. PubMed PMID: 25035951; PMCID: PMC4470379.
11. Holt PG. Inhibitory activity of unstimulated alveolar macrophages on T-lymphocyte blastogenic response. Am Rev Respir Dis. 1978;118(4):791-3. Epub 1978/10/01. doi: 10.1164/arrd.1978.118.4.791. PubMed PMID: 309295.
12. Hoidal JR, Schmeling D, Peterson PK. Phagocytosis, bacterial killing, and metabolism by purified human lung phagocytes. J Infect Dis. 1981;144(1):61-71. Epub 1981/07/01. PubMed PMID: 7021701.
13. Lyons CR, Ball EJ, Toews GB, Weissler JC, Stastny P, Lipscomb MF. Inability of human alveolar macrophages to stimulate resting T cells correlates with decreased antigen-specific T cell-macrophage binding. J Immunol. 1986;137(4):1173-80. Epub 1986/08/15. PubMed PMID: 2426354.
14. Gibbings SL, Thomas SM, Atif SM, McCubbrey AL, Desch AN, Danhorn T, Leach SM, Bratton DL, Henson PM, Janssen WJ, Jakubzick CV. Three Unique

Interstitial Macrophages in the Murine Lung at Steady State. Am J Respir Cell Mol Biol. 2017;57(1):66-76. Epub 2017/03/04. doi: 10.1165/rcmb.2016-0361OC. PubMed PMID: 28257233; PMCID: PMC5516280.
15. Cai Y, Sugimoto C, Arainga M, Alvarez X, Didier ES, Kuroda MJ. In vivo characterization of alveolar and interstitial lung macrophages in rhesus macaques: implications for understanding lung disease in humans. J Immunol. 2014;192(6):2821-9. Epub 2014/02/19. doi: 10.4049/jimmunol.1302269. PubMed PMID: 24534529; PMCID: PMC3959879.
16. Draijer C, Penke LRK, Peters-Golden M. Distinctive Effects of GM-CSF and M-CSF on Proliferation and Polarization of Two Major Pulmonary Macrophage Populations. J Immunol. 2019. Epub 2019/03/15. doi: 10.4049/jimmunol.1801387. PubMed PMID: 30867240.
17. Westphalen K, Gusarova GA, Islam MN, Subramanian M, Cohen TS, Prince AS, Bhattacharya J. Sessile alveolar macrophages communicate with alveolar epithelium to modulate immunity. Nature. 2014;506(7489):503-6. Epub 2014/01/28. doi: 10.1038/nature12902. PubMed PMID: 24463523; PMCID: PMC4117212.
18. Bedoret D, Wallemacq H, Marichal T, Desmet C, Quesada Calvo F, Henry E, Closset R, Dewals B, Thielen C, Gustin P, de Leval L, Van Rooijen N, Le Moine A, Vanderplasschen A, Cataldo D, Drion PV, Moser M, Lekeux P, Bureau F. Lung interstitial macrophages alter dendritic cell functions to prevent airway allergy in mice. J Clin Invest. 2009;119(12):3723-38. Epub 2009/11/13. doi: 10.1172/JCI39717. PubMed PMID: 19907079; PMCID: PMC2786798.
19. Janssen WJ, McPhillips KA, Dickinson MG, Linderman DJ, Morimoto K, Xiao YQ, Oldham KM, Vandivier RW, Henson PM, Gardai SJ. Surfactant proteins A and D suppress alveolar macrophage phagocytosis via interaction with SIRP alpha. Am J Respir Crit Care Med. 2008;178(2):158-67. doi: 10.1164/rccm.200711-1661OC. PubMed PMID: 18420961; PMCID: 2453510.
20. Zaslona Z, Przybranowski S, Wilke C, van Rooijen N, Teitz-Tennenbaum S, Osterholzer JJ, Wilkinson JE, Moore BB, Peters-Golden M. Resident alveolar macrophages suppress, whereas recruited monocytes promote, allergic lung inflammation in murine models of asthma. J Immunol. 2014;193(8):4245-53. doi: 10.4049/jimmunol.1400580. PubMed PMID: 25225663; PMCID: 4185233.
21. Fernandez S, Jose P, Avdiushko MG, Kaplan AM, Cohen DA. Inhibition of IL-10 receptor function in alveolar macrophages by Toll-like receptor agonists. J Immunol. 2004;172(4):2613-20. Epub 2004/02/07. PubMed PMID: 14764735.
22. Coker RK, Laurent GJ, Shahzeidi S, Hernandez-Rodriguez NA, Pantelidis P, du Bois RM, Jeffery PK, McAnulty RJ. Diverse cellular TGF-beta 1 and TGF-beta 3 gene expression in normal human and murine lung. Eur Respir J. 1996;9(12):2501-7. Epub 1996/12/01. PubMed PMID: 8980960.
23. Yona S, Kim KW, Wolf Y, Mildner A, Varol D, Breker M, Strauss-Ayali D, Viukov S, Guilliams M, Misharin A, Hume DA, Perlman H, Malissen B, Zelzer E, Jung S. Fate mapping reveals origins and dynamics of monocytes and tissue macrophages under homeostasis. Immunity. 2013;38(1):79-91. doi: 10.1016/j.immuni.2012.12.001. PubMed PMID: 23273845; PMCID: 3908543.
24. Gibbings SL, Goyal R, Desch AN, Leach SM, Prabagar M, Atif SM, Bratton DL, Janssen W, Jakubzick CV. Transcriptome analysis highlights the conserved difference

between embryonic and postnatal-derived alveolar macrophages. Blood. 2015;126(11):1357-66. doi: 10.1182/blood-2015-01-624809. PubMed PMID: 26232173; PMCID: 4566811.
25. Mould KJ, Barthel L, Mohning MP, Thomas SM, McCubbrey AL, Danhorn T, Leach SM, Fingerlin TE, O'Connor BP, Reisz JA, D'Alessandro A, Bratton DL, Jakubzick CV, Janssen WJ. Cell Origin Dictates Programming of Resident versus Recruited Macrophages during Acute Lung Injury. Am J Respir Cell Mol Biol. 2017;57(3):294-306. doi: 10.1165/rcmb.2017-0061OC. PubMed PMID: 28421818.
26. Okuma T, Terasaki Y, Kaikita K, Kobayashi H, Kuziel WA, Kawasuji M, Takeya M. C-C chemokine receptor 2 (CCR2) deficiency improves bleomycin-induced pulmonary fibrosis by attenuation of both macrophage infiltration and production of macrophage-derived matrix metalloproteinases. J Pathol. 2004;204(5):594-604. doi: 10.1002/path.1667. PubMed PMID: 15538737.
27. Misharin AV, Morales-Nebreda L, Reyfman PA, Cuda CM, Walter JM, McQuattie-Pimentel AC, Chen CI, Anekalla KR, Joshi N, Williams KJN, Abdala-Valencia H, Yacoub TJ, Chi M, Chiu S, Gonzalez-Gonzalez FJ, Gates K, Lam AP, Nicholson TT, Homan PJ, Soberanes S, Dominguez S, Morgan VK, Saber R, Shaffer A, Hinchcliff M, Marshall SA, Bharat A, Berdnikovs S, Bhorade SM, Bartom ET, Morimoto RI, Balch WE, Sznajder JI, Chandel NS, Mutlu GM, Jain M, Gottardi CJ, Singer BD, Ridge KM, Bagheri N, Shilatifard A, Budinger GRS, Perlman H. Monocyte-derived alveolar macrophages drive lung fibrosis and persist in the lung over the life span. J Exp Med. 2017;214(8):2387-404. Epub 2017/07/12. doi: 10.1084/jem.20162152. PubMed PMID: 28694385; PMCID: PMC5551573.
28. Barletta KE, Cagnina RE, Wallace KL, Ramos SI, Mehrad B, Linden J. Leukocyte compartments in the mouse lung: distinguishing between marginated, interstitial, and alveolar cells in response to injury. J Immunol Methods. 2012;375(1-2):100-10. Epub 2011/10/15. doi: 10.1016/j.jim.2011.09.013. PubMed PMID: 21996427; PMCID: PMC3328189.
29. Kugathasan K, Roediger EK, Small CL, McCormick S, Yang P, Xing Z. CD11c+ antigen presenting cells from the alveolar space, lung parenchyma and spleen differ in their phenotype and capabilities to activate naive and antigen-primed T cells. BMC Immunol. 2008;9:48. doi: 10.1186/1471-2172-9-48. PubMed PMID: 18700962; PMCID: 2527294.
30. Kambara K, Ohashi W, Tomita K, Takashina M, Fujisaka S, Hayashi R, Mori H, Tobe K, Hattori Y. In vivo depletion of CD206+ M2 macrophages exaggerates lung injury in endotoxemic mice. Am J Pathol. 2015;185(1):162-71. Epub 2014/12/03. doi: 10.1016/j.ajpath.2014.09.005. PubMed PMID: 25447055.
31. Moon HG, Cao Y, Yang J, Lee JH, Choi HS, Jin Y. Lung epithelial cell-derived extracellular vesicles activate macrophage-mediated inflammatory responses via ROCK1 pathway. Cell Death Dis. 2015;6:e2016. doi: 10.1038/cddis.2015.282. PubMed PMID: 26658190; PMCID: 4720875.
32. Emura I, Usuda H, Togashi K, Satou K. Minute lesions of alveolar damage in lungs of patients with stable idiopathic pulmonary fibrosis. Histopathology. 2015;67(1):90-5. doi: 10.1111/his.12631. PubMed PMID: 25491592.
33. Sunil VR, Francis M, Vayas KN, Cervelli JA, Choi H, Laskin JD, Laskin DL. Regulation of ozone-induced lung inflammation and injury by the beta-galactoside-

binding lectin galectin-3. Toxicol Appl Pharmacol. 2015;284(2):236-45. Epub 2015/03/01. doi: 10.1016/j.taap.2015.02.002. PubMed PMID: 25724551; PMCID: PMC4408237.
34. Huang X, Xiu H, Zhang S, Zhang G. The Role of Macrophages in the Pathogenesis of ALI/ARDS. Mediators Inflamm. 2018;2018:1264913. Epub 2018/06/29. doi: 10.1155/2018/1264913. PubMed PMID: 29950923; PMCID: PMC5989173.
35. Tao B, Jin W, Xu J, Liang Z, Yao J, Zhang Y, Wang K, Cheng H, Zhang X, Ke Y. Myeloid-specific disruption of tyrosine phosphatase Shp2 promotes alternative activation of macrophages and predisposes mice to pulmonary fibrosis. J Immunol. 2014;193(6):2801-11. doi: 10.4049/jimmunol.1303463. PubMed PMID: 25127857.
36. Xi Y, Tan K, Brumwell AN, Chen SC, Kim YH, Kim TJ, Wei Y, Chapman HA. Inhibition of epithelial-to-mesenchymal transition and pulmonary fibrosis by methacycline. Am J Respir Cell Mol Biol. 2014;50(1):51-60. doi: 10.1165/rcmb.2013-0099OC. PubMed PMID: 23944988; PMCID: 3930932.
37. Ueno M, Maeno T, Nomura M, Aoyagi-Ikeda K, Matsui H, Hara K, Tanaka T, Iso T, Suga T, Kurabayashi M. Hypoxia-inducible factor-1alpha mediates TGF-beta-induced PAI-1 production in alveolar macrophages in pulmonary fibrosis. Am J Physiol Lung Cell Mol Physiol. 2011;300(5):L740-52. doi: 10.1152/ajplung.00146.2010. PubMed PMID: 21239537.
38. Prasse A, Pechkovsky DV, Toews GB, Jungraithmayr W, Kollert F, Goldmann T, Vollmer E, Muller-Quernheim J, Zissel G. A vicious circle of alveolar macrophages and fibroblasts perpetuates pulmonary fibrosis via CCL18. American journal of respiratory and critical care medicine. 2006;173(7):781-92. doi: 10.1164/rccm.200509-1518OC. PubMed PMID: 16415274.
39. Daba MH, El-Tahir KE, Al-Arifi MN, Gubara OA. Drug-induced pulmonary fibrosis. Saudi Med J. 2004;25(6):700-6. Epub 2004/06/15. PubMed PMID: 15195196.
40. Gibbons MA, MacKinnon AC, Ramachandran P, Dhaliwal K, Duffin R, Phythian-Adams AT, van Rooijen N, Haslett C, Howie SE, Simpson AJ, Hirani N, Gauldie J, Iredale JP, Sethi T, Forbes SJ. Ly6Chi monocytes direct alternatively activated profibrotic macrophage regulation of lung fibrosis. Am J Respir Crit Care Med. 2011;184(5):569-81. Epub 2011/06/18. doi: 10.1164/rccm.201010-1719OC. PubMed PMID: 21680953.
41. Wynn TA, Vannella KM. Macrophages in Tissue Repair, Regeneration, and Fibrosis. Immunity. 2016;44(3):450-62. Epub 2016/03/18. doi: 10.1016/j.immuni.2016.02.015. PubMed PMID: 26982353; PMCID: PMC4794754.
42. Byrne AJ, Maher TM, Lloyd CM. Pulmonary Macrophages: A New Therapeutic Pathway in Fibrosing Lung Disease? Trends Mol Med. 2016;22(4):303-16. Epub 2016/03/17. doi: 10.1016/j.molmed.2016.02.004. PubMed PMID: 26979628.
43. Lopez-Rodriguez E, Gay-Jordi G, Mucci A, Lachmann N, Serrano-Mollar A. Lung surfactant metabolism: early in life, early in disease and target in cell therapy. Cell Tissue Res. 2017;367(3):721-35. Epub 2016/10/27. doi: 10.1007/s00441-016-2520-9. PubMed PMID: 27783217.

44. Carey B, Trapnell BC. The molecular basis of pulmonary alveolar proteinosis. Clin Immunol. 2010;135(2):223-35. Epub 2010/03/27. doi: 10.1016/j.clim.2010.02.017. PubMed PMID: 20338813; PMCID: PMC2866141.
45. Marcus A, Gowen BG, Thompson TW, Iannello A, Ardolino M, Deng W, Wang L, Shifrin N, Raulet DH. Recognition of tumors by the innate immune system and natural killer cells. Adv Immunol. 2014;122:91-128. Epub 2014/02/11. doi: 10.1016/B978-0-12-800267-4.00003-1. PubMed PMID: 24507156; PMCID: PMC4228931.
46. Tveita AA, Schjesvold F, Haabeth OA, Fauskanger M, Bogen B. Tumors Escape CD4+ T-cell-Mediated Immunosurveillance by Impairing the Ability of Infiltrating Macrophages to Indirectly Present Tumor Antigens. Cancer research. 2015;75(16):3268-78. doi: 10.1158/0008-5472.CAN-14-3640. PubMed PMID: 26038231.
47. Feng M, Chen JY, Weissman-Tsukamoto R, Volkmer JP, Ho PY, McKenna KM, Cheshier S, Zhang M, Guo N, Gip P, Mitra SS, Weissman IL. Macrophages eat cancer cells using their own calreticulin as a guide: roles of TLR and Btk. Proc Natl Acad Sci U S A. 2015;112(7):2145-50. Epub 2015/02/04. doi: 10.1073/pnas.1424907112. PubMed PMID: 25646432; PMCID: PMC4343163.
48. Yoshihama S, Roszik J, Downs I, Meissner TB, Vijayan S, Chapuy B, Sidiq T, Shipp MA, Lizee GA, Kobayashi KS. NLRC5/MHC class I transactivator is a target for immune evasion in cancer. Proc Natl Acad Sci U S A. 2016;113(21):5999-6004. Epub 2016/05/11. doi: 10.1073/pnas.1602069113. PubMed PMID: 27162338; PMCID: PMC4889388.
49. Prado-Garcia H, Romero-Garcia S, Puerto-Aquino A, Rumbo-Nava U. The PD-L1/PD-1 pathway promotes dysfunction, but not "exhaustion", in tumor-responding T cells from pleural effusions in lung cancer patients. Cancer Immunol Immunother. 2017;66(6):765-76. Epub 2017/03/16. doi: 10.1007/s00262-017-1979-x. PubMed PMID: 28289860.
50. Stronen E, Toebes M, Kelderman S, van Buuren MM, Yang W, van Rooij N, Donia M, Boschen ML, Lund-Johansen F, Olweus J, Schumacher TN. Targeting of cancer neoantigens with donor-derived T cell receptor repertoires. Science. 2016;352(6291):1337-41. Epub 2016/05/21. doi: 10.1126/science.aaf2288. PubMed PMID: 27198675.
51. Ribatti D. The concept of immune surveillance against tumors. The first theories. Oncotarget. 2016. doi: 10.18632/oncotarget.12739. PubMed PMID: 27764780.
52. Folkman J, Merler E, Abernathy C, Williams G. Isolation of a tumor factor responsible for angiogenesis. J Exp Med. 1971;133(2):275-88. PubMed PMID: 4332371; PMCID: 2138906.
53. Li S, Wang N, Brodt P. Metastatic cells can escape the proapoptotic effects of TNF-alpha through increased autocrine IL-6/STAT3 signaling. Cancer research. 2012;72(4):865-75. doi: 10.1158/0008-5472.CAN-11-1357. PubMed PMID: 22194466.
54. Bunt SK, Sinha P, Clements VK, Leips J, Ostrand-Rosenberg S. Inflammation induces myeloid-derived suppressor cells that facilitate tumor progression. J Immunol. 2006;176(1):284-90. PubMed PMID: 16365420.

55. Gajewski TF, Schreiber H, Fu YX. Innate and adaptive immune cells in the tumor microenvironment. Nat Immunol. 2013;14(10):1014-22. doi: 10.1038/ni.2703. PubMed PMID: 24048123; PMCID: 4118725.
56. Chao T, Furth EE, Vonderheide RH. CXCR2-Dependent Accumulation of Tumor-Associated Neutrophils Regulates T-cell Immunity in Pancreatic Ductal Adenocarcinoma. Cancer Immunol Res. 2016;4(11):968-82. doi: 10.1158/2326-6066.CIR-16-0188. PubMed PMID: 27737879; PMCID: 5110270.
57. Peppicelli S, Andreucci E, Ruzzolini J, Laurenzana A, Margheri F, Fibbi G, Del Rosso M, Bianchini F, Calorini L. The acidic microenvironment as a possible niche of dormant tumor cells. Cell Mol Life Sci. 2017. doi: 10.1007/s00018-017-2496-y. PubMed PMID: 28331999.
58. Miligy I, Mohan P, Gaber A, Aleskandarany MA, Nolan CC, Diez-Rodriguez M, Mukherjee A, Chapman C, Ellis IO, Green AR, Rakha EA. Prognostic significance of Tumour infiltrating B-Lymphocytes in Breast Ductal Carcinoma in Situ. Histopathology. 2017. doi: 10.1111/his.13217. PubMed PMID: 28326600.
59. Prado-Garcia H, Romero-Garcia S, Puerto-Aquino A, Rumbo-Nava U. The PD-L1/PD-1 pathway promotes dysfunction, but not "exhaustion", in tumor-responding T cells from pleural effusions in lung cancer patients. Cancer Immunol Immunother. 2017. doi: 10.1007/s00262-017-1979-x. PubMed PMID: 28289860.
60. Duechler M, Peczek L, Zuk K, Zalesna I, Jeziorski A, Czyz M. The heterogeneous immune microenvironment in breast cancer is affected by hypoxia-related genes. Immunobiology. 2014;219(2):158-65. doi: 10.1016/j.imbio.2013.09.003. PubMed PMID: 24091277.
61. Van Overmeire E, Laoui D, Keirsse J, Van Ginderachter JA, Sarukhan A. Mechanisms driving macrophage diversity and specialization in distinct tumor microenvironments and parallelisms with other tissues. Front Immunol. 2014;5:127. doi: 10.3389/fimmu.2014.00127. PubMed PMID: 24723924; PMCID: 3972476.
62. Piccolo V, Curina A, Genua M, Ghisletti S, Simonatto M, Sabo A, Amati B, Ostuni R, Natoli G. Opposing macrophage polarization programs show extensive epigenomic and transcriptional cross-talk. Nat Immunol. 2017;18(5):530-40. doi: 10.1038/ni.3710. PubMed PMID: 28288101.
63. Weitsman G, Mitchell NJ, Evans R, Cheung A, Kalber TL, Bofinger R, Fruhwirth GO, Keppler M, Wright ZV, Barber PR, Gordon P, de Koning T, Wulaningsih W, Sander K, Vojnovic B, Ameer-Beg S, Lythgoe M, Arnold JN, Arstad E, Festy F, Hailes HC, Tabor AB, Ng T. Detecting intratumoral heterogeneity of EGFR activity by liposome-based in vivo transfection of a fluorescent biosensor. Oncogene. 2017. doi: 10.1038/onc.2016.522. PubMed PMID: 28166195.
64. Egeblad M, Ewald AJ, Askautrud HA, Truitt ML, Welm BE, Bainbridge E, Peeters G, Krummel MF, Werb Z. Visualizing stromal cell dynamics in different tumor microenvironments by spinning disk confocal microscopy. Dis Model Mech. 2008;1(2-3):155-67; discussion 65. doi: 10.1242/dmm.000596. PubMed PMID: 19048079; PMCID: 2562195.
65. Lesokhin AM, Hohl TM, Kitano S, Cortez C, Hirschhorn-Cymerman D, Avogadri F, Rizzuto GA, Lazarus JJ, Pamer EG, Houghton AN, Merghoub T, Wolchok JD. Monocytic CCR2(+) myeloid-derived suppressor cells promote immune escape

by limiting activated CD8 T-cell infiltration into the tumor microenvironment. Cancer research. 2012;72(4):876-86. doi: 10.1158/0008-5472.CAN-11-1792. PubMed PMID: 22174368; PMCID: 3288305.
66. Wang A, Lu C, Ning Z, Gao W, Xie Y, Zhang N, Liang J, Abbasi FS, Yan Q, Liu J. Tumor-associated macrophages promote Ezrin phosphorylation-mediated epithelial-mesenchymal transition in lung adenocarcinoma through FUT4/LeY up-regulation. Oncotarget. 2017;8(17):28247-59. doi: 10.18632/oncotarget.16001. PubMed PMID: 28423676; PMCID: 5438647.
67. Sharma SK, Chintala NK, Vadrevu SK, Patel J, Karbowniczek M, Markiewski MM. Pulmonary alveolar macrophages contribute to the premetastatic niche by suppressing antitumor T cell responses in the lungs. J Immunol. 2015;194(11):5529-38. doi: 10.4049/jimmunol.1403215. PubMed PMID: 25911761.
68. Hochst B, Mikulec J, Baccega T, Metzger C, Welz M, Peusquens J, Tacke F, Knolle P, Kurts C, Diehl L, Ludwig-Portugall I. Differential induction of Ly6G and Ly6C positive myeloid derived suppressor cells in chronic kidney and liver inflammation and fibrosis. PLoS One. 2015;10(3):e0119662. doi: 10.1371/journal.pone.0119662. PubMed PMID: 25738302; PMCID: PMC4349817.
69. Movahedi K, Laoui D, Gysemans C, Baeten M, Stange G, Van den Bossche J, Mack M, Pipeleers D, In't Veld P, De Baetselier P, Van Ginderachter JA. Different tumor microenvironments contain functionally distinct subsets of macrophages derived from Ly6C(high) monocytes. Cancer research. 2010;70(14):5728-39. doi: 10.1158/0008-5472.CAN-09-4672. PubMed PMID: 20570887.
70. Movahedi K, Guilliams M, Van den Bossche J, Van den Bergh R, Gysemans C, Beschin A, De Baetselier P, Van Ginderachter JA. Identification of discrete tumor-induced myeloid-derived suppressor cell subpopulations with distinct T cell-suppressive activity. Blood. 2008;111(8):4233-44. doi: 10.1182/blood-2007-07-099226. PubMed PMID: 18272812.
71. De Santa F, Narang V, Yap ZH, Tusi BK, Burgold T, Austenaa L, Bucci G, Caganova M, Notarbartolo S, Casola S, Testa G, Sung WK, Wei CL, Natoli G. Jmjd3 contributes to the control of gene expression in LPS-activated macrophages. EMBO J. 2009;28(21):3341-52. Epub 2009/09/26. doi: 10.1038/emboj.2009.271. PubMed PMID: 19779457; PMCID: PMC2752025.
72. Ishii M, Wen H, Corsa CA, Liu T, Coelho AL, Allen RM, Carson WFt, Cavassani KA, Li X, Lukacs NW, Hogaboam CM, Dou Y, Kunkel SL. Epigenetic regulation of the alternatively activated macrophage phenotype. Blood. 2009;114(15):3244-54. Epub 2009/07/02. doi: 10.1182/blood-2009-04-217620. PubMed PMID: 19567879; PMCID: PMC2759649.
73. Chen S, Ma J, Wu F, Xiong LJ, Ma H, Xu W, Lv R, Li X, Villen J, Gygi SP, Liu XS, Shi Y. The histone H3 Lys 27 demethylase JMJD3 regulates gene expression by impacting transcriptional elongation. Genes Dev. 2012;26(12):1364-75. Epub 2012/06/21. doi: 10.1101/gad.186056.111. PubMed PMID: 22713873; PMCID: PMC3387663.
74. Mullican SE, Gaddis CA, Alenghat T, Nair MG, Giacomin PR, Everett LJ, Feng D, Steger DJ, Schug J, Artis D, Lazar MA. Histone deacetylase 3 is an epigenomic brake in macrophage alternative activation. Genes Dev. 2011;25(23):2480-8. Epub

2011/12/14. doi: 10.1101/gad.175950.111. PubMed PMID: 22156208; PMCID: PMC3243058.
75. Chen X, Barozzi I, Termanini A, Prosperini E, Recchiuti A, Dalli J, Mietton F, Matteoli G, Hiebert S, Natoli G. Requirement for the histone deacetylase Hdac3 for the inflammatory gene expression program in macrophages. Proceedings of the National Academy of Sciences of the United States of America. 2012;109(42):E2865-74. Epub 2012/07/18. doi: 10.1073/pnas.1121131109. PubMed PMID: 22802645; PMCID: PMC3479529.
76. Heinz S, Glass CK. Roles of lineage-determining transcription factors in establishing open chromatin: lessons from high-throughput studies. Curr Top Microbiol Immunol. 2012;356:1-15. Epub 2011/07/12. doi: 10.1007/82_2011_142. PubMed PMID: 21744305.
77. Kaikkonen MU, Spann NJ, Heinz S, Romanoski CE, Allison KA, Stender JD, Chun HB, Tough DF, Prinjha RK, Benner C, Glass CK. Remodeling of the enhancer landscape during macrophage activation is coupled to enhancer transcription. Mol Cell. 2013;51(3):310-25. Epub 2013/08/13. doi: 10.1016/j.molcel.2013.07.010. PubMed PMID: 23932714; PMCID: PMC3779836.
78. Ostuni R, Piccolo V, Barozzi I, Polletti S, Termanini A, Bonifacio S, Curina A, Prosperini E, Ghisletti S, Natoli G. Latent enhancers activated by stimulation in differentiated cells. Cell. 2013;152(1-2):157-71. Epub 2013/01/22. doi: 10.1016/j.cell.2012.12.018. PubMed PMID: 23332752.
79. Heinz S, Romanoski CE, Benner C, Allison KA, Kaikkonen MU, Orozco LD, Glass CK. Effect of natural genetic variation on enhancer selection and function. Nature. 2013;503(7477):487-92. doi: 10.1038/nature12615. PubMed PMID: 24121437; PMCID: 3994126.
80. Caescu CI, Guo X, Tesfa L, Bhagat TD, Verma A, Zheng D, Stanley ER. Colony stimulating factor-1 receptor signaling networks inhibit mouse macrophage inflammatory responses by induction of microRNA-21. Blood. 2015;125(8):e1-13. Epub 2015/01/13. doi: 10.1182/blood-2014-10-608000. PubMed PMID: 25573988; PMCID: PMC4335087.
81. Das A, Ganesh K, Khanna S, Sen CK, Roy S. Engulfment of apoptotic cells by macrophages: a role of microRNA-21 in the resolution of wound inflammation. J Immunol. 2014;192(3):1120-9. Epub 2014/01/07. doi: 10.4049/jimmunol.1300613. PubMed PMID: 24391209; PMCID: PMC4358325.
82. Tang B, Li X, Ren Y, Wang J, Xu D, Hang Y, Zhou T, Li F, Wang L. MicroRNA-29a regulates lipopolysaccharide (LPS)-induced inflammatory responses in murine macrophages through the Akt1/ NF-kappaB pathway. Exp Cell Res. 2017;360(2):74-80. Epub 2017/08/16. doi: 10.1016/j.yexcr.2017.08.013. PubMed PMID: 28811129.
83. Zhang L, Huang C, Guo Y, Gou X, Hinsdale M, Lloyd P, Liu L. MicroRNA-26b Modulates the NF-kappaB Pathway in Alveolar Macrophages by Regulating PTEN. J Immunol. 2015;195(11):5404-14. Epub 2015/10/28. doi: 10.4049/jimmunol.1402933. PubMed PMID: 26503952; PMCID: PMC4655123.
84. Graff JW, Dickson AM, Clay G, McCaffrey AP, Wilson ME. Identifying functional microRNAs in macrophages with polarized phenotypes. J Biol Chem. 2012;287(26):21816-25. Epub 2012/05/03. doi: 10.1074/jbc.M111.327031. PubMed PMID: 22549785; PMCID: PMC3381144.

85. Park JE, Dutta B, Tse SW, Gupta N, Tan CF, Low JK, Yeoh KW, Kon OL, Tam JP, Sze SK. Hypoxia-induced tumor exosomes promote M2-like macrophage polarization of infiltrating myeloid cells and microRNA-mediated metabolic shift. Oncogene. 2019. Epub 2019/03/16. doi: 10.1038/s41388-019-0782-x. PubMed PMID: 30872795.
86. Wang S, Zhang X, Ju Y, Zhao B, Yan X, Hu J, Shi L, Yang L, Ma Z, Chen L, Liu Y, Duan Z, Chen X, Meng S. MicroRNA-146a feedback suppresses T cell immune function by targeting Stat1 in patients with chronic hepatitis B. J Immunol. 2013;191(1):293-301. Epub 2013/05/24. doi: 10.4049/jimmunol.1202100. PubMed PMID: 23698745.
87. Wu W, Takanashi M, Borjigin N, Ohno SI, Fujita K, Hoshino S, Osaka Y, Tsuchida A, Kuroda M. MicroRNA-18a modulates STAT3 activity through negative regulation of PIAS3 during gastric adenocarcinogenesis. Br J Cancer. 2013;108(3):653-61. Epub 2013/01/17. doi: 10.1038/bjc.2012.587. PubMed PMID: 23322197; PMCID: PMC3593546.
88. Tu K, Zheng X, Dou C, Li C, Yang W, Yao Y, Liu Q. MicroRNA-130b promotes cell aggressiveness by inhibiting peroxisome proliferator-activated receptor gamma in human hepatocellular carcinoma. Int J Mol Sci. 2014;15(11):20486-99. Epub 2014/11/12. doi: 10.3390/ijms151120486. PubMed PMID: 25387077; PMCID: PMC4264179.
89. Roy S, Sen CK. MiRNA in innate immune responses: novel players in wound inflammation. Physiol Genomics. 2011;43(10):557-65. Epub 2010/12/09. doi: 10.1152/physiolgenomics.00160.2010. PubMed PMID: 21139022; PMCID: PMC3110889.
90. Fanucchi S, Fok ET, Dalla E, Shibayama Y, Borner K, Chang EY, Stoychev S, Imakaev M, Grimm D, Wang KC, Li G, Sung WK, Mhlanga MM. Immune genes are primed for robust transcription by proximal long noncoding RNAs located in nuclear compartments. Nat Genet. 2019;51(1):138-50. Epub 2018/12/12. doi: 10.1038/s41588-018-0298-2. PubMed PMID: 30531872.
91. Cui H, Banerjee S, Guo S, Xie N, Ge J, Jiang D, Zornig M, Thannickal VJ, Liu G. Long noncoding RNA Malat1 regulates differential activation of macrophages and response to lung injury. JCI Insight. 2019;4(4). Epub 2019/01/25. doi: 10.1172/jci.insight.124522. PubMed PMID: 30676324.
92. Lu Y, Liu X, Xie M, Liu M, Ye M, Li M, Chen XM, Li X, Zhou R. The NF-kappaB-Responsive Long Noncoding RNA FIRRE Regulates Posttranscriptional Regulation of Inflammatory Gene Expression through Interacting with hnRNPU. J Immunol. 2017;199(10):3571-82. Epub 2017/10/11. doi: 10.4049/jimmunol.1700091. PubMed PMID: 28993514; PMCID: PMC5672816.
93. Hu G, Gong AY, Wang Y, Ma S, Chen X, Chen J, Su CJ, Shibata A, Strauss-Soukup JK, Drescher KM, Chen XM. LincRNA-Cox2 Promotes Late Inflammatory Gene Transcription in Macrophages through Modulating SWI/SNF-Mediated Chromatin Remodeling. J Immunol. 2016;196(6):2799-808. Epub 2016/02/18. doi: 10.4049/jimmunol.1502146. PubMed PMID: 26880762; PMCID: PMC4779692.
94. Ma S, Ming Z, Gong AY, Wang Y, Chen X, Hu G, Zhou R, Shibata A, Swanson PC, Chen XM. A long noncoding RNA, lincRNA-Tnfaip3, acts as a coregulator of NF-kappaB to modulate inflammatory gene transcription in mouse macrophages.

FASEB J. 2017;31(3):1215-25. Epub 2016/12/17. doi: 10.1096/fj.201601056R. PubMed PMID: 27979905; PMCID: PMC6191062.
95. Tugal D, Liao X, Jain MK. Transcriptional control of macrophage polarization. Arterioscler Thromb Vasc Biol. 2013;33(6):1135-44. Epub 2013/05/04. doi: 10.1161/ATVBAHA.113.301453. PubMed PMID: 23640482.
96. Juhas U, Ryba-Stanislawowska M, Szargiej P, Mysliwska J. Different pathways of macrophage activation and polarization. Postepy Hig Med Dosw (Online). 2015;69:496-502. Epub 2015/05/20. doi: 10.5604/17322693.1150133. PubMed PMID: 25983288.
97. Czimmerer Z, Daniel B, Horvath A, Ruckerl D, Nagy G, Kiss M, Peloquin M, Budai MM, Cuaranta-Monroy I, Simandi Z, Steiner L, Nagy B, Jr., Poliska S, Banko C, Bacso Z, Schulman IG, Sauer S, Deleuze JF, Allen JE, Benko S, Nagy L. The Transcription Factor STAT6 Mediates Direct Repression of Inflammatory Enhancers and Limits Activation of Alternatively Polarized Macrophages. Immunity. 2018;48(1):75-90 e6. Epub 2018/01/19. doi: 10.1016/j.immuni.2017.12.010. PubMed PMID: 29343442; PMCID: PMC5772169.
98. Zhu L, Zhao Q, Yang T, Ding W, Zhao Y. Cellular metabolism and macrophage functional polarization. Int Rev Immunol. 2015;34(1):82-100. Epub 2014/10/24. doi: 10.3109/08830185.2014.969421. PubMed PMID: 25340307.
99. Haschemi A, Kosma P, Gille L, Evans CR, Burant CF, Starkl P, Knapp B, Haas R, Schmid JA, Jandl C, Amir S, Lubec G, Park J, Esterbauer H, Bilban M, Brizuela L, Pospisilik JA, Otterbein LE, Wagner O. The sedoheptulose kinase CARKL directs macrophage polarization through control of glucose metabolism. Cell Metab. 2012;15(6):813-26. Epub 2012/06/12. doi: 10.1016/j.cmet.2012.04.023. PubMed PMID: 22682222; PMCID: PMC3370649.
100. Tavakoli S, Zamora D, Ullevig S, Asmis R. Bioenergetic profiles diverge during macrophage polarization: implications for the interpretation of 18F-FDG PET imaging of atherosclerosis. J Nucl Med. 2013;54(9):1661-7. Epub 2013/07/28. doi: 10.2967/jnumed.112.119099. PubMed PMID: 23886729; PMCID: PMC4037161.
101. Diskin C, Palsson-McDermott EM. Metabolic Modulation in Macrophage Effector Function. Front Immunol. 2018;9:270. Epub 2018/03/10. doi: 10.3389/fimmu.2018.00270. PubMed PMID: 29520272; PMCID: PMC5827535.
102. Zhou D, Huang C, Lin Z, Zhan S, Kong L, Fang C, Li J. Macrophage polarization and function with emphasis on the evolving roles of coordinated regulation of cellular signaling pathways. Cell Signal. 2014;26(2):192-7. Epub 2013/11/14. doi: 10.1016/j.cellsig.2013.11.004. PubMed PMID: 24219909.
103. Wilson HM. SOCS Proteins in Macrophage Polarization and Function. Front Immunol. 2014;5:357. Epub 2014/08/15. doi: 10.3389/fimmu.2014.00357. PubMed PMID: 25120543; PMCID: PMC4112788.
104. Lloberas J, Valverde-Estrella L, Tur J, Vico T, Celada A. Mitogen-Activated Protein Kinases and Mitogen Kinase Phosphatase 1: A Critical Interplay in Macrophage Biology. Front Mol Biosci. 2016;3:28. Epub 2016/07/23. doi: 10.3389/fmolb.2016.00028. PubMed PMID: 27446931; PMCID: PMC4923182.
105. Kim HS, Asmis R. Mitogen-activated protein kinase phosphatase 1 (MKP-1) in macrophage biology and cardiovascular disease. A redox-regulated master controller of monocyte function and macrophage phenotype. Free Radic Biol Med.

2017;109:75-83. Epub 2017/03/24. doi: 10.1016/j.freeradbiomed.2017.03.020. PubMed PMID: 28330703; PMCID: PMC5462841.
106. Sha Y, Marshall HE. S-nitrosylation in the regulation of gene transcription. Biochim Biophys Acta. 2012;1820(6):701-11. doi: 10.1016/j.bbagen.2011.05.008. PubMed PMID: 21640163; PMCID: PMC4403761.
107. Stomberski CT, Hess DT, Stamler JS. Protein S-Nitrosylation: Determinants of Specificity and Enzymatic Regulation of S-Nitrosothiol-Based Signaling. Antioxid Redox Signal. 2019;30(10):1331-51. Epub 2017/11/14. doi: 10.1089/ars.2017.7403. PubMed PMID: 29130312; PMCID: PMC6391618.
108. Matsumoto A, Gow AJ. Membrane transfer of S-nitrosothiols. Nitric Oxide. 2011;25(2):102-7. Epub 2011/03/08. doi: 10.1016/j.niox.2011.02.006. PubMed PMID: 21377531; PMCID: PMC3130086.
109. Ryerson TB, Trainer M, Holloway JS, Parrish DD, Huey LG, Sueper DT, Frost GJ, Donnelly SG, Schauffler S, Atlas EL, Kuster WC, Goldan PD, Hubler G, Meagher JF, Fehsenfeld FC. Observations of ozone formation in power plant plumes and implications for ozone control strategies. Science. 2001;292(5517):719-23. doi: 10.1126/science.1058113. PubMed PMID: 11326097.
110. Avissar NE, Reed CK, Cox C, Frampton MW, Finkelstein JN. Ozone, but not nitrogen dioxide, exposure decreases glutathione peroxidases in epithelial lining fluid of human lung. American journal of respiratory and critical care medicine. 2000;162(4 Pt 1):1342-7. doi: 10.1164/ajrccm.162.4.9912041. PubMed PMID: 11029342.
111. Bassett D, Elbon-Copp C, Otterbein S, Barraclough-Mitchell H, Delorme M, Yang H. Inflammatory cell availability affects ozone-induced lung damage. Journal of toxicology and environmental health Part A. 2001;64(7):547-65. doi: 10.1080/15287390152627237. PubMed PMID: 11760153.
112. Balmes JR, Chen LL, Scannell C, Tager I, Christian D, Hearne PQ, Kelly T, Aris RM. Ozone-induced decrements in FEV1 and FVC do not correlate with measures of inflammation. American journal of respiratory and critical care medicine. 1996;153(3):904-9. doi: 10.1164/ajrccm.153.3.8630571. PubMed PMID: 8630571.
113. Veninga TS, Wagenaar J, Lemstra W. Distinct enzymatic responses in mice exposed to a range of low doses of ozone. Environ Health Perspect. 1981;39:153-7. Epub 1981/06/01. doi: 10.1289/ehp.8139153. PubMed PMID: 7238452; PMCID: PMC1568736.
114. Lee MS, Moon KY, Bae DJ, Park MK, Jang AS. The effects of pycnogenol on antioxidant enzymes in a mouse model of ozone exposure. Korean J Intern Med. 2013;28(2):216-23. Epub 2013/03/26. doi: 10.3904/kjim.2013.28.2.216. PubMed PMID: 23526176; PMCID: PMC3604612.
115. Michaudel C, Fauconnier L, Jule Y, Ryffel B. Functional and morphological differences of the lung upon acute and chronic ozone exposure in mice. Sci Rep. 2018;8(1):10611. Epub 2018/07/15. doi: 10.1038/s41598-018-28261-9. PubMed PMID: 30006538; PMCID: PMC6045627.
116. Francis M, Sun R, Cervelli JA, Choi H, Mandal M, Abramova EV, Gow AJ, Laskin JD, Laskin DL. Editor's Highlight: Role of Spleen-Derived Macrophages in Ozone-Induced Lung Inflammation and Injury. Toxicol Sci. 2017;155(1):182-95. doi: 10.1093/toxsci/kfw192. PubMed PMID: 27708193; PMCID: PMC6080856.

117. Fakhrzadeh L, Laskin JD, Laskin DL. Deficiency in inducible nitric oxide synthase protects mice from ozone-induced lung inflammation and tissue injury. Am J Respir Cell Mol Biol. 2002;26(4):413-9. doi: 10.1165/ajrcmb.26.4.4516. PubMed PMID: 11919077.
118. Bonadonna G, De Lena M, Monfardini S, Bartoli C, Bajetta E, Beretta G, Fossati-Bellani F. Clinical trials with bleomycin in lymphomas and in solid tumors. European journal of cancer. 1972;8(2):205-15. PubMed PMID: 4116302.
119. Hecht SM. Bleomycin: new perspectives on the mechanism of action. Journal of natural products. 2000;63(1):158-68. PubMed PMID: 10650103.
120. Spangler M, Sartiano GP, Coetzee ML, Ove P. Effect of bleomycin on [3H]Thymidine 5'-Triphosphate incorporation into host liver and hepatoma nuclei. Cancer research. 1976;36(4):1339-46. PubMed PMID: 56997.
121. Tashiro M, Izumikawa K, Yoshioka D, Nakamura S, Kurihara S, Sakamoto N, Seki M, Kakeya H, Yamamoto Y, Yanagihara K, Mukae H, Hayashi T, Fukushima K, Tashiro T, Kohno S. Lung fibrosis 10 years after cessation of bleomycin therapy. The Tohoku journal of experimental medicine. 2008;216(1):77-80. PubMed PMID: 18719341.
122. Yatomi M, Hisada T, Ishizuka T, Koga Y, Ono A, Kamide Y, Seki K, Aoki-Saito H, Tsurumaki H, Sunaga N, Kaira K, Dobashi K, Yamada M, Okajima F. 17(R)-resolvin D1 ameliorates bleomycin-induced pulmonary fibrosis in mice. Physiological reports. 2015;3(12). doi: 10.14814/phy2.12628. PubMed PMID: 26660549; PMCID: 4760456.
123. Liang M, Lv J, Zou L, Yang W, Xiong Y, Chen X, Guan M, He R, Zou H. A modified murine model of systemic sclerosis: bleomycin given by pump infusion induced skin and pulmonary inflammation and fibrosis. Laboratory investigation; a journal of technical methods and pathology. 2015;95(3):342-50. doi: 10.1038/labinvest.2014.145. PubMed PMID: 25502178.
124. Liu W, Wan J, Han JZ, Li C, Feng DD, Yue SJ, Huang YH, Chen Y, Cheng QM, Li Y, Luo ZQ. Antiflammin-1 attenuates bleomycin-induced pulmonary fibrosis in mice. Respir Res. 2013;14:101. doi: 10.1186/1465-9921-14-101. PubMed PMID: 24098933; PMCID: 3856527.
125. Misharin AV, Morales-Nebreda L, Mutlu GM, Budinger GR, Perlman H. Flow cytometric analysis of macrophages and dendritic cell subsets in the mouse lung. Am J Respir Cell Mol Biol. 2013;49(4):503-10. Epub 2013/05/16. doi: 10.1165/rcmb.2013-0086MA. PubMed PMID: 23672262; PMCID: PMC3824047.
126. Guo C, Atochina-Vasserman E, Abramova H, George B, Manoj V, Scott P, Gow A. Role of NOS2 in pulmonary injury and repair in response to bleomycin. Free Radic Biol Med. 2016;91:293-301. doi: 10.1016/j.freeradbiomed.2015.10.417. PubMed PMID: 26526764; PMCID: PMC5059840.
127. Samoilenko capital O CAC, Milinevska OA, Karnaushenko OV, Shlyakhovenko VA, Zaletok SP. Effect of polyamine metabolism inhibitors on Lewis lung carcinoma growth and metastasis. Exp Oncol. 2015;37(2):151-3. Epub 2015/06/27. PubMed PMID: 26112945.
128. Rashidi B, Yang M, Jiang P, Baranov E, An Z, Wang X, Moossa AR, Hoffman RM. A highly metastatic Lewis lung carcinoma orthotopic green fluorescent protein

model. Clinical & experimental metastasis. 2000;18(1):57-60. PubMed PMID: 11206839.
129. Cuccarese MF, Dubach JM, Pfirschke C, Engblom C, Garris C, Miller MA, Pittet MJ, Weissleder R. Heterogeneity of macrophage infiltration and therapeutic response in lung carcinoma revealed by 3D organ imaging. Nat Commun. 2017;8:14293. Epub 2017/02/09. doi: 10.1038/ncomms14293. PubMed PMID: 28176769; PMCID: PMC5309815.
130. Bouillez A, Adeegbe D, Jin C, Hu X, Tagde A, Alam M, Rajabi H, Wong KK, Kufe D. MUC1-C promotes the suppressive immune microenvironment in non-small cell lung cancer. Oncoimmunology. 2017;6(9):e1338998. Epub 2017/09/22. doi: 10.1080/2162402X.2017.1338998. PubMed PMID: 28932637; PMCID: PMC5599083.
131. Zaynagetdinov R, Sherrill TP, Gleaves LA, McLoed AG, Saxon JA, Habermann AC, Connelly L, Dulek D, Peebles RS, Jr., Fingleton B, Yull FE, Stathopoulos GT, Blackwell TS. Interleukin-5 facilitates lung metastasis by modulating the immune microenvironment. Cancer Res. 2015;75(8):1624-34. Epub 2015/02/19. doi: 10.1158/0008-5472.CAN-14-2379. PubMed PMID: 25691457; PMCID: PMC4401663.
132. Arnold JN, Magiera L, Kraman M, Fearon DT. Tumoral immune suppression by macrophages expressing fibroblast activation protein-alpha and heme oxygenase-1. Cancer Immunol Res. 2014;2(2):121-6. Epub 2014/04/30. doi: 10.1158/2326-6066.CIR-13-0150. PubMed PMID: 24778275; PMCID: PMC4007628.
133. Wang J, Yu F, Jia X, Iwanowycz S, Wang Y, Huang S, Ai W, Fan D. MicroRNA-155 deficiency enhances the recruitment and functions of myeloid-derived suppressor cells in tumor microenvironment and promotes solid tumor growth. Int J Cancer. 2015;136(6):E602-13. Epub 2014/08/22. doi: 10.1002/ijc.29151. PubMed PMID: 25143000; PMCID: PMC4289468.
134. Yan X, Li W, Pan L, Fu E, Xie Y, Chen M, Mu D. Lewis Lung Cancer Cells Promote SIGNR1(CD209b)-Mediated Macrophages Polarization Induced by IL-4 to Facilitate Immune Evasion. J Cell Biochem. 2016;117(5):1158-66. Epub 2015/10/09. doi: 10.1002/jcb.25399. PubMed PMID: 26447454.
135. Lee C, Bae SS, Joo H, Bae H. Melittin suppresses tumor progression by regulating tumor-associated macrophages in a Lewis lung carcinoma mouse model. Oncotarget. 2017;8(33):54951-65. Epub 2017/09/15. doi: 10.18632/oncotarget.18627. PubMed PMID: 28903394; PMCID: PMC5589633.
136. Frampton MW. Ozone air pollution: how low can you go? Am J Respir Crit Care Med. 2011;184(2):150-1. doi: 10.1164/rccm.201104-0606ED. PubMed PMID: 21765027; PMCID: PMC3172884.
137. Goodman JE, Prueitt RL, Chandalia J, Sax SN. Evaluation of adverse human lung function effects in controlled ozone exposure studies. J Appl Toxicol. 2014;34(5):516-24. doi: 10.1002/jat.2905. PubMed PMID: 23836463.
138. Huang J, Li G, Xu G, Qian X, Zhao Y, Pan X, Huang J, Cen Z, Liu Q, He T, Guo X. The burden of ozone pollution on years of life lost from chronic obstructive pulmonary disease in a city of Yangtze River Delta, China. Environ Pollut. 2018;242(Pt B):1266-73. doi: 10.1016/j.envpol.2018.08.021. PubMed PMID: 30121480.

139. Nnoli NC, Linder SH, Smith MA, Gemeinhardt GL, Zhang K. The combined effect of ambient ozone exposure and toxic air releases on hospitalization for asthma among children in Harris County, Texas. Int J Environ Health Res. 2018;28(4):358-78. doi: 10.1080/09603123.2018.1479515. PubMed PMID: 29962221.
140. Alexis NE, Carlsten C. Interplay of air pollution and asthma immunopathogenesis: a focused review of diesel exhaust and ozone. Int Immunopharmacol. 2014;23(1):347-55. doi: 10.1016/j.intimp.2014.08.009. PubMed PMID: 25194677.
141. Valavanidis A, Vlachogianni T, Fiotakis K, Loridas S. Pulmonary oxidative stress, inflammation and cancer: respirable particulate matter, fibrous dusts and ozone as major causes of lung carcinogenesis through reactive oxygen species mechanisms. Int J Environ Res Public Health. 2013;10(9):3886-907. doi: 10.3390/ijerph10093886. PubMed PMID: 23985773; PMCID: PMC3799517.
142. Kosmider B, Loader JE, Murphy RC, Mason RJ. Apoptosis induced by ozone and oxysterols in human alveolar epithelial cells. Free Radic Biol Med. 2010;48(11):1513-24. doi: 10.1016/j.freeradbiomed.2010.02.032. PubMed PMID: 20219673; PMCID: PMC2965594.
143. Leroy P, Tham A, Wong H, Tenney R, Chen C, Stiner R, Balmes JR, Paquet AC, Arjomandi M. Inflammatory and repair pathways induced in human bronchoalveolar lavage cells with ozone inhalation. PLoS One. 2015;10(6):e0127283. doi: 10.1371/journal.pone.0127283. PubMed PMID: 26035830; PMCID: PMC4452717.
144. Pryor WA, Squadrito GL, Friedman M. The cascade mechanism to explain ozone toxicity: the role of lipid ozonation products. Free Radic Biol Med. 1995;19(6):935-41. PubMed PMID: 8582671.
145. Sunil VR, Patel-Vayas K, Shen J, Laskin JD, Laskin DL. Classical and alternative macrophage activation in the lung following ozone-induced oxidative stress. Toxicol Appl Pharmacol. 2012;263(2):195-202. doi: 10.1016/j.taap.2012.06.009. PubMed PMID: 22727909; PMCID: PMC3670689.
146. Yousefi S, Sharma SK, Stojkov D, Germic N, Aeschlimann S, Ge MQ, Flayer CH, Larson ED, Redai IG, Zhang S, Koziol-White CJ, Kariko K, Simon HU, Haczku A. Oxidative damage of SP-D abolishes control of eosinophil extracellular DNA trap formation. J Leukoc Biol. 2018;104(1):205-14. doi: 10.1002/JLB.3AB1117-455R. PubMed PMID: 29733456.
147. Kumarathasan P, Blais E, Saravanamuthu A, Bielecki A, Mukherjee B, Bjarnason S, Guenette J, Goegan P, Vincent R. Nitrative stress, oxidative stress and plasma endothelin levels after inhalation of particulate matter and ozone. Part Fibre Toxicol. 2015;12:28. doi: 10.1186/s12989-015-0103-7. PubMed PMID: 26376633; PMCID: PMC4573945.
148. Kumarathasan P, Vincent R, Goegan P, Potvin M, Guenette J. Hydroxyl radical adduct of 5-aminosalicylic acid: a potential marker of ozone-induced oxidative stress. Biochem Cell Biol. 2001;79(1):33-42. PubMed PMID: 11235916.
149. Heinrich TA, da Silva RS, Miranda KM, Switzer CH, Wink DA, Fukuto JM. Biological nitric oxide signalling: chemistry and terminology. Br J Pharmacol.

2013;169(7):1417-29. doi: 10.1111/bph.12217. PubMed PMID: 23617570; PMCID: PMC3724101.
150. Hess DT, Matsumoto A, Kim SO, Marshall HE, Stamler JS. Protein S-nitrosylation: purview and parameters. Nat Rev Mol Cell Biol. 2005;6(2):150-66. Epub 2005/02/03. doi: 10.1038/nrm1569. PubMed PMID: 15688001.
151. Jia J, Arif A, Terenzi F, Willard B, Plow EF, Hazen SL, Fox PL. Target-selective protein S-nitrosylation by sequence motif recognition. Cell. 2014;159(3):623-34. doi: 10.1016/j.cell.2014.09.032. PubMed PMID: 25417112; PMCID: PMC4243042.
152. Kovacs I, Lindermayr C. Nitric oxide-based protein modification: formation and site-specificity of protein S-nitrosylation. Front Plant Sci. 2013;4:137. Epub 2013/05/30. doi: 10.3389/fpls.2013.00137. PubMed PMID: 23717319; PMCID: PMC3653056.
153. Marino SM, Gladyshev VN. Structural analysis of cysteine S-nitrosylation: a modified acid-based motif and the emerging role of trans-nitrosylation. J Mol Biol. 2010;395(4):844-59. Epub 2009/10/27. doi: 10.1016/j.jmb.2009.10.042. PubMed PMID: 19854201; PMCID: PMC3061812.
154. Sun J, Steenbergen C, Murphy E. S-nitrosylation: NO-related redox signaling to protect against oxidative stress. Antioxid Redox Signal. 2006;8(9-10):1693-705. doi: 10.1089/ars.2006.8.1693. PubMed PMID: 16987022; PMCID: PMC2443861.
155. Sugahara K, Tokumine J, Teruya K, Oshiro T. Alveolar epithelial cells: differentiation and lung injury. Respirology. 2006;11 Suppl:S28-31. Epub 2006/01/21. doi: 10.1111/j.1440-1843.2006.00804.x. PubMed PMID: 16423267.
156. Kim J, Won JS, Singh AK, Sharma AK, Singh I. STAT3 regulation by S-nitrosylation: implication for inflammatory disease. Antioxid Redox Signal. 2014;20(16):2514-27. Epub 2013/09/26. doi: 10.1089/ars.2013.5223. PubMed PMID: 24063605; PMCID: PMC4026100.
157. Kenyon NJ, van der Vliet A, Schock BC, Okamoto T, McGrew GM, Last JA. Susceptibility to ozone-induced acute lung injury in iNOS-deficient mice. Am J Physiol Lung Cell Mol Physiol. 2002;282(3):L540-5. doi: 10.1152/ajplung.00297.2001. PubMed PMID: 11839550.
158. Batra J, Chatterjee R, Ghosh B. Inducible nitric oxide synthase (iNOS): role in asthma pathogenesis. Indian J Biochem Biophys. 2007;44(5):303-9. Epub 2008/03/18. PubMed PMID: 18341205.
159. Mashimo H, Goyal RK. Lessons from genetically engineered animal models. IV. Nitric oxide synthase gene knockout mice. Am J Physiol. 1999;277(4):G745-50. Epub 1999/10/12. doi: 10.1152/ajpgi.1999.277.4.G745. PubMed PMID: 10516139.
160. Torrisi JS, Hespe GE, Cuzzone DA, Savetsky IL, Nitti MD, Gardenier JC, Garcia Nores GD, Jowhar D, Kataru RP, Mehrara BJ. Inhibition of Inflammation and iNOS Improves Lymphatic Function in Obesity. Sci Rep. 2016;6:19817. Epub 2016/01/23. doi: 10.1038/srep19817. PubMed PMID: 26796537; PMCID: PMC4726274.
161. Luzina IG, Lockatell V, Todd NW, Kopach P, Pentikis HS, Atamas SP. Pharmacological In Vivo Inhibition of S-Nitrosoglutathione Reductase Attenuates Bleomycin-Induced Inflammation and Fibrosis. J Pharmacol Exp Ther. 2015;355(1):13-22. Epub 2015/07/26. doi: 10.1124/jpet.115.224675. PubMed PMID: 26209236.

162. Foster MW, Yang Z, Gooden DM, Thompson JW, Ball CH, Turner ME, Hou Y, Pi J, Moseley MA, Que LG. Proteomic characterization of the cellular response to nitrosative stress mediated by s-nitrosoglutathione reductase inhibition. J Proteome Res. 2012;11(4):2480-91. Epub 2012/03/07. doi: 10.1021/pr201180m. PubMed PMID: 22390303; PMCID: PMC3327136.
163. Wei W, Li B, Hanes MA, Kakar S, Chen X, Liu L. S-nitrosylation from GSNOR deficiency impairs DNA repair and promotes hepatocarcinogenesis. Sci Transl Med. 2010;2(19):19ra3. Epub 2010/04/08. doi: 10.1126/scitranslmed.3000328. PubMed PMID: 20371487; PMCID: PMC3085984.
164. Liu L, Yan Y, Zeng M, Zhang J, Hanes MA, Ahearn G, McMahon TJ, Dickfeld T, Marshall HE, Que LG, Stamler JS. Essential roles of S-nitrosothiols in vascular homeostasis and endotoxic shock. Cell. 2004;116(4):617-28. Epub 2004/02/26. PubMed PMID: 14980227.
165. Que LG, Yang Z, Lugogo NL, Katial RK, Shoemaker SA, Troha JM, Rodman DM, Tighe RM, Kraft M. Effect of the S-nitrosoglutathione reductase inhibitor N6022 on bronchial hyperreactivity in asthma. Immun Inflamm Dis. 2018;6(2):322-31. Epub 2018/04/12. doi: 10.1002/iid3.220. PubMed PMID: 29642282; PMCID: PMC5946144.
166. Barnett SD, Buxton ILO. The role of S-nitrosoglutathione reductase (GSNOR) in human disease and therapy. Crit Rev Biochem Mol Biol. 2017;52(3):340-54. Epub 2017/04/11. doi: 10.1080/10409238.2017.1304353. PubMed PMID: 28393572; PMCID: PMC5597050.
167. Blonder JP, Mutka SC, Sun X, Qiu J, Green LH, Mehra NK, Boyanapalli R, Suniga M, Look K, Delany C, Richards JP, Looker D, Scoggin C, Rosenthal GJ. Pharmacologic inhibition of S-nitrosoglutathione reductase protects against experimental asthma in BALB/c mice through attenuation of both bronchoconstriction and inflammation. BMC Pulm Med. 2014;14:3. Epub 2014/01/11. doi: 10.1186/1471-2466-14-3. PubMed PMID: 24405692; PMCID: PMC3893392.
168. Gonzalez H, Hagerling C, Werb Z. Roles of the immune system in cancer: from tumor initiation to metastatic progression. Genes Dev. 2018;32(19-20):1267-84. Epub 2018/10/03. doi: 10.1101/gad.314617.118. PubMed PMID: 30275043; PMCID: PMC6169832.
169. Zanganeh S, Spitler R, Hutter G, Ho JQ, Pauliah M, Mahmoudi M. Tumor-associated macrophages, nanomedicine and imaging: the axis of success in the future of cancer immunotherapy. Immunotherapy. 2017;9(10):819-35. Epub 2017/09/08. doi: 10.2217/imt-2017-0041. PubMed PMID: 28877626.
170. Awad RM, De Vlaeminck Y, Maebe J, Goyvaerts C, Breckpot K. Turn Back the TIMe: Targeting Tumor Infiltrating Myeloid Cells to Revert Cancer Progression. Front Immunol. 2018;9:1977. Epub 2018/09/21. doi: 10.3389/fimmu.2018.01977. PubMed PMID: 30233579; PMCID: PMC6127274.
171. Kiss M, Van Gassen S, Movahedi K, Saeys Y, Laoui D. Myeloid cell heterogeneity in cancer: not a single cell alike. Cell Immunol. 2018;330:188-201. Epub 2018/02/28. doi: 10.1016/j.cellimm.2018.02.008. PubMed PMID: 29482836.
172. Gharaee-Kermani M, Phan SH. The role of eosinophils in pulmonary fibrosis (Review). Int J Mol Med. 1998;1(1):43-53. Epub 1998/12/16. PubMed PMID: 9852197.

173. Huaux F, Liu T, McGarry B, Ullenbruch M, Xing Z, Phan SH. Eosinophils and T lymphocytes possess distinct roles in bleomycin-induced lung injury and fibrosis. J Immunol. 2003;171(10):5470-81. Epub 2003/11/11. PubMed PMID: 14607953.
174. Cormier SA, Taranova AG, Bedient C, Nguyen T, Protheroe C, Pero R, Dimina D, Ochkur SI, O'Neill K, Colbert D, Lombari TR, Constant S, McGarry MP, Lee JJ, Lee NA. Pivotal Advance: eosinophil infiltration of solid tumors is an early and persistent inflammatory host response. J Leukoc Biol. 2006;79(6):1131-9. Epub 2006/04/18. doi: 10.1189/jlb.0106027. PubMed PMID: 16617160; PMCID: PMC3496422.
175. Klion A. Recent advances in understanding eosinophil biology. F1000Res. 2017;6:1084. Epub 2017/07/29. doi: 10.12688/f1000research.11133.1. PubMed PMID: 28751971; PMCID: PMC5506535.
176. Percopo CM, Brenner TA, Ma M, Kraemer LS, Hakeem RM, Lee JJ, Rosenberg HF. SiglecF+Gr1hi eosinophils are a distinct subpopulation within the lungs of allergen-challenged mice. J Leukoc Biol. 2017;101(1):321-8. Epub 2016/08/18. doi: 10.1189/jlb.3A0416-166R. PubMed PMID: 27531929; PMCID: PMC5166438.
177. Shaul ME, Fridlender ZG. Cancer related circulating and tumor-associated neutrophils - subtypes, sources and function. FEBS J. 2018. Epub 2018/06/01. doi: 10.1111/febs.14524. PubMed PMID: 29851227.
178. Youn JI, Nagaraj S, Collazo M, Gabrilovich DI. Subsets of myeloid-derived suppressor cells in tumor-bearing mice. J Immunol. 2008;181(8):5791-802. Epub 2008/10/04. PubMed PMID: 18832739; PMCID: PMC2575748.
179. Zhang L, Huang G, Li X, Zhang Y, Jiang Y, Shen J, Liu J, Wang Q, Zhu J, Feng X, Dong J, Qian C. Hypoxia induces epithelial-mesenchymal transition via activation of SNAI1 by hypoxia-inducible factor -1alpha in hepatocellular carcinoma. BMC Cancer. 2013;13:108. Epub 2013/03/19. doi: 10.1186/1471-2407-13-108. PubMed PMID: 23496980; PMCID: PMC3614870.
180. Yue X, Zhao Y, Zhang C, Li J, Liu Z, Liu J, Hu W. Leukemia inhibitory factor promotes EMT through STAT3-dependent miR-21 induction. Oncotarget. 2016;7(4):3777-90. Epub 2015/12/31. doi: 10.18632/oncotarget.6756. PubMed PMID: 26716902; PMCID: PMC4826169.
181. Langley RR, Fidler IJ. The seed and soil hypothesis revisited--the role of tumor-stroma interactions in metastasis to different organs. Int J Cancer. 2011;128(11):2527-35. Epub 2011/03/03. doi: 10.1002/ijc.26031. PubMed PMID: 21365651; PMCID: PMC3075088.
182. Wickremasinghe MI, Thomas LH, O'Kane CM, Uddin J, Friedland JS. Transcriptional mechanisms regulating alveolar epithelial cell-specific CCL5 secretion in pulmonary tuberculosis. J Biol Chem. 2004;279(26):27199-210. Epub 2004/05/01. doi: 10.1074/jbc.M403107200. PubMed PMID: 15117956.
183. Hiscott J, Marois J, Garoufalis J, D'Addario M, Roulston A, Kwan I, Pepin N, Lacoste J, Nguyen H, Bensi G, et al. Characterization of a functional NF-kappa B site in the human interleukin 1 beta promoter: evidence for a positive autoregulatory loop. Mol Cell Biol. 1993;13(10):6231-40. Epub 1993/10/01. PubMed PMID: 8413223; PMCID: PMC364682.
184. Sica A, Tan TH, Rice N, Kretzschmar M, Ghosh P, Young HA. The c-rel protooncogene product c-Rel but not NF-kappa B binds to the intronic region of the human interferon-gamma gene at a site related to an interferon-stimulable response

element. Proc Natl Acad Sci U S A. 1992;89(5):1740-4. Epub 1992/03/01. PubMed PMID: 1542667; PMCID: PMC48528.
185. Shakhov AN, Collart MA, Vassalli P, Nedospasov SA, Jongeneel CV. Kappa B-type enhancers are involved in lipopolysaccharide-mediated transcriptional activation of the tumor necrosis factor alpha gene in primary macrophages. J Exp Med. 1990;171(1):35-47. Epub 1990/01/01. PubMed PMID: 2104921; PMCID: PMC2187654.
186. Libermann TA, Baltimore D. Activation of interleukin-6 gene expression through the NF-kappa B transcription factor. Mol Cell Biol. 1990;10(5):2327-34. Epub 1990/05/01. PubMed PMID: 2183031; PMCID: PMC360580.
187. Hein H, Schluter C, Kulke R, Christophers E, Schroder JM, Bartels J. Genomic organization, sequence, and transcriptional regulation of the human eotaxin gene. Biochem Biophys Res Commun. 1997;237(3):537-42. Epub 1997/08/28. doi: 10.1006/bbrc.1997.7169. PubMed PMID: 9299399.
188. Moya MP, Gow AJ, Califf RM, Goldberg RN, Stamler JS. Inhaled ethyl nitrite gas for persistent pulmonary hypertension of the newborn. Lancet. 2002;360(9327):141-3. Epub 2002/07/20. doi: 10.1016/S0140-6736(02)09385-6. PubMed PMID: 12126827.
189. Sheller JR, Polosukhin VV, Mitchell D, Cheng DS, Peebles RS, Blackwell TS. Nuclear factor kappa B induction in airway epithelium increases lung inflammation in allergen-challenged mice. Exp Lung Res. 2009;35(10):883-95. Epub 2009/12/10. doi: 10.3109/01902140903019710. PubMed PMID: 19995280; PMCID: PMC3419942.
190. Zhao Q, Simpson LG, Driscoll KE, Leikauf GD. Chemokine regulation of ozone-induced neutrophil and monocyte inflammation. Am J Physiol. 1998;274(1 Pt 1):L39-46. Epub 1998/02/12. PubMed PMID: 9458799.
191. Fakhrzadeh L, Laskin JD, Laskin DL. Ozone-induced production of nitric oxide and TNF-alpha and tissue injury are dependent on NF-kappaB p50. Am J Physiol Lung Cell Mol Physiol. 2004;287(2):L279-85. Epub 2004/04/06. doi: 10.1152/ajplung.00348.2003. PubMed PMID: 15064226.
192. Kim J, Choi S, Saxena N, Singh AK, Singh I, Won JS. Regulation of STAT3 and NF-kappaB activations by S-nitrosylation in multiple myeloma. Free Radic Biol Med. 2017;106:245-53. Epub 2017/02/25. doi: 10.1016/j.freeradbiomed.2017.02.039. PubMed PMID: 28232202; PMCID: PMC5826580.
193. Yu H, Pardoll D, Jove R. STATs in cancer inflammation and immunity: a leading role for STAT3. Nat Rev Cancer. 2009;9(11):798-809. Epub 2009/10/24. doi: 10.1038/nrc2734. PubMed PMID: 19851315; PMCID: PMC4856025.
194. Liegeois M, Legrand C, Desmet CJ, Marichal T, Bureau F. The interstitial macrophage: A long-neglected piece in the puzzle of lung immunity. Cell Immunol. 2018;330:91-6. doi: 10.1016/j.cellimm.2018.02.001. PubMed PMID: 29458975.
195. Novak ML, Koh TJ. Macrophage phenotypes during tissue repair. J Leukoc Biol. 2013;93(6):875-81. Epub 2013/03/19. doi: 10.1189/jlb.1012512. PubMed PMID: 23505314; PMCID: PMC3656331.